Solitons in Bose-Einstein Condensates

– Solitonen in Bose-Einstein-Kondensaten –

Diplomarbeit

Matthias Söhn

April 2002

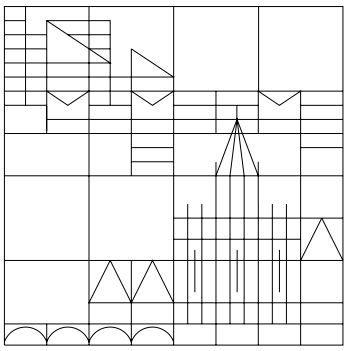

Fachbereich für Physik
Universität Konstanz

Solitonen in Bose-Einstein-Kondensaten

Einführung

Bose-Einstein-Kondensation

Die quantenstatistischen Eigenschaften von Vielteilchensystemen identischer Teilchen werden grundlegend bestimmt durch den *Spin* der Teilchen: *Bosonen* sind Teilchen mit *ganzzahligem Spin* und werden durch Wellenfunktionen beschrieben, die sich *symmetrisch* unter Vertauschung der Teilchenvariablen verhalten; demgegenüber werden Teilchen mit *halbzahligen Spin* (*"Fermionen"*) durch *antisymmetrische* Wellenfunktionen beschrieben. Obwohl im klassischen Limes, d.h. insbesondere bei hohen Temperaturen, die Unterschiede zwischen bosonischen und fermionischen Gasen klein sind, zeigen sich deutliche Unterschiede der Quantenstatistik im Bereich kleiner Temperaturen.

Eine direkte Folge der obenerwähnten Symmetrieeigenschaften ist, daß im Falle von Fermionen ein einzelner Quantenzustand höchstens von einem Teilchen besetzt werden kann (Pauli-Prinzip). Für Bosonen gibt es eine solche Beschränkung nicht.
Das letztere manifestiert sich insbesondere beim Phänomen der *Bose-Einstein-Kondensation*, die der makroskopischen Besetzung eines einzelnen Quantenzustandes entspricht. Dieser bemerkenswerte Effekt wurde erstmals 1924/25 von S. N. Bose und A. Einstein für ein nicht-wechselwirkendes, homogenes Gas vorausgesagt ([1], [2]).
Die direkte experimentelle Verwirklichung dieses Effektes jedoch, nämlich in Systemen schwach wechselwirkender atomarer Gase, stellt eine beträchtliche Herausforderung dar und ließ 70 Jahre auf sich warten: Nachdem experimentelle Techniken wie magnetische Fallen, Laser-Kühlung von Atomen und Verdampfungskühlung von Atomen den Vorstoß in den Bereich ultratiefer Temperaturen ermöglicht hatten, wurden im Jahre 1995 die ersten Bose-Einstein-Kondensate (im folgenden mitunter abgekürzt durch "BECs") in verdünnten Gasen von ^{87}Rb ([3]), Spin-polarisiertem ^{7}Li ([4]) und Na ([5]) erzeugt. Hierfür wurde im Jahre 2001 der Nobelpreis für Physik an E. A. Cornell, W. Ketterle und C. E.

Wiemann verliehen. Schon allein dies bezeugt die große Bedeutung, die dieser experimentellen Errungenschaft sowohl für die Grundlagenforschung, als auch für eventuelle spätere Anwendungen beigemessen wird.

Bei Systemen atomarer Gase liegt der typische Wert der kritischen Temperatur für das Einsetzen des Bose-Einstein-Kondensationseffektes im Bereich von Nanokelvin, wobei der Effekt der makroskopischen Besetzung des Einteilchen-Grundzustandes mitunter auch als quantenmechanischer Phasenübergang in einen 'neuen Materiezustand' gekennzeichnet wird. Dieser ist dadurch charakterisiert, daß die DeBroglie-Wellenlänge der kalten Bosonen in die Größenordnung des mittleren Teilchenabstandes kommt. Anschaulich gesprochen verlieren die Bosonen ihre individuelle Identität; stattdessen beginnt die ganze Menge von Atomen, sich wie eine einzige makroskopische Wellenfunktion zu verhalten — und kann in der Tat auch derart beschrieben werden. Im Falle schwach wechselwirkender Kondensate führt ein 'mean-field'-Zugang auf die sog. Gross-Pitaevskii-Gleichung (im folgenden mitunter abgekürzt durch "GPE"), die die Zeitentwicklung ebendieser makroskopischen Wellenfunktion bestimmt. Man beachte, daß in diesem Zugang beispielsweise Teilchenkorrelationen, 'Quanten-depletion' und Effekten endlicher Temperatur nicht korrekt Rechnung getragen wird.

Solitonen

Die Gross-Pitaevskii-Gleichung ist eine nichtlineare Differentialgleichung, wobei der nichtlineare Term von den Teilchenwechselwirkungen herrührt. Es zeigt sich, daß diese Gleichung sog. *Solitonenlösungen* hat. Solitonen sind Wellenpakete mit der wesentlichen Eigenschaft, daß sie stabil gegen ein 'Zerfliessen' sind: Ohne den nichtlinearen Term würden Dispersionseffekte zu einer Verbreiterung des Wellenpaketes führen, da sich die unterschiedlichen Spektralkomponenten mit unterschiedlichen Geschwindigkeiten ausbreiten. Es ist jedoch möglich, daß sich die Effekte von Nichtlinearität und Dispersion gegenseitig aufheben — dies ermögicht Solitonenlösungen, bei denen die Dispersion *effektiv* verschwindet.

Solitonen als Phänomen sind schon seit langem bekannt: In Form von Wasserwellen-Solitonen in einem flachen Kanal wurden diese im 19ten Jahrhundert durch Zufall von J. Scott Russell entdeckt. Seitdem wurden solitonenartige Lösungen in vielen anderen nichtlinearen physikalischen Systemen entdeckt. Um nur ein Beispiel zu nennen: Solitonen in Glasfasern sind auf dem Gebiet der optischen Kommunikation von großem Interesse, da solche Lichtpulse — als Datenbits interpretiert — unter entsprechenden Bedingungen in wesentlichen dispersionsfrei propagieren können. Tatsächlich haben in den letzten Jahren auf diesem Gebiet die ersten echten 'Anwendungen' des Solitonenphänomens Produktreife erlangt.

Man unterscheidet — abhängig von den Vorzeichen der Nichtlinearität und des Dispersionstermes — sog. *helle* und *dunkle* Solitonen. Erstere sind Wellenpakete im eigentlichen Sinne mit Intensitätsmaxima, letztere stellen eine lokalisierte Intensitätsverminderung innerhalb nichtverschwindender Hintergrundintensität

dar. Bis jetzt gelang in BECs atomarer Gase experimentell nur die Erzeugung dunkler Solitonen. Es werden derzeit jedoch auch experimentelle Anstrengungen bezüglich heller Solitonen unternommen: Beispielsweise arbeitet an der Universität Konstanz eine Gruppe um Markus Oberthaler an einem entsprechenden Experiment zur Erzeugung einer speziellen Art heller Solitonen (sog. helle 'gap'-Solitonen, siehe hierzu Abschnitt 3.2.2).

Zusammenfassende Übersicht über diese Arbeit

Die Gross-Pitaevskii-Gleichung ist unter anderem gut für Stabilitätsuntersuchungen von Solitonenlösungen geeignet. Effekte endlicher Temperatur oder endlicher Teilchenzahl, sowie Teilchenkorrelationen werden jedoch im Rahmen eines solchen 'mean-field'-Zuganges nicht hinreichend beschrieben. In diesem Sinne widmet sich diese Diplomarbeit der Untersuchung der genaueren "Quantenstruktur" von Solitonen in Bose-Einstein-Kondensaten, wobei quantenfeldtheoretische Modelle jenseits des üblichen 'mean-field'-Zuganges diskutiert werden.

Kapitel 2 stellt eine Einführung in die Theorie der Bose-Einstein-Kondensation dar. Es wird gezeigt, daß in Systemen ultrakalter, verdünnter Gase Teilchenwechselwirkungen näherungsweise durch s-Wellen-Streuung beschrieben werden können. Dies erlaubt die Einführung des sog. 'zero-range pseudo-Potentials' ("Delta-Potential") als Modellpotential, welches die s-Wellen-Streulänge als einzigen Parameter hat. Dies hat wesentliche Vereinfachungen bei der Beschreibung des Systems zur Folge: Es wird gezeigt, daß im Heisenbergbild ein 'mean-field'-Zugang auf die grundlegende Gross-Pitaevskii-Gleichung für die makroskopische Wellenfunktion des Kondensates führt, bei der der nichtlineare Term von den Teilchenwechselwirkungen herrührt.

Nachdem im Kapitel 3 zunächst allgemein das Phänomen "Solitonen" anhand optischer Solitonen in Glasfasern eingeführt wird, wird gezeigt, daß die Gross-Pitaevskii-Gleichung sowohl dunkle und helle Solitonen als Lösungen hat.

Im Schrödingerbild wird das System durch eine n-Teilchen Schrödinger-Gleichung beschrieben, wobei die Wellenfunktion explizit von den n Variablen der Teilchenpositionen abhängt. Im Grenzfall ultrakalter, verdünnter Gase taucht auch in dieser Gleichung wiederum das o.g. 'zero-range pseudo-Potential' als Wechselwirkungsterm auf. Im Kapitel 4 wird nun die eindimensionale Version dieser Gleichung für den Fall diskutiert, daß effektiv attraktive Wechselwirkungen zwischen den Teilchen vorliegen. Es wird gezeigt, daß sowohl ein Hartree-'mean-field'-Zugang, als auch ein exakter, sog. Bethe-Ansatz im Grenzfall großer Teilchenzahlen auf helle Solitonen als Lösung führen, wenn man den Erwartungswert des Feldoperators betrachtet. Im Falle der exakten Bethe-Lösung ergibt sich dabei der Solitonenzustand als Superposition von Teilchenzahl- und Gesamtimpuls-Eigenzuständen. Die sich daraus ergebenden Phasendiffusions- und

Dispersionseffekte werden diskutiert, wobei letztere einen reinen Quanteneffekt darstellen, der sich erst im quantenfeldtheoretischen Zugang ergibt. Es wird gezeigt, daß genannter Quantendispersionseffekt zur Verbreiterung des Solitonenzustandes führt, was — wie abgeschätzt wird — experimentell beobachtbar sein sollte.
Desweiteren werden bestimmte Matrixelemente, die im Zusammenhang mit den räumlichen Zweipunktkorrelationsfunktionen für den Solitonenzustand auftauchen, für die *Bethe*-Zuständen berechnet. Damit wird gezeigt, daß die Wechselwirkungen Korrelationen zwischen den Teilchen hervorrufen. Leider zeigt sich aber, daß im Falle der Bethe-Solitonen Größen wie der Erwartungswert des Feldoperators oder die Zweipunktkorrelationsfunktionen für große Teilchenzahlen numerisch nicht mehr zugänglich sind.

In Kapitel 5 wird wiederum die n-Teilchen Schrödinger-Gleichung betrachtet, wobei allerdings statt des 'zero-range pseudo-Potentials' ein allgemeineres Wechselwirkungspotential angenommen wird. Hierdurch soll eine realistischere Beschreibung der Teilchenwechselwirkungen jenseits des obenerwähnten Grenzfalles $T \to 0$ ermöglicht werden. Es wird zunächst gezeigt, daß man sich bei der Behandlung verdünnter Gase in guter Näherung auf binäre Teilchenwechselwirkungen beschränken kann. Folglich separiert ein entsprechender Ansatz für die n-Teilchen-Wellenfunktion in ein Produkt von (höchstens) *Zwei*-Teilchen-Wellenfunktionen. Ursprünglich wurde erhofft, durch diesen von vereinfachenden Annahmen ausgehenden Ansatz eine approximative Beschreibung zu bekommen, die — anders als beim obengenannten Bethe-Modell — auch im Falle großer Teilchenzahlen rechentechnisch anwendbar ist. Es zeigt sich jedoch, daß die sich ergebenden Ausdrücke sowohl analytisch, als auch numerisch selbst bei relativ kleinen Teilchenzahlen nicht vernünftig behandelbar sind. In diesem Zusammenhang wurden computeralgebraische Methoden entwickelt, mit denen die Kommutatoralgebra des Modelles implementiert wird; durch kleinere Anpassungen sollten hiermit im Prinzip jedoch auch verwandte Probleme, die bei quantenfeldtheoretischen Rechnungen auftauchen, behandelbar sein.

Zusammenfassend hat sich im Rahmen dieser Arbeit gezeigt, daß bei der Behandlung von Systemen wechselwirkender Teilchen mit quantenfeldtheoretischen Methoden, die über den üblichen 'mean-field'/Hartree-Zugang hinausgehen, die konkrete Berechnung wichtiger Größen allenfalls für kleine Teilchenzahlen möglich ist; bei hohen Teilchenzahlen scheitert man typischerweise am großen Rechenaufwand.

Solitons in Bose-Einstein Condensates

Diploma Thesis

Matthias Söhn

April 2002

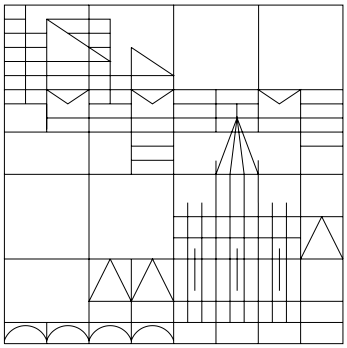

Fachbereich für Physik
Universität Konstanz

Acknowlegdements

First of all and generally I want to thank my parents: Who knows whether I would ever have managed to go the long way of becoming "Dipl. Phys." — stated here not as a "title", of course, but as 'pars pro toto' for my personal and academic growth — without their continuous promotion, backing, support – and love...? Especially for them I explicitly change to my native language to say: *Danke für Alles, was Ihr für mich getan habt!*

Concerning this thesis I am deeply indebted to my supervisor Peter Marzlin. More than once — indeed every time again — I have been impressed by his great knowledge, his ability to show a way out of emerging physical, mathematical and numerical problems and his flexibility to always have enough time for me despite all his other commitments.

Moreover, I wish to thank Prof. Audretsch and his group — here especially mentioning our excellent Linux sysadmin Jan Krüger: It's due to him that I pondered over publishing this diploma thesis under the GNU general public license. Unfortunately, this is not possible — but it is written in the "general public language" English at least...!

I also want to explicitly mention my friends and numerous flatmates from all over the world that I have had in the legendary 'Haus E': It is no question that I am grateful to them for preventing me from completely forgetting that there is a world besides physics... These experiences definitely left their mark on my $3\frac{1}{2}$ years of staying in Konstanz.

I also acknowledge the Universität Konstanz for providing the probably best university library in Germany. Almost never I left it without having found the books, media and information I have been searching for.

Finally, special thanks to my flatmates Morvern McLean from Australia and Mike Welham from South Africa — two native speakers — for their thorough proof reading of parts of this thesis.

Contents

Chapter 1

Introduction

1.1 Bose-Einstein Condensation

The quantum-statistical properties of many-particle systems of identical particles are fundamentally determined by the *spin* of the particles: *Bosons* with *integral spin* are represented by wavefunctions that are *symmetric* under permutation of particles, whereas particles with *half-integral spin* (*"fermions"*) are described by *antisymmetric* wavefunctions. Though in the classical limit, i.e. especially at high temperatures, the differences between bosonic and fermionic gases are small, striking differences of the quantum statistics are revealed in the low temperature regime.

A direct consequence of the abovementioned symmetry properties is that in the case of fermions at most one particle can occupy a single quantum state (Pauli exclusion principle), whereas for bosons no such fundamental restriction exists.
The latter is clearly revealed by the phenomenon of *Bose-Einstein condensation*, where a single quantum state is macroscopically occupied. This fascinating effect was first predicted by S. N. Bose and A. Einstein in 1924-25 ([1], [2]) for a non-interacting homogeneous Bose gas.
However, the direct experimental realization of this effect, namely in systems of weakly interacting atomic gases, has been a great challenge and was only accomplished 70 years later: After techniques like magnetic trapping, laser cooling of atoms and evaporative cooling made it possible to venture into the ultra-low temperature regime, the first Bose-Einstein condensates (BECs) were finally realized in 1995 in dilute gases of ^{87}Rb ([3]), spin polarized ^{7}Li ([4]) and Na ([5]). For this the 2001 Nobel price in physics was awarded to E. A. Cornell, W. Ketterle and C. E. Wiemann. This shows the great importance that is attached to this experimental achievement both for fundamental research and for possible later application.

In systems of atomic gases the typical critical temperature for the onset of

Bose-Einstein condensation is in the order of nanokelvin, where the macroscopic population of the quantum-mechanical single-particle ground state is often referred to as a quantum phase transition into a 'new state of matter'. This is characterized by the DeBroglie wavelength of the cold bosons reaching the mean particle separation. In effect, the bosons lose their individual identity and the whole assembly starts behaving like — and can be described by — a single macroscopic wavefunction. In the case of weakly interacting condensates a mean field approach leads to the so-called Gross-Pitaevskii equation (GPE), which governs the time evolution of the macroscopic wave function. In this appoach particle correlations, depletion and finite temperature effects are not correctly accounted for.

1.2 Solitons

The Gross-Pitaevskii equation is a nonlinear differential equation with the nonlinear term being due to the particle interactions. It turns out that this equation supports so-called *soliton solutions*. Solitons are wave packets that have the essential property of stability with respect to the spreading out: Without the nonlinearity, *dispersion* would lead to broadening of the pulse width due to the different spectral components propagating with different velocities. However, it is possible that the effects of the nonlinearity and the dispersion cancel each other out — making possible solitonic solutions with *effectively* vanishing dispersion.

The soliton phenomenon itself has been known for many years, having been accidentally discovered by J. S. Russell in the 19th century in a shallow channel as water-wave soliton. Since then solitonic solutions have been found in many other nonlinear physical systems. As an example, solitons in optical fibers have recently been of great interest to the optical communication industry, as the pulses — interpreted as bits — essentially propagate without dispersion. This industry has produced the first real-world applications of the soliton phenomenon.

Depending on the signs of the nonlinearity and the dispersion term, one has to distinguish *bright* and *dark* solitons. The former are wave packets with intensity maxima and the latter consist of a localized intensity reduction in a non-vanishing background. So far only the creation of dark solitons in BECs of atomic gases has been successful. However, attempts are also being made for bright solitons: As an example, the group of Markus Oberthaler in Konstanz is working on an experiment for the creation of a special type of bright solitons (so-called bright "gap solitons", cp. sect. 3.2.2).

1.3 Thesis outline

The GROSS-PITAEVSKII equation is well suited, among other applications, for the analysis of soliton stability. However, the effects of finite temperature and finite particle number, or particle correlations are not correctly described in such a mean field approach. In this thesis aspects of the 'quantum structure' of BEC-solitons are investigated with quantum-field theoretical models beyond the usual mean field approach being discussed.

Chapter 2 introduces the reader to the general theoretical background of BOSE-EINSTEIN condensation. Starting with ideal BOSE gases, the framework of second quantization is employed for adequately describing interacting gases. Introducing the so-called zero-range pseudo potential as simplifying model potential for ultra-cold, weakly interacting gases, a mean-field approach leads to the GROSS-PITAEVSKII equation. Subsequently, a n-particle SCHRÖDINGER equation is derived as an alternative, non-mean field approach. The latter will be the starting point for the discussions in chapter chapter 4.

In chapter 3 the soliton phenomenon is introduced on the basis of optical solitons. Moreover, the solitonic solutions of the GPE are discussed.

In chapter 4 the n-particle SCHRÖDINGER equation with the zero-range pseudo potential as interaction potential is focused on for the 1D case. Both an approximate HARTREE approach and the exact, so-called BETHE ansatz are presented, both of which are shown to provide bright soliton solutions. Subsequently, the relevance of a so-called quantum-diffusion effect, which is revealed by the latter approach, is discussed for typical experimental situations. Finally, some aspects of the coherence properties of BETHE solitons are considered showing that the interactions induce particle correlations.

In chapter 5 the zero-range pseudo model potential is substituted by a more realistic potential. Restricting to binary interactions, an approximate ansatz for solving the corresponding n-particle SCHRÖDINGER equation is presented. The emerging mathematical structure is investigated and its applicability for concrete calculations is discussed. In this context a computeralgebraic approach developed for handling the commutator algebra of this model is presented.

Finally, in chapter 6 we present the conclusions from this thesis.

The work presented in this diploma thesis has been done at the *Fachbereich für Physik*, *Universität Konstanz*, in the theoretical quantum optics group of Prof. Dr. JÜRGEN AUDRETSCH under the supervision of Dr. habil. PETER MARZLIN.

Chapter 2

Bose-Einstein Condensation

In this chapter an introduction into the theoretical framework for describing Bose-Einstein condensation will be given.
First some concepts of Bose statistics will be presented on the basis of the ideal Bose gas (sec. 2.1) before concentrating on interacting Bose gases in sec. 2.2. The framework of second quantization will be introduced as a suitable formalism for handling interacting many-particle systems (sec. 2.2.1). Subsequently, in sec. 2.2.2 an adequate model potential for describing interactions in systems of ultracold dilute atomic gases will be derived. Having obtained a corresponding Hamiltonian, the system's time-dependence then can be described both in the Heisenberg picture (sec. 2.2.3), where a mean field approach provides the fundamental Gross-Pitaevskii equation for describing condensates in the limit $T \to 0$, and in the Schrödinger picture (sec. 2.2.4), where a Schrödinger equation for the n-particle wave function can be derived. Both equations support solitonic solutions, which will be investigated in the following chapters.

2.1 The ideal Bose gas

In the grand canonical ensemble the Bose-Einstein distribution function, which gives the mean occupation number of the ν-th single particle eigenstate (energy ϵ_ν), is:[1]

$$\langle n_\nu \rangle = \frac{1}{e^{\beta(\epsilon_\nu - \mu)} - 1} = \frac{1}{z^{-1} e^{\beta \epsilon_\nu} - 1}, \tag{2.1}$$

where $\beta = 1/k_B T$, k_B is Boltzmann's constant, $\mu = \mu(T)$ denotes the chemical potential and $z = e^{\beta\mu}$ is called *fugacity*. In order to avoid negative values of $\langle n_\nu \rangle$ or divergence for $T \to 0$, the chemical potential is limited to values smaller than the ground state energy ($-\infty < \mu < \epsilon_0$).

[1] The ideal Bose gas and corresponding calculations are extensively treated in all standard statistical physics-textbooks, cf. eg. [6], [7].

The total number N of particles in the system then is given by $\sum_\nu \langle n_\nu \rangle$; anticipating the special role of the ground state, N is split into two parts:

$$N = N_0 + N_{\epsilon>\epsilon_0} = \frac{1}{z^{-1}e^{\beta\epsilon_0} - 1} + \sum_{\nu\neq 0} \frac{1}{z^{-1}e^{\beta\epsilon_\nu} - 1} \tag{2.2}$$

In the thermodynamic limit ($N\to\infty$, $V\to\infty$, $\rho = \frac{N}{V} = const$) the discrete sum in (2.2) can be substituted by an integral:

$$N = N_0 + N_{\epsilon>\epsilon_0} = \frac{z}{1-z} + \int_{\epsilon_0=0}^{\infty} d\epsilon\, f(\epsilon) \frac{1}{z^{-1}e^{\beta\epsilon} - 1}, \tag{2.3}$$

where it has been set $\epsilon_0 = 0$, and $f(\epsilon)$ is the density of states, which is

$$f(\epsilon) = \frac{V(2m)^{3/2}}{4\pi^2\hbar^3}\sqrt{\epsilon} \tag{2.4}$$

for a three-dimensional system of free spin-0 particles with $\epsilon = \hbar^2k^2/(2m)$ as dispersion relation.

For high temperatures ($z \ll 1$ as $\mu \ll 0$; classical limit) the population of the ground state $\frac{N_0}{N}$ is vanishingly small, whereas for $T\to 0$ ($\mu\to\epsilon_0{=}0$, $z\to 1$) the expression for N_0 diverges, which already is a hint for Bose-Einstein condensation.

A closer analysis of the expression for $N_{\epsilon>\epsilon_0}$ finally reveals the essenence of this effect: Bose-Einstein condensation is actually the phenomenon of *saturation* of the population of the excited states! Mathematically this can be seen by rewriting (2.3) with $f(\epsilon)$ given by (2.4) in terms of the particle density $\rho_{(0)} = N_{(0)}/V$:[1]

$$\rho = \rho_0 + \rho_{\epsilon>\epsilon_0} = \rho_0 + \frac{g_{3/2}(z)}{\lambda_{dB}^3}, \tag{2.5}$$

where $\lambda_{\mathrm{dB}} = h/\sqrt{2\pi m k_B T}$ is the so called thermal De'Broglie wavelength and $g_{3/2}(z) = \sum_{n=1}^{\infty} z^n/n^{3/2}$. For $z \to 1$ the latter function has the upper bound $g_{3/2}(1) = \zeta(\frac{3}{2}) \approx 2.612$, where $\zeta(z)$ denotes the Riemann zeta function. Thus this system indeed shows the abovementioned saturation of the excited states' population, and the process of Bose-Einstein condensation starts when $\rho = \max(\rho_{\epsilon>\epsilon_0})$, i.e. :

$$\rho\lambda_{\mathrm{dB}}^3 = \zeta(\frac{3}{2}) \tag{2.6}$$

As $\lambda_{\mathrm{dB}} = \lambda_{\mathrm{dB}}(T)$ this corresponds to a *critical temperature* T_C for the Bose-Einstein phase transition:

$$T_C = \frac{2\pi\hbar^2}{mk_B[\zeta(\frac{3}{2})]^{2/3}}\rho^{2/3} \tag{2.7}$$

The population of the ground state for $T \leq T_0$ follows from (2.5) using (2.7):

$$\frac{N_0}{N} = \left[1 - \left(\frac{T}{T_C}\right)^{3/2}\right] \tag{2.8}$$

(2.6) provides another illustration of the BOSE-EINSTEIN phase transition: It starts when the thermal DE'BROGLIE wavelength has the order of magnitude of the mean interparticle distance ($\propto \rho^{-1/3}$) — then the wave character of the particles comes into play forming a collective *"macroscopic wavefunction"* of the BOSE-EINSTEIN condensate fraction.

So far only the special case of a gas of *free* particles in three dimensions, for which $f(\epsilon)$ is given by (2.4), has been looked at; different physical situations are described by other expressions for the density of states. Some examples:

- *external potentials:* All experiments with dilute gases make use of external trapping potentials; one can show that this, of course, has influence on the concrete form of the expressions (2.4)-(2.8)[2], but that the existence of an BEC phase transition is not affected.

- *dimensionality:* It can be shown that both one- and two-dimensional systems of untrapped bosons do *not* undergoe a BEC phase transition for a finite temperature *in the thermodynamic limit* (formally $T_C = 0$ in this case).[3] An external trapping potential changes the whole situation: two-dimensional systems of trapped bosons show a finite transition temperature $T_C > 0$; however, in one-dimensional system of trapped bosons no BEC phase transition occurs for finite temperatures.[4]
  Nevertheless, so-called *quasi-1D* situations can experimentally be realized (see chap. 3.2.1), where a three-dimensional condensate can effectively be described in terms of a one-dimensional theoretical framework.

- *massless Bosons:* Given $\epsilon = \hbar ck$ as dispersion relation a critical temperature can be defined (cf. eg. [6], exercises 3.3.3, 3.3.7). Photons are a typical example here and indeed the *laser*-principle — "macroscopic population of single optical modes" — is related to BOSE-EINSTEIN condensation; however, there are major differences as "lasing" is a non-equilibrium process resulting from the fact that the photon number is not conserved; thus simply lowering the temperature of a photon gas will not lead to a "photonic BEC" (cf. [10] (chap. 1.1.3)).

It should be explicitly noted that the BOSE-EINSTEIN phase transition is a genuine quantum effect — unlike for the phase transitions solid/fluid/gas no particle interactions are needed. However, in all real atomic gases interactions exist

[2]For the typical case of an *harmonic* trapping potential explicit calculations are carried out in [8]; as an example: in (2.8) the exponent changes from $\frac{3}{2}$ to 3.

[3]For the two-dimensional case an explicit proof can be found in [6], exercise 3.3.4.

[4]Refer to [9] (II.D) for a more detailed discussion.

and it turns out that the simple ideal-gas model is not sufficient for a satisfying description of effects beyond those stated above. In the following section the influence of interactions on BOSE-EINSTEIN condensation will be discussed; actually, it will turn out that the nonlinearity leading to the existence of solitons directly results from particle interactions.

2.2 Interacting Bose gas

2.2.1 Second quantized Hamiltonian

In second quantized formulation[5] a system of interacting particles in an external potential V_{ext} is described by the following Hamiltonian:

$$\begin{aligned}\hat{H} &= \int d\mathbf{r}\ \hat{\Psi}^+(\mathbf{r})\left[-\frac{\hbar^2}{2m}\nabla^2 + V_{\text{ext}}(\mathbf{r})\right]\hat{\Psi}(\mathbf{r}) \\ &\quad + \frac{1}{2}\iint d\mathbf{r}d\mathbf{r}'\ \hat{\Psi}^+(\mathbf{r})\hat{\Psi}^+(\mathbf{r}')V(\mathbf{r}-\mathbf{r}')\hat{\Psi}(\mathbf{r}')\hat{\Psi}(\mathbf{r}) \qquad (2.9)\end{aligned}$$

$\hat{\Psi}(\mathbf{r})$ resp. $\hat{\Psi}^+(\mathbf{r})$ are *field operators* annihilating resp. creating a particle at position $\mathbf{r}$, and $V(\mathbf{r},\mathbf{r}') = V(\mathbf{r}-\mathbf{r}')$ is the two-body interatomic potential. Taking into account only a two-body interatomic potential is a very good approximation for systems of atomic gases, as higher-order interactions (eg. interaction with induced multipoles) are completely negligible for such systems.

The bosonic character of the system is implemented by subjecting the field operators to the following *bosonic commutation relations*:

$$\left[\hat{\Psi}(\mathbf{r}), \hat{\Psi}^+(\mathbf{r}')\right] = \delta(\mathbf{r}-\mathbf{r}') \qquad (2.10a)$$

$$\left[\hat{\Psi}(\mathbf{r}), \hat{\Psi}(\mathbf{r}')\right] = 0 = \left[\hat{\Psi}^+(\mathbf{r}), \hat{\Psi}^+(\mathbf{r}')\right] \qquad (2.10b)$$

In the framework of second quantization these commutation relations are the algebraic counterpart of the symmetry properties of bosonic wavefunctions.

The field operator can be decomposed in the following way:

$$\hat{\Psi}(\mathbf{r}) = \sum_\alpha \phi_\alpha(\mathbf{r})\,\hat{a}_\alpha, \qquad \hat{\Psi}^+(\mathbf{r}) = \sum_\alpha \phi^*_\alpha(\mathbf{r})\,\hat{a}^+_\alpha \qquad (2.11)$$

where the $\{\phi_\alpha\}$ represent a complete set of orthonormal single-particle wave functions and $\hat{a}_\alpha$ resp. $\hat{a}^+_\alpha$ are the corresponding operators for annihilation resp. creation of a boson with the wave function ϕ_α ("a boson in the mode α"). These

[5] For an introduction into the formalism of second quantization the interested reader is referred to standard textbooks, eg. [11].

operators are defined in FOCK space as acting like:

$$\hat{a}_\alpha^+ \, |n_0, n_1, \ldots, n_\alpha, \ldots\rangle = \sqrt{n_\alpha + 1} \, |n_0, n_1, \ldots, n_\alpha + 1, \ldots\rangle \quad (2.12a)$$

$$\hat{a}_\alpha \, |n_0, n_1, \ldots, n_\alpha, \ldots\rangle = \sqrt{n_\alpha} \, |n_0, n_1, \ldots, n_\alpha - 1, \ldots\rangle \quad (2.12b)$$

Here $|n_0, n_1, \ldots, n_\alpha, \ldots\rangle$ is the system's state with n_0 particles occupying the mode 0, n_1 particles occupying the mode 1 etc.
Inserting (2.11) into (2.10) one obtains the bosonic commutions relations for $\hat{a}_\alpha$, $\hat{a}_\alpha^+$:

$$\left[\hat{a}_\alpha, \hat{a}_\beta^+\right] = \delta_{\alpha,\beta} \quad (2.13a)$$

$$\left[\hat{a}_\alpha, \hat{a}_\beta\right] = 0 = \left[\hat{a}_\alpha^+, \hat{a}_\beta^+\right] \quad (2.13b)$$

Employing the completeness relation for the states $\{\phi_\alpha\}$, i.e. $\sum_\alpha \phi_\alpha^*(\mathbf{r})\phi_\alpha(\mathbf{r}') = \delta(\mathbf{r} - \mathbf{r}')$, the creation/annihilation operators can be expressed in terms of the field operators, which will be needed later:

$$\hat{a}_\alpha = \int d\mathbf{r}' \, \phi_\alpha^*(\mathbf{r}')\hat{\Psi}(\mathbf{r}'), \qquad \hat{a}_\alpha^+ = \int d\mathbf{r}' \, \phi_\alpha(\mathbf{r}')\hat{\Psi}^+(\mathbf{r}'), \quad (2.14)$$

So far the model is quite general; in the following certain approximations for the case of $T \to 0$ will be introduced for the description of the condensate fraction.

2.2.2 The zero-range pseudo-potential as model potential

For alkali atoms the exact interaction potential $V(\mathbf{r} - \mathbf{r}') =: V(\mathbf{r}_{\text{rel}}) =: V(\mathbf{r})$ has a rather complicated structure ([8]): It has a repulsive hard core (eg. ^{133}Cs: for $r \lesssim 0.5$nm), a very deep minimum (^{133}Cs: $V_{\min} \approx -500\text{K} \cdot k_B$ at $r_{\min} \approx 0.6$nm) and consequently many bound states[6]; the long range attractive part is of VAN DER WAALS-nature scaling as $1/r^6$ for large r.

For ultracold condensates ($T \to 0$) there is no need to model the the interaction by the exact potential: as will be justified in the following, a much simpler model potential is sufficient in this limit.[7]

Some elementary results of scattering theory

Neglecting for simplicity an external potential[8] the relative motion of two such atoms is described by the Hamiltonian

$$H_{\text{rel}} = -\frac{\hbar^2}{2\mu} \frac{\partial^2}{\partial \mathbf{r}_{\text{rel}}^2} + V(\mathbf{r}_{\text{rel}}) \quad (2.15)$$

[6] Numerical studies of the ground state are presented in appendix C.

[7] For a more detailed discussion the interested reader is referred to eg. [8].

[8] As typical scales over which external potentials considerably change are orders of magnitude larger than the scales of interaction potentials, this is indeed a very good approximation for the relative motion (compare the discussion in the context of (C.5) in appendix C).

with $\mathbf{r}-\mathbf{r}' =: \mathbf{r}_{\text{rel}}$ (this will be simply denoted as "$\mathbf{r}$" in the following) and $\mu = \frac{m}{2}$ as reduced mass.

In the context of BEC scattering states of this Hamiltonian have to be considered.[9] As known from standard quantum mechanics, for finite potentials[10] ($V(r > b) = 0$) the *asymptotic* scattering solution of the SCHRÖDINGER equation $H_{\text{rel}}\psi = E\psi$ can be written as

$$\psi(\mathbf{r}) = \psi_0(\mathbf{r}) + \frac{e^{ikr}}{r} f_{\mathbf{k}}(\mathbf{n}), \tag{2.16}$$

where ψ_0 denotes the incoming wave and $f_{\mathbf{k}} = f_{\mathbf{k}}(\mathbf{n}) \in \mathbb{C}$ is the so-called *scattering amplitude*, which depends on $\mathbf{n} = \mathbf{r}/r$.
In the asymptotic region, which is given by $r \gg b, kb^2$ ([8]), the scattering potential V enters the wave function solely in terms of $f_{\mathbf{k}}(\mathbf{n})$. For atomic gases (mean distance between the particles: $\sim \rho^{-1/3}$) this means, that in the dilute regime $\rho^{-1/3} \gg b, kb^2$ binary particle interactions are sufficiently accounted for by the scattering amplitude, as the atoms rarely come close enough to each other to see more than an "average effect" of the potential.
Moreover, for $k \to 0$, i.e. $T \to 0$, the situation becomes even simpler as the scattering amplitude in this limit is no longer dependent on $\mathbf{n}$ ([8]) — one speaks of pure *s-wave scattering*:

$$f_{\mathbf{k}}(\mathbf{n}) \xrightarrow{\mathbf{k}\to 0}: -a \tag{2.17}$$

a is the so-called *s-wave scattering length* and represents the only parameter needed to describe the atomic interactions in the dilute, ultra-low temperature limit. The value of a is accessible by experimental measurements and can be positive (effective repulsive interactions in the s-wave limit) or negative (effective attractive interactions) depending on the atomic species.[11]

The zero range pseudo potential

Consequently, in the ultra-low temperature limit a simpler model potential having the same scattering length can be substituted for the exact potential; the so-called *zero range pseudo potential*

$$V(\mathbf{r}-\mathbf{r}') = g\,\delta(\mathbf{r}-\mathbf{r}') \tag{2.18}$$

[9] Bound states would correspond to molecular states of two atoms, which are typically untrapped due to spin-antispin pairing to total spin 0.

[10] Interaction potentials between atoms are typically not of finite range due to VAN-DER-WAALS interactions scaling as $\sim r^{-6}$; however, it can be shown ([8] sect. 3.1.3) that all central results from scattering theory, esp. the existence of the limit (2.17), are valid also in this case.

[11] It is worth noting that for $a < 0$ (eg. ^7Li) only *trapped* condensates *not exceeding* a certain maximal number of particles (depending on the strength of the confinement) are stable as the attractive forces tend to increase the condensate's density, which can lead to a collapse into the solid phase for large particle numbers (cf. eg. [9]).

with the *coupling constant*

$$g = \frac{4\pi\hbar^2}{m}a. \tag{2.19}$$

fulfills this requirement[12].

Inserting the model potential (2.18) into (2.9) results in the following expression for the second quantized Hamiltonian:

$$\begin{aligned}\hat{H} &= \int d\mathbf{r}\ \ \hat{\Psi}^+(\mathbf{r})\left[-\frac{\hbar^2}{2m}\nabla^2 + V_{\text{ext}}(\mathbf{r})\right]\hat{\Psi}(\mathbf{r}) \\ &\quad + \frac{g}{2}\int d\mathbf{r}\ \ \hat{\Psi}^+(\mathbf{r})\hat{\Psi}^+(\mathbf{r})\hat{\Psi}(\mathbf{r})\hat{\Psi}(\mathbf{r})\end{aligned} \tag{2.20}$$

In the following this Hamiltonian will play a central role: not only will it serve as a starting point for a mean field description of condensates leading to the so-called GROSS-PITAEVSKII equation (sec. 2.2.3), which is a nonlinear SCHRÖDINGER equation showing solitonic solutions (see sec. 3.2), but also the *exact* solution of the corresponding n-particle SCHRÖDINGER equation (sec. 2.2.4) will be presented for the 1D case in chap. 4; this solution will be shown to be of soliton form in the asymptotic regime of large particle numbers.

2.2.3 Heisenberg picture: The Gross-Pitaevskii equation — mean field description of the condensate

In the HEISENBERG picture the time-dependence of the field operator is given by the HEISENBERG equation of motion:

$$\begin{aligned}i\hbar\,\partial_t\hat{\Psi}_H(\mathbf{r},t) &= \left[\hat{\Psi}_H(\mathbf{r},t), \hat{H}_{\text{H}}\right] \\ &= \left[-\frac{\hbar^2}{2m}\nabla^2 + V_{\text{ext}}(\mathbf{r},t) + g\hat{\Psi}_H^+(\mathbf{r},t)\hat{\Psi}_H(\mathbf{r},t)\right]\hat{\Psi}_H(\mathbf{r},t),\end{aligned} \tag{2.21}$$

where $\hat{H}_{\text{H}}$ denotes the second quantized Hamiltonian (2.20) in the HEISENBERG picture[13]. (2.21) has the form of a *nonlinear* SCHRÖDINGER *equation* (NLSE) for the field operator and thus is sometimes referred to as *"Quantum-NLSE"*.

[12] To be exact, (2.18) is the correct expression only in the 1D case; actually, in 3D an additional regularizing operator removes $1/r$-divergences of the wavefunction, which can occur for 3D ([8]): $V\psi = g\,\delta(\mathbf{r}-\mathbf{r}')\,[\partial_r(r\,\psi)]$

[13] $\hat{H}_{\text{H}}$ arises from (2.20), which is the Hamiltonian $\hat{H}_{\text{S}}$ in the SCHRÖDINGER picture, by simply substituting $\hat{\Psi}_{\text{S}}^{(+)} := \hat{\Psi}^{(+)}(\mathbf{r}) \to \hat{\Psi}^{(+)}(\mathbf{r},t) =: \hat{\Psi}_{\text{H}}^{(+)}$. (2.21) is derived using the commutation relations (2.10), which are also valid as equal-time commutation relations for the HEISENBERG field operators $\hat{\Psi}_{\text{H}}^{(+)}$.

Mean field theory: The Gross-Pitaevskii equation

From the quantum field theoretic point of view the many body Hamiltonians (2.9) and (2.20) fully describe the behaviour of the particles in the system. However, it turns out that in the case of BOSE-EINSTEIN condensation in dilute, ultra-cold ($T \approx 0$) atomic gases a mean field approach yields a satisfying description of many properties of the condensate fraction. Of course, effects like depletion of the condensate by higher order interactions with other condensate or thermal atoms are not accounted for in such a description.

In the following the so-called BOGOLIUBOV approach will be presented for deriving the GROSS-PITAEVSKII equation. There are other ways of introducing a mean field description, one of which is a variational ansatz (cf. [8], [9]; see also chap. 4.1).
The idea is to explicitly separate out the condensate contribution to the field operator: following (2.11), the latter can generally be written as

$$\hat{\Psi}(\mathbf{r},t) = \phi_0(\mathbf{r},t)\,\hat{a}_0 + \delta\hat{\Psi}(\mathbf{r},t) \tag{2.22}$$

with the operator $\delta\hat{\Psi}(\mathbf{r},t)$ describing the excited states. For ultracold condensates ($T \to 0$) in dilute atomic gases the occupation of the ground state N_0/N comes close to unity, whereas the thermal fraction — represented by $\delta\hat{\Psi}$ in (2.22) — is very small: $N'/N = 1 - N_0/N$. Under these circumstances the following approximative assumptions are valid:

- For large N_0 there is no significant physical difference between states with N_0 and $N_0 + 1$ particles; according to (2.12a) the action of $\hat{a}_0$ and $\hat{a}_0^+$ on FOCK-states can then approximately be replaced by the c-number $\sqrt{N_0}$ ($\approx \sqrt{N_0 + 1}$).
- $\delta\hat{\Psi}(\mathbf{r},t)$ representing the comparatively small fraction of non-condensed particles can be treated as a *small perturbation*.

Thus the field operator can be written as a sum of its expectation value $\langle\hat{\Psi}\rangle = \sqrt{N_0}\,\phi_0(\mathbf{r},t)$ — the c-valued ("macroscopic") *condensate wave function* ϕ_0 being normalized to $\int d\mathbf{r}\ |\phi_0(\mathbf{r},t)|^2 = 1$ — and a small operator-valued thermal perturbation:

$$\hat{\Psi}(\mathbf{r},t) = \sqrt{N_0}\,\phi_0(\mathbf{r},t) + \delta\hat{\Psi}(\mathbf{r},t) \tag{2.23}$$

Finally, substituting (2.23) into the Quantum-NLSE (2.21) and neglecting all terms containing excitations $\delta\hat{\Psi}$ leads to the GROSS-PITAEVSKII *equation (GPE)* for the condensate wave function:

$$\boxed{i\hbar\,\partial_t\phi_0(\mathbf{r},t) = \left[-\frac{\hbar^2}{2m}\nabla^2 + V_{\text{ext}}(\mathbf{r},t) + gN_0|\phi_0(\mathbf{r},t)|^2\right]\phi_0(\mathbf{r},t)} \tag{2.24}$$

Whereas the BOGOLIUBOV approximation is generally quite good for ultracold ($T \ll T_C$) atomic gases with $N_0 \gg N' = N - N_0$, i.e. in the case of small

quantum depletion, there are cases where this approximation is not valid: A typical example is suprafluid ^4He, where strong particle interactions lead to a dominating quantum depletion ($(N - N_0)/N \approx 90\%$).
However, even for atomic gases with $T = 0$ there is *on principle* a non-vanishing quantum depletion due to particle interactions. This can be described by taking into account higher order terms $\delta\hat{\Psi}$ when substituting (2.23) into (2.21), which leads to the so-called BOGOLIUBOV-DE GENNES *equations* describing small excitations of the condensate ([12], [9]).

2.2.4 Schrödinger picture: n-particle Schrödinger equation with δ-interactions

In the SCHRÖDINGER picture the system's dynamical time-dependence is explicitly carried by the *states* $|\psi\rangle = |\psi\rangle_{\mathrm{S}}(t)$ with the equation of motion given by the SCHRÖDINGER equation

$$i\hbar\,\partial_t\,|\psi\rangle = \hat{H}_{\mathrm{S}}\,|\psi\rangle, \tag{2.25}$$

where $\hat{H}_{\mathrm{S}}$ is the SCHRÖDINGER-Hamiltonian given by (2.20).

The system's state $|\psi\rangle$ can be expanded in FOCK space:

$$|\psi\rangle = \sum_{n=0}^{\infty} a_n |n\rangle \tag{2.26}$$

with the expansion coeffients satisfying the normalization condition

$$\sum_{n=0}^{\infty} |a_n|^2 = 1. \tag{2.27}$$

$|n\rangle$ in (2.26) denotes a general n-particle state:

$$\begin{aligned}
|n\rangle = \sum_{\substack{\{n_i\} \\ \sum_{i=0}^{\infty} n_i \overset{!}{=} n}} c_{n_0,\ldots,n_i,\ldots} \quad & \underbrace{|n_0,\ldots,n_i,\ldots\rangle}_{= \left[\prod_{j=0}^{\infty} \frac{(\hat{a}_j^+)^{n_j}}{\sqrt{n_j!}}\right] |0\rangle} \\
\overset{(2.14)}{=} \int_{-\infty}^{\infty}\cdots\int_{-\infty}^{\infty} d\mathbf{r}_1\cdots d\mathbf{r}_n \quad & \\
\underbrace{\sum_{\substack{\{n_i\} \\ \sum_{i=0}^{\infty} n_i \overset{!}{=} n}} \frac{c_{n_0,\ldots,n_i,\ldots}}{\prod_j \sqrt{n_j!}} \mathcal{S}_n \left[\phi^{(1)}(\mathbf{r}_{\mathcal{P}(1)},t)\cdots\phi^{(n)}(\mathbf{r}_{\mathcal{P}(n)},t)\right]}_{=: \frac{1}{\sqrt{n!}} f_n(\mathbf{r}_1,\ldots,\mathbf{r}_n,t)} & \hat{\Psi}^+(\mathbf{r}_1)\cdots\hat{\Psi}^+(\mathbf{r}_n)\,|0\rangle
\end{aligned} \tag{2.28}$$

As introduced on p. 8, $|n_0, \dots, n_i, \dots\rangle$ is the FOCK-state with n_0 $[\dots n_i, \dots]$ particles populating the 0th- $[\dots i\text{-th}, \dots]$ mode described by the one-particle wave function ϕ_0 $[\dots \phi_i, \dots]$. The *symmetrization operator* $\mathcal{S}_n = \frac{1}{n!}\sum_{\{\mathcal{P}\}}$ (summation over all possible permutations $\mathcal{P}$ of $[1, \dots, n]$ with $\mathcal{P}(k)$ denoting the k-th component of the permutation) had to be introduced, as $|n_0, \dots, n_i, \dots\rangle$ is describing bosons; $\phi^{(j)}$ denotes the wave function of the j-th particle.[14]
Summarizing, this leads to the following representation of $|\psi\rangle$:

$$|\psi\rangle = \sum_n a_n \int \cdots \int d\mathbf{r}_1 \cdots d\mathbf{r}_n \, \frac{1}{\sqrt{n!}} f_n(\mathbf{r}_1, \dots, \mathbf{r}_n, t) \hat{\Psi}^+(\mathbf{r}_1) \cdots \hat{\Psi}^+(\mathbf{r}_n) \, |0\rangle, \quad (2.29)$$

where the n-particle mode function f_n is required to be normalized:

$$\int \cdots \int d\mathbf{r}_1 \cdots d\mathbf{r}_n \, |f_n(\mathbf{r}_1, \dots, \mathbf{r}_n, t)|^2 = 1 \quad (2.30)$$

Substituting (2.29) and the Hamiltonian (2.20) into the $|\psi\rangle$-SCHRÖDINGER equation (2.25) yields uncoupled f_n-SCHRÖDINGER equations for each particle number n:[15]

$$\begin{aligned} & i\hbar \, \partial_t f_n(\mathbf{r}_1, \dots, \mathbf{r}_n, t) \\ & = \left[\sum_{i=1}^{n} \left(-\frac{\hbar^2}{2m} \nabla^2_{\mathbf{r}_i} + V_{\text{ext}}(\mathbf{r}_i) \right) + g \sum_{1 \le i < j \le n} \delta(\mathbf{r}_j - \mathbf{r}_i) \right] f_n(\mathbf{r}_1, \dots, \mathbf{r}_n, t) \end{aligned} \quad (2.31)$$

This result could have been expected even without explicit calculations: As the Hamiltonian (2.20) resulted from taking the zero range pseudo potential (2.18) as model potential for atomic interactions, (2.31) is just the SCHRÖDINGER equation for a system of n bosons with exactly this particle interaction potential.

As usual, one is lead to the corresponding time-independent SCHRÖDINGER equation by factoring out the time-dependence by

$$f_n(\mathbf{r}_1, \dots, \mathbf{r}_n, t) = e^{-\frac{i}{\hbar} E_n t} f_n(\mathbf{r}_1, \dots, \mathbf{r}_n). \quad (2.32)$$

[14] Of course, *numbering* of the (identical!) particles is solely introduced for reasons of notation; with this in mind, the expression $\phi^{(1)} \cdots \phi^{(n)}$ in (2.28) has to be read as $\phi^{(1)} \cdots \phi^{(n)} \equiv (\phi_0)^{n_0} \cdots (\phi_i)^{n_i} \cdots$, which is a product of n functions due to $\sum_i n_i = n$.

[15] The explicit calculation that leads to (2.31) is rather lenghty, but straightforward: Besides employing partial integration for the integral comprising the kinetic term, essentially only the commutation relations (2.10) of the field operator have to be applied repeatedly.

Mind the factor "2" in the interaction term (compared to the corresponding term in the Hamiltonian (2.20)): It effectively originates from rewriting $\sum_{1 \le i,j \le n; i \ne j}(\dots) \to 2\sum_{1 \le i < j \le n}(\dots)$ when summing over a symmetric argument.

$f_n(\mathbf{r}_1, \ldots, \mathbf{r}_n)$ then obeys:

$$\left[\sum_{i=1}^{n}\left(-\frac{\hbar^2}{2m}\nabla^2_{\mathbf{r}_i} + V_{\text{ext}}(\mathbf{r}_i)\right) + g\sum_{1\leq i<j\leq n}\delta(\mathbf{r}_j - \mathbf{r}_i)\right] f_n(\mathbf{r}_1, \ldots, \mathbf{r}_n)$$
$$= E_n\, f_n(\mathbf{r}_1, \ldots, \mathbf{r}_n) \quad (2.33)$$

Recapitulating, one notes that — in contrast to the HEISENBERG picture — the SCHRÖDINGER picture has the advantage of resulting in *linear* equations for $|\psi\rangle$ and the n-particle wave function f_n: (2.25); (2.31) resp. (2.33). However, this, of course, is obtained at the expense of the inevitability to explicitly handle the many degrees of freedom of the wave function $f_n(\mathbf{r}_1, \ldots, \mathbf{r}_n)$.
Both approaches lead to soliton solutions and have their own relevance:

- Solutions to the GPE (2.24) will be discussed in chapter 3; even for the Quantum-NLSE (2.21) a method called *quantum inverse scattering method* ([13])[16] has been developed.
- For the special case of vanishing external potential V_{ext} the *one-dimensional* pendant to the n-particle SCHRÖDINGER equation (2.33) can be solved exactly by the so-called BETHE's ansatz method. This method and an approximative HARTREE-approach will be discussed in chapter 4.

[16] More references concerning this method can be found in [32] (references 12, 15-18 ib); also refer to appendix A of this thesis for a short introduction into the idea of the "classical" inverse scattering method.

Chapter 3

Solitons

The investigation of excitations of the BEC ground state is central to the theoretical understanding of Bose-Einstein condensation. Naturally, basic excitation forms are waves and wave packets. Special wave packet solutions of the Gross-Pitaevskii equation are so-called *solitons* (lat. "solus": alone, solitary; also: *solitary waves*), which first of all have — in addition to some other characteristics — the essential property of stability with respect to the spreading out. As known from mathematical physics, necessarily — but not sufficiently — only *nonlinear* differential equations can have such solutions.
Solitons also appear in many other fields in which nonlinearities play a role such as: in shallow channels of water, where solitons have been observed for the first time by J. Scott Russell in 1834; as so-called *Tsunami*-waves in the oceans; in biology (e.g. in the contex of stimulus propagation in nerves); in particle physics and in nonlinear fiber optics. The essential and well-investigated propagation equation of the latter has the same form as the Gross-Pitaevskii equation, so that it is possible to adopt many of the common known results to solitons in Bose-Einstein condensates.

In order to obtain basic understanding of soliton-phenomena it is instructive to first discuss fundamental properties of solitons by means of the mentioned optical analogue in nonlinear fiber optics (sec. 3.1) — without going into specific optical details of course — before transferring these results to the field of Bose-Einstein condensation, where solitons of the Gross-Pitaevskii equation will be discussed (sec. 3.2).

3.1 Optical solitons

Monochromatic plane waves are usually described by the real (or imaginary) part of a complex wave:[1]

$$E(z,t) = \Re(Ae^{i(kz-\omega t)}), \tag{3.1}$$

where A is the (complex-valued) amplitude of the field.

In vacuum the *dispersion relation* between the wave number k and the frequency ω is linear ($\omega = c_0 k$), i.e. *all* frequency components of a wave packet move with vacuum speed of light c_0 as *phase velocity* ("dispersion-free").

3.1.1 Group-Velocity Dispersion

In media the phase-velocity c_{med} is frequency dependent in general: $c_{\text{med}}(\omega) = c_0/n(\omega)$, where $n = n(\omega)$ denotes the refractive index. Consequently, different frequency components of a wave packet move with different phase velocities — the packet "dissolves" dispersively.

If the wave packet has a narrow frequency distribution around a central frequency ω_0, it can be properly described as a plane wave with position- and time-dependent amplitude (cf. for example [14] (chap. 4.3.4)):

$$E(z,t) = \Re(A(z,t)e^{i(k_0 z-\omega_0 t)}) \tag{3.2}$$

The series expansion of the wave number $k(\omega) = n(\omega)\ \omega/c_0$ about this frequency is:

$$k(\omega) = k_0 + k'(\omega-\omega_0) + \frac{1}{2}k''(\omega-\omega_0)^2 + \mathcal{O}(\omega^3) \tag{3.3}$$

Here $k' = dk/d\omega := 1/v_g$ is connected to the *group velocity* v_g, with which the envelope function $A(z,t)$ moves. $k'' = d^2k/d\omega^2$ is a measure for the so-called *"group velocity dispersion"*: Spreading out of a wave packet is caused by $k'' \neq 0$ to the first order. The differential equation describing this is (cf. [15] (chap. 3.2), [16]):

$$i\frac{\partial A(z,t)}{\partial z} = \frac{1}{2}k''\frac{\partial^2 A(z,t)}{\partial t^2} \tag{3.4}$$

$k'' \neq 0$ expresses a frequency dependence of the phase velocity, so that a position dependence of the momentary frequency (*"frequency chirp"*) emerges along the packet during propagation: For $k'' > 0$ (< 0) one can find low (high) frequencies (relative to the the center frequency ω_0) around the front of the wave packet and high (low) frequencies in the back (cp. fig. 1 (left part)). It can be shown ([15] (chap. 3.2.1)) that in the case of a Gaussian wave group the phase has a parabolic time dependence und thus the frequency chirp $\delta\omega \propto \frac{\partial\phi}{\partial t}$ is linear.

[1] For reasons of simplicity only the scalar electric field E in the one-dimensional case is focused on here.

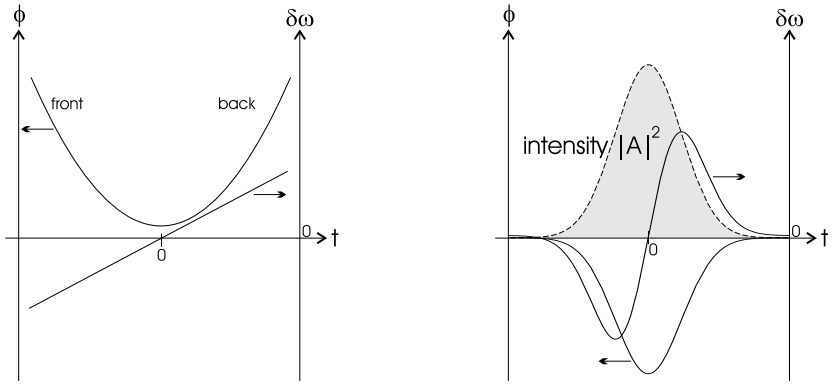

Figure 3.1: Group-velocity dispersion (depicted for $k'' > 0$) (left) and self-phase modulation (right) (see also [17]).

3.1.2 Self-Phase Modulation

For high intensities so-called *nonlinear media* show — in addition to the frequency dependence — an intensity dependence of the refractive index ("positive ($n_2 > 0$) KERR-effekt"):

$$n(\omega, I) = n_0(\omega) + n_2|E|^2 = n_0 + n_2 I \tag{3.5}$$

Under certain circumstances[2] the effect of group-velocity dispersion — caused by the frequency dependence of n_0 — can be neglected compared to the so-called "self-phase modulation", which arises from the second term in (3.5); the resulting propagation equation then is (parameter $\gamma \propto n_2$):

$$i\frac{\partial A(z,t)}{\partial z} = -\gamma|A(z,t)|^2 A(z,t) \tag{3.6}$$

Obviously, this equation has the solution $A(z,t) = A(0,t)\ \exp(-i\phi_{\mathrm{NL}}(z,t))$ with the nonlinear phase-shift $\phi_{\mathrm{NL}}(z,t) = -\gamma\ z\ |A(0,t)|^2$ ($\propto |A(0,t)|^2$ (intensity) — hence "*self*-phase modulation"). As $\delta\omega \propto \frac{\partial\phi}{\partial t} \propto \frac{\partial}{\partial t}(|A(0,t)|^2)\ z$, there is also in this case a frequency chirp, that increases during propagation ($\delta\omega \propto z$) and causes a broadening of the spectrum of the pulse. In the right part of fig. 3.1 ϕ_{NL} and $\delta\omega$ are schematically shown for a Gaussian pulse.

3.1.3 Solitons — Bright and Dark types

The propagation equation for the envelope-function $A(z,t)$ that arises when both group-velocity dispersion and self-phase modulation are relevant, is (cp. eq. (3.4), (3.6)):

$$i\frac{\partial A(z,t)}{\partial z} = \frac{1}{2}k''\frac{\partial^2 A(z,t)}{\partial t^2} - \gamma|A(z,t)|^2 A(z,t) \tag{3.7}$$

[2]for optical pulses with high intensity, but relatively long pulse duration (cf. [15] (chap. 4.1)).

As presented in the following, the interplay of the signs of k'' and γ, i.e. $\mathrm{sign}(k''\gamma)$, determines the character of the solutions of this equation. One is lead to the standard form of eq. (3.7) by the substitution $\zeta = \mathrm{sign}(k''\gamma)\, k''/2\ z$ and the abbreviation $\kappa = \mathrm{sign}(k''\gamma)\ 2\gamma/k'' = 2\,|\gamma/k''|\ (> 0)$:

$$\boxed{i\frac{\partial A}{\partial \zeta} = \mathrm{sign}(k''\gamma)\ \frac{\partial^2 A}{\partial t^2} - \kappa |A|^2 A} \tag{3.8}$$

Except for the permutation of the roles of the position- and time-variables, this equation has the form of a *nonlinear* SCHRÖDINGER-*equation* (NLSE). In the following we are only interested in *soliton*-solutions of this equation, i.e. essentially wave packets that are not spreading out.

"Bright" solitons: $\mathrm{sign}(k''\gamma) = -1$

How can one illustrate the existence of such solutions? — For that so-called *"bright"* types of solitons, i.e. wave packets with intensity *maxima* in the center, should first be looked at in the following.

In the case of *positive* dispersion and positive KERR-effekt ($k'' > 0$, $\gamma > 0$, i.e. $\mathrm{sign}(k''\gamma > 0)$, as depicted in fig. 1) this soliton type shows fast widening, i.e. bright solitons are *not* stable in this case[3]. However, for $k'' < 0$ (this would correspond to a negative derivative of $\delta\omega$ in the left part of fig. 3.1) and $\gamma > 0$ there are pulse shapes for which the frequency chirps caused by dispersion and self-phase modulation compensate exactly[4]: For the above nonlinear equation special *sech*-shaped wave packets fulfill this. Under the boundary condition $A \xrightarrow{t\to\pm\infty} 0$ one finds as *soliton of first order*[5] (cp. for example [18]):

$$\boxed{A(\zeta,t) = \sqrt{\frac{8}{\kappa}}\ \eta\ \exp\big(-4i\,(\xi^2-\eta^2)\,\zeta - 2i\xi\,t + i\varphi\big)\ \mathrm{sech}\big(2\eta\,(t - t_0 + 4\xi\,\zeta)\big)} \tag{3.9}$$

Here η and ξ are parameters determining the soliton's width and velocity. Obviously, the width and intensity of the soliton are not independent of each other (prefactor $\propto \eta$) — a property resulting from the nonlinear character of (3.8). The other parameters characterizing the soliton are the offset-phase φ and -time t_0. Fig. 3.2 (left) schematically shows the propagation of such a bright soliton (for $\xi \neq 0$).

[3] In this case so-called "dark" solitons are stable (see p. 19).

[4] Even Gaussian pulses like in fig. 3.1 fulfill this approximately: Around the center of the pulse the frequency chirp caused by self-phase modulation is linear and thus can compensate the dispersion effect in this region for adequate k''-, γ-values (same values of the gradients around the center, but with opposite sign).

[5] There are also soliton solutions *of N-th order*, which in general consist of N single solitons characterized by $4N$ parameters η_i, ξ_i, φ_i, $t_{0,i}$ (for details: for example refer to [18]).

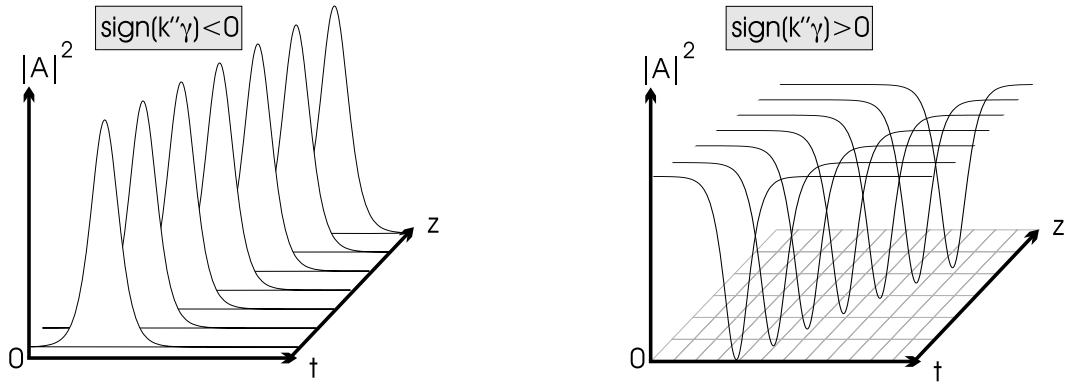

Figure 3.2: Bright (left part) and dark solitons (right part).

A standard method for finding solutions like (3.9) is the so-called *inverse scattering method*, that is also applicable to some other types of nonlinear differential equations; some details about this method will be given in appendix A.
However, the fact that the soliton solutions of the NLSE (3.8) are *sech*-shaped can be illustrated rather easily: The nonlinear term in (3.8) is proportional to $|A|^2$, which is why the solution $A = A(\zeta, t)$ creates its own potential so to say. Thus the soliton-solutions are those solutions, which are "steady" in the self-created potential — in this context one also refers to as "self-focusing". It can be shown that this is closely related to the topic of "reflection-free potentials" — standard quantum-mechanics textbooks ([19] (chap. 25 (ex. 4)); [20] (chap. 19.2)) demonstrate that exactly $sech^2$-shaped potentials have this property.

Besides the major characteristic feature of 'not spreading out', solitons show some other remarkable properties: Two solitons of different velocity which meet each other will survive this *"collision"* essentially[6] *unchanged* (cf. [21], [16]) — as the underlying propagation equation is nonlinear, this is not really to be expected intuitively. Moreover, the *stability* of solitons against deviations from the (mathematically) "ideal shape" is worth mentioning: Even if the initial pulse shape $A(0, t)$ slightly differs from the exact soliton solution of eq. (3.9), an exact soliton develops during propagation (cf. [15] (chap. 5.2.4)). The suffix "-on" in the name "soliton" is a reminiscence of this *"particle-like" behaviour*.

"Dark" solitons: $\mathrm{sign}(k''\gamma) = 1$

The case $\mathrm{sign}(k''\gamma) > 0$ remains to be treated.[7] Soliton solutions of (3.8) are found here requiring the boundary condition $A \xrightarrow{t\to\pm\infty} const \neq 0$. The "wave packet"

[6] After the collision one observes shifts in the positions and phases of the solitons compared to the values expected in case of collisionless propagation; for example, such collisions generally emerge for solitons of N-th order, which have been mentioned in footnote 5.

[7] In fiber-optics this case usually occurs in the combination $k'' > 0$, $\gamma > 0$, i.e. in regions of positive dispersion.

then consists of a localized intensity reduction in a non-vanishing background: so-called *"dark" solitons* (cp. fig. 3.2 (right part)). Solitons of this kind are described by two parameters determining the background-intensity and depth of the intensity minimum. If the minimum-intensity is zero, one speaks of "black" solitons, otherwise of "grey" ones.
The black soliton of the NLSE (3.8) is *tanh*-shaped, i.e. there is a change of sign of the amplitude at the minimum:

$$\boxed{A = \sqrt{\frac{1}{\kappa}}\ \exp(i\zeta)\ \tanh(t/\sqrt{2})} \tag{3.10}$$

There are corresponding analytical solutions for grey solitons; details can be found in [15] (chap. 5.2.5) and [22] for example.

Finally, the nontrivial phase-profile of dark solitons is worth mentioning: The phase is changing more or less abruptly by an amount which depends on the soliton's "darkness" — hence dark solitons always show a chirp; this principally discriminates dark solitons from bright ones, which, ideally, have a phase constant in time.

3.2 Solitons of the 1D Gross-Pitaevskii equation

For quasi-one-dimensional systems the Gross-Pitaevskii equation (2.24)— derived in section 2.2.3 within a mean field description as equation of motion for the macroscopic wavefunction — is a nonlinear PDE of the same type as the propagation equation (3.7) known from fiber optics, which will be shown in the following subsection 3.2.1. Consequently, for the *one-dimensional case* essentially all results can simply be adapted (section 3.2.2). However, systems of more than one dimension typically have to be studied numerically.

3.2.1 The 1D GPE: Derivation; Scaling to dimensionless units

An experimental possibility to realize a quasi-1D situation is to have an only two-dimensional confinement described by an external potential $V_{\text{ext}} = V_{\text{ext}}(y,z) = \frac{1}{2}m\omega_\perp^2(y^2+z^2)$. It can be shown ([23]), that in case of *strong confinement*[8] the solution of the 3D-GPE (2.24) separates like $\phi_0(x,y,z) = \psi_x(x)\,\psi_\perp(y,z)$ with $\psi_\perp(y,z)$ being the ground state of a 2D harmonic oscillator (characterized by $\omega_\perp$

[8]To be more exact: Provided that the energy $\hbar\omega_\perp/2$ of the ground state of the two-dimensional oscillator given by V_{ext} is large in comparison to the energy associated with the nonlinear term $gN_0/A_\perp\,|\psi_x|^2$ (mean-field energy) in the 1D-GPE (3.11), the time evolution of the wave functions ψ_x and $\psi_\perp$ shows to be essentially uncoupled.

or the oscillator length $a_\perp := \sqrt{\hbar/(m\omega_\perp)}$) and $\psi_x(x) =: \psi(x)$ underlying the 1D GROSS-PITAEVSKII equation

$$i\hbar\,\partial_t\psi(x,t) = \left[-\frac{\hbar^2}{2m}\partial_x^2 + \frac{gN_0}{A_\perp}|\psi(x,t)|^2\right]\psi(x,t). \tag{3.11}$$

The only formal difference to the 3D-GPE (2.24) is the introduction of the so-called *transverse area* $A_\perp := 2\pi a_\perp^2$ — a reminiscence of the higher dimensional origin of (3.11). Due to V_{ext} being x-independent, this equation represents a *quasi-free* 1D system of interacting particles.

Introducing new scaled variables according to[9]

$$\widetilde{x} = \frac{x}{x_0} \qquad \text{with} \quad x_0 \in \mathbb{R}^+ \tag{3.12a}$$

$$\widetilde{t} = \frac{t}{t_0} \qquad \text{with} \quad t_0 = -\text{sign}(m\,g)\,\frac{2m}{\hbar}\,x_0^2 \tag{3.12b}$$

$$\widetilde{\psi} = \frac{\psi}{\psi_0} \qquad \text{with} \quad \psi_0 = \frac{1}{\sqrt{x_0}}, \tag{3.12c}$$

where the scaling factor x_0 (unit: $[m]$) can be chosen arbitrarily, equation (3.11) is transformed to:

$$\boxed{i\partial_{\widetilde{t}}\,\widetilde{\psi}(\widetilde{x},\widetilde{t}) = \left[\text{sign}(m\,g)\;\partial_{\widetilde{x}}^2 - \kappa_{\text{BEC}}|\widetilde{\psi}(\widetilde{x},\widetilde{t})|^2\right]\widetilde{\psi}(\widetilde{x},\widetilde{t})} \tag{3.13}$$

(Note that the tilde-symbols "$\widetilde{\ }$" indicating scaled quantities will be omitted for notational convenience in the following.)
The nonlinearity coefficient κ_{BEC} in (3.13) is given by

$$\kappa_{\text{BEC}} = \text{sign}(m\,g)\,\frac{2mgN_0}{\hbar^2 A_\perp} = \frac{2|mg|N_0}{\hbar^2 A_\perp}\,x_0\;(>0). \tag{3.14}$$

Indeed (3.13) is exactly of the same form as the optical nonlinear SCHRÖDINGER equation (3.8).

3.2.2 Soliton solutions

As in the optical case the combination of signs of the mass and the nonlinearity coefficient determines the character of the solitonic solutions. The different cases realizable in BECs will be discussed in the following.

[9] (3.12c) results from the normalizing condition $\int d\widetilde{x}\,|\widetilde{\psi}|^2 \stackrel{!}{=} 1 \stackrel{!}{=} \int dx\,|\psi|^2$.

Bright solitons: $\mathrm{sign}(m\,g) = -1$

Here the solution is of exactly the same form as (3.9); however, depending on the specific combination of the two signs of m and g two significantly different physical situations correspond to it:

Attractive interactions, positive mass

In this case the ground state wave function itself is soliton shaped ($\psi \propto \mathrm{sech}(\dots)$) as described by (3.9)[10]. However, certain general stability problems arise for $a < 0$ ($\Leftrightarrow g < 0$) as indicated in footnote 11 on p. 9 (for a discussion of this case refer to [8]); due to this bright solitons of this type have not been experimentally realized up to now.
Notwithstanding that, the discussion of 1D bright solitons in the following chapters of this thesis will be based on this case.

Repulsive interactions, negative effective mass (bright "gap solitons")

Of course, $\mathrm{sign}(m) = -1 = -\mathrm{sign}(g)$ cannot be realized *directly* for obvious reasons. However, remembering the theory of electronic energy bands in solid state physics there are situations where systems can be described by introducing an *effective mass* M_{eff} that can also take negative values. Something similar can also be achieved in BECs:
Having an additional *periodic* external potential in (3.11)[11]:

$$i\hbar\,\partial_t\psi(x,t) = \Big[\underbrace{-\frac{\hbar^2}{2m}\partial_x^2 + V_0\cos(2k_L x)}_{=:\,H_0} + \frac{4\pi\hbar^2 a N_0}{m A_\perp}|\psi(x,t)|^2\Big]\psi(x,t), \qquad (3.15)$$

where g has been substituted according to (2.19), it can be shown applying a so-called *multiple scales analysis* that the wave function can approximately[12] be cast into a form

$$\psi(x,t) = A(x,t)\,\phi_{\mathrm{Bloch}}^{(n,q_0)}(x,t) \qquad (3.16)$$

with a fast varying Bloch function $\phi_{\mathrm{Bloch}}^{(n,q_0)}$ (n: band index; q: quasi-momentum) as eigenfunction of H_0 and a slowly varying *envelope function* A underlying a

[10] where the wavefunction ψ plays the role of the amplitude A in (3.9), of course.

[11] This can be realized by two laser beams (wavenumber k_L) of opposite direction creating an optical standing wave field $V_{\mathrm{ext}} = V_0\cos(2k_L x)$.

[12] Multiple scale analysis generally can be employed, if a system's behaviour can be separated to variations on distictly different scales (for a general introduction: refer to [24]). Here this means that the quasi-momentum expansion of $\psi(x,t)$ (i.e. the expansion in the fast varying Bloch functions $\phi_{\mathrm{Bloch}}(x,t) = \phi_{\mathrm{Bloch}}^{(n,q)}(x,t)$) has to be centered closely enough around a value q_0, so that the effective mass is approximately constant over all expansion components; typically, this is the case in the regions around the band edges.

GROSS-PITAEVSKII equation ([23]; see also [25], [26]):

$$i\hbar\left(\partial_t + v\partial_x\right) A(x,t) = \left[-\frac{\hbar^2}{2M_{\text{eff}}}\partial_x^2 + \alpha\,\frac{4\pi\hbar^2 a N_0}{m A_\perp}|A(x,t)|^2\right] A(x,t) \qquad (3.17)$$

Here $\alpha > 0$ is a constant, v causes the soliton solution for the envelope function to move with the corresponding *group velocity* and M_{eff} is an *effective mass*[13]. Indeed, for $M_{\text{eff}} < 0$ [14] eq. (3.17) has moving bright soliton solutions similar to (3.9) *for the envelope function*.

This type of bright solitons has not been realized experimentally yet, but attempts are made (cp. eg. [29]; an extensive stability analysis for such an experiment is carried out in [23]).

Dark solitons: $\text{sign}(m\,g) = +1$

(3.10) principally being the basic solution, again the two combinations of signs correspond to different physical situations:

Repulsive interactions, positive mass

The type of dark solitons emerging in this case — the wave function $\psi(x,t)$ having *tanh*-form as described by (3.10) for the optical case — is the first (and up to now *only*) soliton type which has been experimentally realized ([30], [31]). Taking advantage of the characteristic behaviour of a dark soliton's phase, so-called *phase imprinting* techiques have been used for this.

Attractive interactions, negative effective mass

Here the same arguments as in the above case of bright gap solitons lead to the corresponding equation (3.17) with $a < 0$ now. For $M_{\text{eff}} < 0$ one finds a moving envelope function $A(x,t) = A(x - vt)$ of *tanh*-shape. However, as this case is experimentally quite demanding, up to now no experimental realization has been attempted to our knowledge.

[13] Mind that *only* the mass in the kinetic term is substituted by M_{eff} revealing the *dynamic* origin of the effective mass.

[14] Like in solid state physics this is the case, if the soliton is shifted to the edge of the BRILLOUIN zone in reciprocal space (close to the *band "gap"* — this is the origin of the name "gap solitons"); for details to the experimental realization of "moving in reciprocal space": cf. [27], [28].

Chapter 4

1D-solitons of the n-particle Schrödinger equation

In section 2.2.4 the SCHRÖDINGER equation (2.31) for the n-particle wave function f_n has been derived. For quasi-one-dimensional systems this equation becomes

$$i\,\partial_{\widetilde{t}}\,\widetilde{f}_n(\widetilde{x}_1,\ldots,\widetilde{x}_n,\widetilde{t}) = \underbrace{\Big[-\sum_{i=1}^{n}\partial_{\widetilde{x}_i}^2 + \overbrace{\frac{2mgx_0}{\hbar^2 A_\perp}}^{=:\,\kappa}\sum_{1\le i<j\le n}\delta(\widetilde{x}_j-\widetilde{x}_i)\Big]}_{=:\,\widetilde{H}_n}\widetilde{f}_n(\widetilde{x}_1,\ldots,\widetilde{x}_n,\widetilde{t}), \tag{4.1}$$

where the scaling

$$\widetilde{x}_i = \frac{x_i}{x_0} \quad \text{with } x_0 \in \mathbb{R}^+ \tag{4.2a}$$

$$\widetilde{t} = \frac{\hbar}{2mx_0^2}\,t \tag{4.2b}$$

$$\widetilde{f}_n = x_0^{n/2} f_n \tag{4.2c}$$

has already been performed[1]; note, that the tilde-symbols "~ " (indicating scaled quantities) will be omitted in the following for notational convenience.
The nonlinear coefficient is denoted by κ, which is assumed to be negative in the following: $\boxed{\kappa < 0}$. The factor $A_\perp$ ("transverse area"), which arises in the description of quasi-one-dimensional experimental situations, has already been introduced in equation (3.11) in an analogous context (reducing the GPE to quasi-1D situations).
Note that the the value of κ depends on the scaling factor x_0, which can be chosen

[1] This is completely analogous to the scaling (3.12) used for the GPE.

arbitrarily for concrete calculations in dimensionless units. Of course, rescaling to the physical quantities always yields the same results independent of the chosen value of x_0.

Fortunately, it turns out that analogous equations, which arise for the optical analogue (section 3.1), have already been treated in literature: In 1988 LAI and HAUS studied quantum properties of bright solitons in optical fibers discussing both an approximative HARTREE approach ([32]) and the exact BETHE ansatz method ([33]).
In this chapter the essential parts of their results — transformed for BECs — will be recapitulated and discussed (sect. 4.1 and 4.2). However, LAI and HAUS did not focus on the soliton's *coherence properties* as described by higher order *correlation functions*; introducing this in section 4.3.1 explicit calculations for BEC solitons will be presented in section 4.3.2.

4.1 Time-dependent Hartree approximation

In the HARTREE ansatz

$$f_n^{(\mathrm{H})}(x_1, \ldots, x_n, t) = \prod_{k=1}^{n} \Phi_n(x_k, t) \tag{4.3}$$

the system is — for each particle number n — effectively described by a *single particle wave function* Φ_n; in accordance with (2.30) these wave functions are normalized to "1":

$$\int dx \, |\Phi_n(x,t)|^2 \stackrel{!}{=} 1 \tag{4.4}$$

The HARTREE approximation is based on the assumption that every particle effectively experiences the same "average" interaction caused by the other particles, i.e. individual interactions are neglected, which is expressed by (4.3) being a product state[2] of identical single particle wave functions. This, of course, is nothing else but a *mean field approach* that will essentially lead to a GROSS-PITAEVSKII equation like (3.13) for each Φ_n.

In the framework of the time-dependent HARTREE approximation the wave functions $\Phi_n(x,t)$ are to be determined by variationally minimizing the following functional:

$$\mathcal{A}[f_n^{(\mathrm{H})}] = \int \cdots \int dx_1 \cdots dx_n \; f_n^{(\mathrm{H})*}(x_1, \ldots, x_n, t) \Big[i\partial_t - H_n \Big] f_n^{(\mathrm{H})}(x_1, \ldots, x_n, t) \tag{4.5}$$

[2]Due to the individual particle interactions the *exact* solution f_n of (4.1) can not be transformed to product form, but can only be written as a *superposition of product states*: (2.28).

Inserting the HARTREE ansatz (4.3), this can be rewritten to:[3]

$$n \int dx\ \Phi_n^*(x,t)\Big[i\,\partial_t\Phi_n(x,t) + \partial_x^2\Phi_n(x,t) - (n-1)\frac{\kappa}{2}|\Phi_n(x,t)|^2\Phi_n(x,t)\Big] = \mathcal{A}[\Phi_n] \quad (4.6)$$

As $\mathcal{A}$ is a functional of the wave function Φ_n (and Φ_n^*) its minimum is to be determined by taking the variational derivative $\delta_{\Phi_n}\mathcal{A}[\Phi_n]$ (resp. $\delta_{\Phi_n^*}\mathcal{A}[\Phi_n]$); this results in a nonlinear SCHRÖDINGER equation for Φ_n with the nonlinearity scaled by the factor $(n-1)$:

$$i\,\partial_t\Phi_n(x,t) = -\partial_x^2\Phi_n(x,t) + (n-1)\kappa|\Phi_n(x,t)|^2\Phi_n(x,t) \quad (4.7)$$

As known from (3.9) the fundamental bright soliton solution of this equation is:

$$\Phi_n(x,t) = \sqrt{\frac{8}{(n-1)\,|\kappa|}}\ \eta\ \exp\big(-4i\,(\xi^2-\eta^2)\,t - 2i\xi\,(x-x_0)\big) \cdot \operatorname{sech}\big(2\eta\,(x-x_0+4\xi\,t)\big) \quad (4.8)$$

Initially the parameters η and ξ are undetermined. However, the normalization condition (4.4) fixes the value of η, and ξ can be associated with the momentum p (this will be justified below in (4.11)):

$$\eta = \frac{(n-1)\,|\kappa|}{8}, \qquad \xi = -\frac{p}{2} \quad (4.9)$$

This finally yields:

$$\Phi_n(x,t) = \sqrt{\frac{(n-1)\,|\kappa|}{8}}\ \exp\left(-ip^2t + i\frac{(n-1)^2|\kappa|^2}{16}t + ip(x-x_0)\right) \cdot \operatorname{sech}\left(\frac{n-1}{4}|\kappa|\ (x-x_0-2p\,t)\right) \quad (4.10)$$

[3] Some annotations concerning the derivation of (4.6): The factor n of the first addend $\propto i\partial_t\Phi_n$ originates from applying the product rule to $\partial_t f_n^{(\mathrm{H})}$; for the second addend $\propto \partial_x^2\Phi_n$ its origin is obvious; for the third addend the factor $n(n-1)/2$ results from the multiple sum $\sum_{1\le i<j\le n}$ in H_n consisting of exactly this number of addends. Moreover, (4.4) had to be employed.

Energy, total momentum The HARTREE wave functions $f_n^{(\mathrm{H})}$ are exact eigenstates neither of the Hamiltonian H_n as given by (4.1) nor of the total momentum operator given by $-i\sum_{i=1}^n \partial_{x_i}$. However, the average values can be obtained by elementary calculations[4]:

$$\begin{aligned}\langle P\rangle &= \int\cdots\int dx_1\cdots dx_n\, f_n^{(\mathrm{H})^*}(x_1,\ldots,x_n,t)\Big[-i\sum_{i=1}^n \partial_{x_i}\Big] f_n^{(\mathrm{H})}(x_1,\ldots,x_n,t)\\ &= np \qquad (4.11)\\ \langle E\rangle &= \int\cdots\int dx_1\cdots dx_n\, f_n^{(\mathrm{H})^*}(x_1,\ldots,x_n,t)\, H_n\, f_n^{(\mathrm{H})}(x_1,\ldots,x_n,t)\\ &= np^2 - \frac{1}{48}|\kappa|^2 n(n^2-1) \qquad (4.12)\end{aligned}$$

The mean energy obviously is the kinetic energy of the particles with net momentum p each reduced by the (negative) interaction energy. It will be interesting to compare these results with the values for the exact BETHE eigenstates in the following section.

4.1.1 Phase spreading effects

Eq. (4.7) is indeed the GROSS-PITAEVSKII equation (3.13)[5] for Φ_n; however, the factor N_0 in the nonlinearity coefficient (3.14) was introduced as *average* number of particles, whereas (4.7) makes a proposition for a FOCK subspace with *definite* particle number. According to (2.26) the general solution within the HARTREE approach is a *superposition* of these states:

$$|\psi\rangle^{(\mathrm{H})} = \sum_n a_n\,|n\rangle^{(\mathrm{H})} = \sum_n \frac{a_n}{\sqrt{n!}}\left[\int dx\ \Phi_n(x,t)\hat{\Psi}^+(x)\right]^n |0\rangle \qquad (4.13)$$

Due to the n dependence of the phase factor in (4.10) ($\propto \exp(i\frac{1}{16}(n-1)^2|\kappa|^2 t)$) the superposition (4.13) shows *phase spreading* during time evolution: The phase of of each part Φ_n evolves differently. It can be shown that this effect is irrelevant only for short times — then the *mean field* ${}^{(\mathrm{H})}\langle\psi|\hat{\Psi}(x)|\psi\rangle^{(\mathrm{H})}$ turns out to be essentially of the form (4.10) with n replaced by the *average number* of particles $\langle n\rangle$. The interested reader is referred to [32] for a detailed discussion of the phase spreading effects emerging in the HARTREE approximation.

Not enough, noting that (4.10) has the momentum p as parameter, one could have the idea to generalize (4.13) even further by additionally integrating over a

[4] cp. (4.5) and footnote 3.

[5] The nonlinearity coefficient in (3.13) is proportional to N_0 (cp. (3.14)); however, for large particle numbers — this is the validity condition for the mean field approach anyhow — $N_0-1 \approx N_0$, which shows that (3.13) and (4.7) are essentially the same equations.

distribution of momenta; however, $|n\rangle^{(\mathrm{H})}$ is *not* an eigenstate of the momentum operator, and thus a distribution of momenta is already associated with every $|n\rangle^{(\mathrm{H})}$. The exact BETHE eigenstates presented in the following section will turn out to be simultaneous eigenstates of both n *and* p, which makes a momentum superposition inevitable for the construction of *localized* (soliton) states; analoguously to the phase spreading effect, this, of course, leads to a *dispersion effect* of its own.

4.2 Exact solution: Bethe ansatz

For $\kappa < 0$ the so-called BETHE ansatz provides *bound states* of the time-independent n-particle SCHRÖDINGER equation

$$\Big[-\sum_{i=1}^{n} \partial_{x_i}^2 + \kappa \sum_{1\le i<j\le n} \delta(x_j - x_i) \Big] f_n(x_1, \ldots, x_n) = E_n\, f_n(x_1, \ldots, x_n), \quad (4.14)$$

which follows from the time-dependent equation (4.1) by assuming the time-dependence

$$f_n(\mathbf{r}_1, \ldots, \mathbf{r}_n, t) = e^{-iE_n t} f_n(\mathbf{r}_1, \ldots, \mathbf{r}_n). \quad (4.15)$$

First of all one notices that it is enough to specify $f_n(x_1, \ldots, x_n)$ only in a so-called *simplex* subspace of the $\mathbb{R}^n$, eg. in the $\boxed{\text{simplex } x_1 \le x_2 \le \ldots \le x_n}$, as f_n is a *symmetric function* of its arguments and thus the solution in all the other simplex parts of the $\mathbb{R}^n$ can simply be obtained by adequate permutation and renaming of the arguments.
Moreover, *inside* such a simplex region, i.e. for $x_i \neq x_j$, all δ functions in (4.14) vanish; consequently, in these regions the solution is of the form $\exp(i \sum_{l=1}^{n} k_l x_l)$. However, requiring symmetry one has to perform an *explicit symmetrization* of this expression which leads to the following general form of the solution *inside* a simplex region:

$$f_n^{(\mathrm{B})}(x_1, \ldots, x_n) = \sum_{\{\mathcal{P}\}} A_{\mathcal{P}} \exp\left(i \sum_{l=1}^{n} k_{\mathcal{P}(l)} x_l \right) \quad (4.16)$$

Here $\sum_{\{\mathcal{P}\}}$ symbolizes the summation over all possible permutations $\mathcal{P}$ of $[1, \ldots, n]$ and $\mathcal{P}(l)$ denotes the j-th component of such a permutation; the $A_{\mathcal{P}}$ are coefficients of the *exp*-terms specified by the permutation "$\mathcal{P}$" as index.

(4.16) is called BETHE-*ansatz*. The $n!$ coefficients $A_{\mathcal{P}}$ and n wave vectors k_i are to be determined with the help of boundary conditions at the boundaries $x_i = x_j$ of adjacent simplex regions: The principle is similar to that of the corresponding...

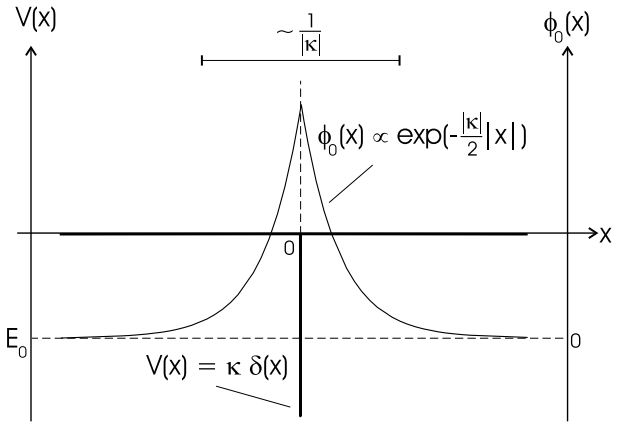

Figure 4.1: One particle analogue (cf. eg. [34]): The δ-function causes a discontinuity in the slope of the wave function at $x = 0$.

One-particle analogue (fig. 4.1) Given

$$\left[-\partial_x^2 + \kappa\,\delta(x)\right]\phi(x) = E\phi(x)$$

as SCHRÖDINGER equation, bound states ($E < 0$), i.e. states with $\phi(x) \xrightarrow{|x|\to\infty} 0$, imply the ansatz

$$\phi(x) = \begin{cases} A\ \exp(+k\,x) & \text{for } x < 0 \\ A'\exp(-k\,x) & \text{for } x > 0 \end{cases}$$

with *real* $k > 0$. The boundary conditions at $x = 0$ are *continuity of* ϕ, i.e. $\phi(0^-) \stackrel{!}{=} \phi(0^+)$, and — as the potential is of δ-form — a *finite discontinuity of* $\partial_x\phi$: $(\partial_x\phi)(0^+) - (\partial_x\phi)(0^-) \stackrel{!}{=} \kappa\phi(0)$. The former provides $A = A'$ and the latter gives $k = -\kappa/2$. Thus only for $\kappa < 0$ a (single!) bound state exists.

Generalization This can be generalized for solving the n-particle equation (4.14) with the BETHE ansatz: One finds[6] that the function $f_n(x_1, \ldots, x_n)$ remains finite for $|x_i| \to \infty$, only if the wave vectors k_l ($l = 1, \ldots, n$) satisfy

$$k_l = p + i\,\frac{\kappa}{4}(n - 2l + 1) \stackrel{\kappa<0}{=} p - i\,\frac{|\kappa|}{4}(n - 2l + 1). \tag{4.17}$$

The quantity $p \in \mathbb{R}$ will turn out to be the (mean) momentum per particle.
Moreover, it can be shown[6] that all coeffients $A_{\mathcal{P}}$ except $A_{[1,\ldots,n]}$ vanish for the k_l

[6] Here only the main results are stated; the interested reader is referred to [32] for detailed calculations.

given by (4.17). Thus the BETHE ansatz yields the solution[7]

$$f^{(\mathrm{B})}_{n,p}\Big|_{x_1\le\cdots\le x_n}(x_1,\ldots,x_n) = \mathcal{N}_n \exp\left(ip\sum_{l=1}^{n} x_l + \frac{|\kappa|}{4}\sum_{l=1}^{n}\left[(n-2l+1)\,x_l\right]\right)$$

$$\equiv \mathcal{N}_n \exp\left(ip\sum_{l=1}^{n} x_l - \frac{|\kappa|}{4}\sum_{1\le i<j\le n}\left(x_j - x_i\right)\right], \quad (4.18)$$

where the single sum has been rewritten in terms of a double sum; $\mathcal{N}_n := A_{[1,\ldots,n]}$ is the normalization factor, that will be calculated below.
(4.18) is valid only in the simplex region $x_1 \le x_2 \le \ldots \le x_n$. However, explicitly restoring symmetry by introducing an $abs(\ldots)$ function the validity of this solution can be extended to the whole $\mathbb{R}^n$:

$$\boxed{f^{(\mathrm{B})}_{n,p}(x_1,\ldots,x_n) = \mathcal{N}_n \exp\left(ip\sum_{j=1}^{n} x_j - \frac{|\kappa|}{4}\sum_{1\le i<j\le n}|x_j - x_i|\right)} \quad (4.19)$$

Note the analogy of the second term in the *exp*-argument to the bound state described in fig. 4.1 for the one-particle analogue. With this in mind the (exact!) BETHE solution can be regarded as "bound state" of the zero range pseudo potential in the multidimensional configuration space.[8]

Energy, total momentum The energy eigenvalue of the wave function $f^{(\mathrm{B})}_{n,p}$ is given by $E_{n,p} = \sum_l k_j^2$, which can be seen by considering the eigenvalue equation (4.14) for the general ansatz (4.16) *inside* a simplex region, where the δ-expressions vanish. This yields:

$$E_{n,p} = \sum_{l=1}^{n} k_j^2 = np^2 - \frac{1}{48}|\kappa|^2 n(n^2-1) \quad (4.20)$$

As mentioned above, $f^{(\mathrm{B})}_{n,p}$ is also an eigenstate of the *total momentum* operator $-i\left[\sum_i \partial_{x_i}\right]$:

$$-i\left[\sum_{i=1}^{n}\partial_{x_i}\right] f^{(\mathrm{B})}_{n,p}(x_1,\ldots,x_n) = np\, f^{(\mathrm{B})}_{n,p}(x_1,\ldots,x_n), \quad (4.21)$$

which can be proved easily using $\sum_{l=1}^{n}(n-2l+1) = 0$. Comparing these exact eigenvalues with (4.11) and (4.12) one notices that the HARTREE mean field approach reproduces the same values — however, not surprisingly — only in the average.

[7] The additional index "p" indicates that the BETHE solution is also an exact eigenstate of the total momentum operator (see below).

[8] The zero range pseudo potential has been introduced as *model potential* describing certain *scattering properties* of the actual interaction potential (see chap. 2.2.2). Thus it has to be emphasized that the BETHE state is *not* a "bound state in multidimensional space" of the actual potential. This will be discussed more detailed in sect. 5.1.3.

FOCK **state representation** According to (2.28) the FOCK eigenket corresponding to the n-particle BETHE wave function $f^{(\mathrm{B})}_{n,p}$ is:

$$|n,p\rangle^{(\mathrm{B})} = \frac{1}{\sqrt{n!}} \int_{-\infty}^{\infty} \cdots \int_{-\infty}^{\infty} dx_1 \cdots dx_n \; f^{(\mathrm{B})}_{n,p}(x_1,\ldots,x_n) \hat{\Psi}^+(x_1)\cdots\hat{\Psi}^+(x_n)\,|0\rangle \tag{4.22a}$$

$$= \sqrt{n!} \int\limits_{-\infty<x_1\leq\cdots\leq x_n<\infty} \cdots \int dx_1 \cdots dx_n \; f^{(\mathrm{B})}_{n,p}(x_1,\ldots,x_n) \hat{\Psi}^+(x_1)\cdots\hat{\Psi}^+(x_n)\,|0\rangle \tag{4.22b}$$

In the second line the integration region has been restricted to a simplex region, which is possible here due to the symmetry of the integrand. As will be seen in appendix B, the form (4.22b) is advantageous for concrete calculations as no expressions containing absolute values $|\ldots|$ are involved. Note the factor "$n!$", as the $\mathbb{R}^n$ is build up of $n!$ simplices.

Eq. (4.22) is an eigenstate of the Hamiltonian[9]

$$\hat{H} = \int dx \;\; \left(\hat{\Psi}^+(x) \left[-\partial_x^2\right] \hat{\Psi}(x) - \frac{|\kappa|}{2} \hat{\Psi}^+(x)\hat{\Psi}^+(x)\hat{\Psi}(x)\hat{\Psi}(x) \right), \tag{4.23}$$

i.e. $\hat{H}\,|n,p\rangle^{(\mathrm{B})} = E_{n,p}\,|n,p\rangle^{(\mathrm{B})}$ with $E_{n,p}$ as given by (4.20).
Hence in the SCHRÖDINGER picture the time-dependence of the eigenkets takes on the form:

$$|n,p\rangle(t) = e^{-iE_{n,p}\,t}|n,p\rangle \tag{4.24}$$

Normalization It can be shown[10] that the BETHE solutions can be normalized according to

$$\langle n',p'|n,p\rangle \stackrel{!}{=} \delta_{n,n'}\,\delta(p-p'), \tag{4.25}$$

which provides the value of the normalization factor $\mathcal{N}_n$:

$$\mathcal{N}_n = \sqrt{\frac{(n-1)!\,|\kappa|^{n-1}}{2^n\pi}} \tag{4.26}$$

4.2.1 Construction of soliton states

The question arises, if the states $|n,p\rangle$ — as eigenstates of the Hamiltonian (4.23) — are already the soliton solutions searched for. For this one may focus on the

[9] The second quantized Hamiltonian (4.23) is the one-dimensional version of (2.20).
[10] see appendix B.1

corresponding matrix elements of the field operator:[11]

$$\langle n', p'|\hat{\Psi}(x)|n, p\rangle = \delta_{n,n'+1}\frac{2^{2n}}{\sqrt{2|\kappa|}\,\pi}\sqrt{n(n+1)}\,n!(n-1)!\,e^{i[(n+1)p-np']\,x}$$

$$\cdot\prod_{r=1}^{n}\frac{1}{(2r-1)^2+\frac{16}{|\kappa|^2}\,(p-p')^2} \tag{4.27a}$$

$$\overset{n\gg 1}{\approx}\ \delta_{n,n'+1}\frac{1}{\sqrt{2|\kappa|}}\sqrt{n(n+1)}\,e^{i[(n+1)p-np']\,x}\ \mathrm{sech}\left(\frac{2\pi}{|\kappa|}\,(p-p')\right) \tag{4.27b}$$

The mean field expressed by $\langle n, p|\hat{\Psi}(x)|n, p\rangle$ vanishes. Moreover, as the $|n, p\rangle$ are eigenstates of the *particle-number* and *total momentum* operator, the corresponding uncertainty relations imply that both *phase* and *position* are completely undefined for these states, which consequently cannot describe a localized soliton state with mean phase and position. However, the latter can be constructed by a adequate superposition of the Hamiltonian's eigenstates:

$$|\psi\rangle = \sum_{n=0}^{\infty} a_n \int_{-\infty}^{\infty} dp\; g_n(p)\;|n, p\rangle(t), \tag{4.28}$$

where normalization of the distributions is required:

$$\sum_n |a_n|^2 \;=\; 1 \tag{4.29}$$

$$\int dp\;|g_n(p)|^2 \;=\; 1 \tag{4.30}$$

Choosing the subsequent distributions[12]

$$a_n = \frac{\alpha_0^n}{\sqrt{n!}}\,\exp\left(-\frac{|\alpha_0|^2}{2}\right) \qquad \textit{Poissonian distribution} \tag{4.31}$$

$$g_n(p) = \frac{1}{\sqrt{\Delta p\,\sqrt{\pi}}}\exp\left(-\frac{1}{2}\frac{(p-p_0)^2}{(\Delta p)^2}\right)e^{-inpx_0} =: g(p)\,e^{-inpx_0}$$

$$\textit{Gaussian distribution} \tag{4.32}$$

[11] See appendix B.2 for some details concerning the derivation of (4.27).

[12] The particle number distribution is chosen as Poissonian distribution (4.31), as this is the distribution for coherent states.

The n-dependent phase factor in the momentum distribution (4.32) is introduced for convenience: It has the effect of providing a translational offset x_0 of the soliton.

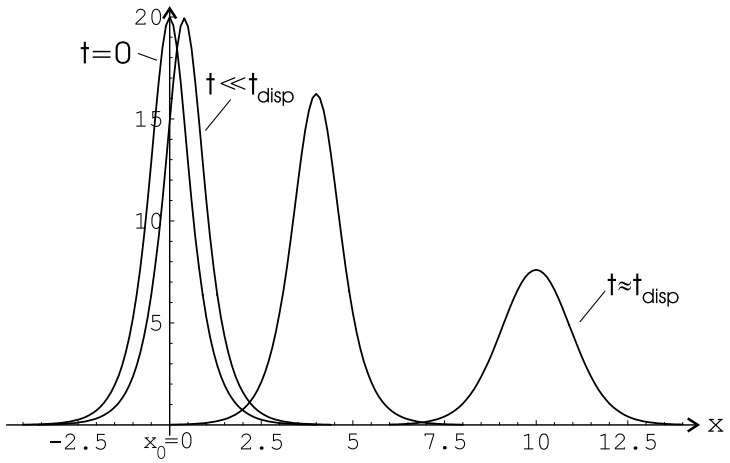

Figure 4.2: Soliton dynamics: Plot of $|\langle\psi|\hat{\Psi}(x)|\psi\rangle|(t)$ according to eq. (4.33) for $t = 0, 0.1, 1, 2.5$ with the following trial values: $|\kappa| = 0.02$, $\Delta p = 0.2$, $p_0 = 2$, $\alpha_0 = 20 \Leftrightarrow n_0 = \langle n\rangle \overset{(4.31)}{=} |\alpha_0|^2 = 400$. The quantity t_{disp} will be introduced in sect. 4.2.2, eq. (4.34), as characteristic time of the soliton's quantum dispersion. The calculation of the plots has been performed using [39].

gives the following approximative expression for the expectation value of the field operator:[13]

$$\begin{aligned}\langle\psi|\hat{\Psi}(x)|\psi\rangle(t) \approx \sum_n \frac{\alpha_0\,|\alpha_0|^{2n}}{n!} e^{-|\alpha_0|^2} \sqrt{\frac{n}{8}}\,\sqrt{|\kappa|}\,\exp\left(i\frac{|\kappa|^2}{16} n(n+1)\,t\right) \\ \cdot \int_{-\infty}^{\infty} dp\;\frac{1}{(\Delta p)\sqrt{\pi}}\exp\left(-\frac{(p-p_0)^2}{(\Delta p)^2}\right)\exp\left(ip(x-x_0)-p^2t\right) \\ \cdot \operatorname{sech}\left(\frac{|\kappa|}{4}(n+\tfrac{1}{2})(x-x_0-2pt)\right) \qquad (4.33)\end{aligned}$$

Plots of the modulus of this function for various times are depicted in fig. 4.2. A surprising observation here is the obvious *broadening* of the soliton during propagation — a remarkable nonclassical effect revealed only by the quantum field description of the soliton.
This *quantum dispersion* effect and its relevance for BEC solitons will be studied more detailed in the following subsection.

[13] The derivation of (4.33) is carried out in the paper of Lai/Haus [33], Appendix D. However, due to some typing errors and their rather terse discussion of the approximations that lead to (4.33) the reader is also referred to appendix B.3 of this thesis.

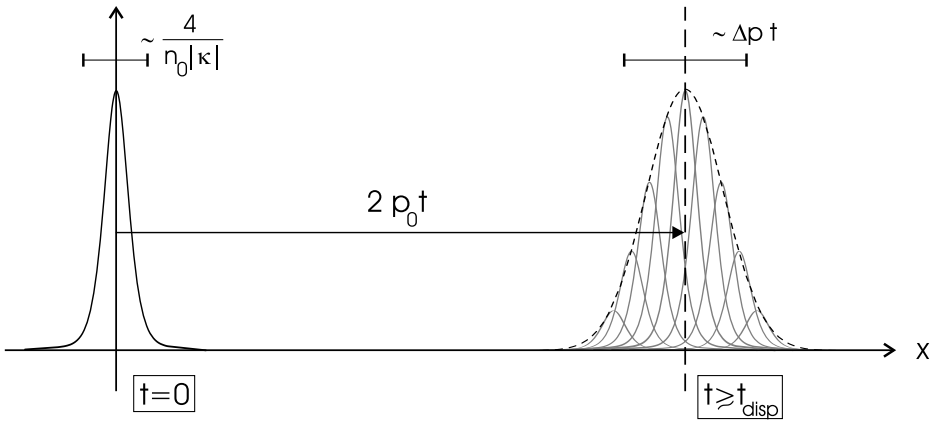

Figure 4.3: Illustration of the quantum dispersion effect (see the text for comments). The dashed line represents the Gaussian distribution of the amplitudes of the *sech*-components when integrating over p in (4.33).

4.2.2 Quantum dispersion of the soliton state

According to eq. (4.33) the expectation value of the field operator essentially is a weighted superpositon or 'average' of "classical" solitons (cp. the HARTREE solution (4.10)) with different values of the particle number n and the momentum p. The former leads to a *phase spreading* effect (cp. sect. 4.1.1) and the latter to *quantum dispersion*, i.e. broadening of the soliton.

The quantum dispersion effect can be illustrated as follows: For $t = 0$ the width of the soliton is in the order of $4/(n_0\,|\kappa|)$ as can be seen from the *sech* term in (4.33).[14] However, due to the momentum dependence of the *sech* term components with different p move with different velocity and thus cover different distances after propagating for a time t. The spreading of the center-positions of the different *sech*-components will be in the order of $\Delta p \cdot t$, where Δp is the momentum bandwidth of the Gaussian momentum distribution (4.32). As illustrated in fig. 4.3, significant broadening will emerge, if $\Delta p \cdot t$ comes into the order of the *sech*-width $4/(n_0\,|\kappa|)$. The characteristic time $t_{\rm disp}$ of dispersion thus is given by

$$t_{\rm disp} \approx \frac{4}{n_0\,|\kappa|\,\Delta p} \tag{4.34}$$

This is to be compared with the so-called *soliton period* $t_{\rm s}$, which is given by the periodicity of the phase in "$\exp(i\,|\kappa|^2\,n(n+1)\,t/16)$" (cp. (4.33)):

$$t_{\rm s} \approx \frac{32\pi}{n_0^2\,|\kappa|^2} \tag{4.35}$$

[14] n_0 denotes the average number of particles $\langle n\rangle$, which is $n_0 = |\alpha_0|^2$ for a Poissonian distribution (4.31).

Hence:

$$\frac{t_{\text{disp}}}{t_{\text{s}}} \approx \frac{n_0 \, |\kappa|}{8\pi \, \Delta p} \tag{4.36}$$

Consequently, if $\Delta p \ll n_0 \, |\kappa|$ the dispersion effect is significant only after many soliton periods. Remembering that eq. (4.33) for the expectation value of the field is valid only for $|\kappa| \ll \Delta p$ (eq. (B.24)), one finds that stable solitons with constant width $\sim 4/(n_0 \, |\kappa|)$ exist for times $t \lesssim t_{\text{s}}$, only if the condition

$$|\kappa| \overset{!}{\ll} \Delta p \overset{!}{\ll} n_0 \, |\kappa| \tag{4.37}$$

is fulfilled.

It is interesting to compare the effect of quantum dispersion with the "classical" effect of pulse-dispersion in linear, dispersive media: In the latter case a momentum bandwidth of the order of $\Delta p \sim \hbar/\Delta x$ is required for the construction of a pulse with a width Δx. However, the bandwidth Δp required for constructing a soliton with a width $\Delta x \approx 1/(n_0 \, |\kappa|)$ can be — it even *has to* be! — *much smaller than* $1/\Delta x$ as indicated by (4.37). As in both cases the dispersion effect is proportional to Δp, the effect of quantum dispersion of solitons in *nonlinear* media is much less than that of pulses with comparable width in *linear*, dispersive media.

Relevance of the effect for BEC solitons The quantities in eq. (4.37) are scaled, i.e. dimensionless quantities:

- As defined in equation (4.1), the nonlinearity coefficient is given by[15] $\kappa = 4am\omega_\perp x_0/\hbar$, where a is the scattering length, $\omega_\perp$ is the transversal trap frequency ($\rightarrow$ quasi-1D experimental situation) and x_0 is a scaling factor as introduced in (4.2a).
- Rescaling the momentum bandwidth $\Delta p =: \Delta p^{(\text{scaled})}$ to the corresponding physical quantity $\Delta p^{(\text{unscaled})}$, one is lead to the relation $\Delta p^{(\text{scaled})} = x_0/\hbar \cdot \Delta p^{(\text{unscaled})}$.

Eq. (4.37) thus reads as:

$$\underbrace{4am\omega_\perp}_{\approx 1.3 \cdot 10^{-32} \text{ kg m/s}} \overset{!}{\ll} \Delta p^{(\text{unscaled})} \overset{!}{\ll} n_0 \cdot \underbrace{4am\omega_\perp}_{\text{dito}} \tag{4.38}$$

The given numerical value results from taking the data of ^7Li ($m = 1.17 \cdot 10^{-26}$kg, $a = -1.44 \cdot 10^{-9}$m) and the typical value $\omega_\perp \sim 200$Hz as a basis.

As a first attempt, one might estimate the value of $\Delta p^{(\text{unscaled})}$ using the thermal relation $\Delta p^{(\text{therm})} \sim \sqrt{2mk_{\text{B}}T}$. For a typical temperature of $T \sim 500$nK

[15] Here $g = 4\pi\hbar^2 a/m$ from (2.19) and $A_\perp = 2\pi a_\perp^2 = 2\pi\hbar/(m\omega_\perp)$ as introduced in the context of (3.11) have been used.

this yields $\Delta p^{(\mathrm{therm})} \approx 4.0 \cdot 10^{-28}$ kg m/s — thus the first condition $4am\omega_\perp \ll \Delta p^{(\mathrm{unscaled})}$ would be fulfilled. However, the second condition would require $n_0 \gtrsim 10^6$. This is an unrealistic value remembering that ^7Li-condensates cannot be created with such a high number of particles, as ^7Li has a negative scattering length (see the remark in footnote 11 on p. 9). Typical experimental values here are $n_0 = 10^3 - 10^4$ particles, which gives[16] $t_{\mathrm{s}}^{(\mathrm{unscaled})} \approx 1.3$s and $t_{\mathrm{disp}}^{(\mathrm{unscaled})} \approx 1.8$ms (for $n_0 = 10^3$), when Δp is estimated by $\Delta p^{(\mathrm{therm})}$ for $T = 500$nK.
These values clearly show that Δp cannot be estimated by the thermal relation $\Delta p^{(\mathrm{therm})} \sim \sqrt{2mk_{\mathrm{B}}T}$. This is not surprising as the momentum bandwidth of the condensate fraction is much smaller — indeed it is $\Delta p \approx 0$ ideally. Assuming a value of $\Delta p^{(\mathrm{unscaled})} \approx 5.0 \cdot 10^{-31}$ kg m/s for the first condition in (4.38) to be fulfilled, a soliton with $n_0 = 10^3$ particles would have a characteristic time of quantum dispersion of about $t_{\mathrm{disp}} \approx 1.5$s and, incidentally, a width[17] of $\sim 30\mu$m and hence should be observable experimentally.

4.3 Correlations induced by the particle interactions

4.3.1 Correlation function and coherence properties

Besides the macroscopic population of the ground state, further crucial characteristics of Bose-Einstein condensates are its coherence properties: For example, the ability of a condensate to form an interference pattern[18] is closely related to its long-range spatial phase coherence. The preferred tools to study coherence properties are so-called *correlation functions*: As known from the optical analogue[19], for the case of an interference experiment the visibility of interference fringes can be quantified by the so-called *first-order correlation function* $g^{(1)}(x, x')$, which for quantum mechanical systems is given by ([38]):

$$g^{(1)}(x, x') = \frac{\langle\psi|\hat{\Psi}^+(x)\hat{\Psi}(x')|\psi\rangle}{\sqrt{\langle\psi|\hat{\Psi}^+(x)\hat{\Psi}(x)|\psi\rangle} \cdot \sqrt{\langle\psi|\hat{\Psi}^+(x')\hat{\Psi}(x')|\psi\rangle}} \tag{4.39}$$

[16] Rescaling the time variables according to (4.2b), one finds for the unscaled versions of eqs. (4.34), (4.35): $t_{\mathrm{disp}}^{(\mathrm{unscaled})} = 2\hbar/\big(n_0 a\omega_\perp \Delta p^{(\mathrm{unscaled})}\big)$; $t_{\mathrm{s}}^{(\mathrm{unscaled})} = 4\pi\hbar/(n_0^2 a^2 m\omega_\perp^2)$.

[17] As mentioned on p. 34 the soliton's width is in the order of $\sim 4/(n_0|\kappa|)$ in *scaled variables*. Using the definition of κ in eq. (4.1) and rescaling the according to (4.2a) one finds: $\Delta x^{(\mathrm{unscaled})} \sim \hbar/(n_0 am\omega_\perp)$.

[18] The first realisation of such an interference experiment succeeded in 1997 ([35]); a more systematic experimental investigation of the first-order coherence properties of a condensate is described in [36].

[19] For a detailed discussion of coherence properties of light and its relevance for optical interference experiments refer to the textbook [37].

$g^{(1)}(x,x')$ is a measure for *field* correlations between the two points x and x'. As an example, if the system were in a pure *coherent state* — defined by the action of the field operator as being $\hat{\Psi}(x)|\psi\rangle = \psi(x)|\psi\rangle$ — the modulus of the function $g^{(1)}(x,x')$ would yield the value "1" for all x, x' expressing perfect first order coherence. The opposite case, i.e. *no* spatial first order coherence, is expressed by $g^{(1)}(x,x') = 0$. In this case interference patterns would be completely washed out due to entirely uncorrelated field fluctuations.

Whereas $g^{(1)}(x,x')$ describes spatial coherence of the *field*, i.e. also its phase, higher order correlation functions can be defined analogously: For example, $g^{(2)}(x,x') \propto \langle\psi|\hat{\Psi}^+(x)\hat{\Psi}^+(x')\hat{\Psi}(x')\hat{\Psi}(x)|\psi\rangle$ is a measure for spatial correlations of the field's *intensity*.[20]

In this section we will focus on some properties of the first order correlation function for a system of n interacting particles as described by the SCHRÖDINGER equation (4.14).

4.3.2 First order correlations for the soliton state

Calculating $g^{(1)}(x,x') \propto \langle\psi|\hat{\Psi}^+(x)\hat{\Psi}(x')|\psi\rangle$ for the state (4.28), one is lead to the following expression:

$$\langle\psi|\hat{\Psi}^+(x)\hat{\Psi}(x')|\psi\rangle = \sum_n |a_n|^2 \iint dp dp'\; g_n^*(p') g_n(p) \cdot \underline{\langle n,p'|\hat{\Psi}^+(x)\hat{\Psi}(x')|n,p\rangle} \tag{4.40}$$

Regarding the underlined matrix element, it will be shown that the particle interactions modeled by the zero-range pseudo potential induce spatial correlations. For that first the corresponding matrix element for a system of non-interacting particles will be calculated, which then can be compared to the result for the matrix element when using the exact BETHE states from sect. 4.2.

Non-interacting bosons

The SCHRÖDINGER equation describing n non-interacting, untrapped particles is (eq. (4.14) for $\kappa = 0$):

$$\Big[-\sum_{i=1}^{n} \partial_{x_i}^2 \Big]\, f_n(x_1,\ldots,x_n) = E_n\, f_n(x_1,\ldots,x_n), \tag{4.41}$$

A special solution of this equation obviously is the (symmetric) eigenfunction

$$f_{n,p}^{(\kappa=0)}(x_1,\ldots,x_n) = \frac{1}{(2\pi)^{n/2}} \exp\left(i\,p \sum_{l=1}^{n} x_l \right), \tag{4.42}$$

[20] The interested reader is referred to the article [38] for more details about higher order correlation functions.

which corresponds to a system of n particles with the momentum p *each*; the total momentum thus is np. The prefactor $(2\pi)^{-n/2}$ results from postulating the normalization condition $\langle n', p'|n, p\rangle = \delta_{n,n'}\delta(p - p')$. Obviously eq. (4.42) is a solution for the non-interacting case which corresponds to the BETHE solution (4.19).

Introducing the operator $\hat{a}_p^+ = \frac{1}{\sqrt{2\pi}} \int dx\, \exp(ipx)\, \hat{\Psi}^+(x)$, i.e. the operator creating one particle with the wave function $\propto \exp(ipx)$ (cp. eq. (2.14)), the FOCK state corresponding to (4.42) can be written as:

$$\begin{aligned} |n, p\rangle^{(\kappa=0)} &= \frac{1}{\sqrt{n!}} \int_{-\infty}^{\infty} \cdots \int_{-\infty}^{\infty} dx_1 \cdots dx_n\, f_{n,p}^{(\kappa=0)}(x_1, \ldots, x_n) \hat{\Psi}^+(x_1) \cdots \hat{\Psi}^+(x_n)\, |0\rangle \\ &= \frac{1}{\sqrt{n!}} (\hat{a}_p^+)^n\, |0\rangle \end{aligned} \tag{4.43}$$

The matrix element $\langle n, p'|\hat{\Psi}^+(x)\hat{\Psi}(x')|n, p\rangle$ thus can be written as:

$$\langle n, p'|\hat{\Psi}^+(x)\hat{\Psi}(x')|n, p\rangle = \frac{1}{n!} \underbrace{\langle 0|(\hat{a}_{p'})^n \quad \hat{\Psi}^+(x)}_{=\langle 0|\,[(\hat{a}_{p'})^n, \hat{\Psi}^+(x)]} \quad \underbrace{\hat{\Psi}(x') \quad (\hat{a}_p^+)^n|0\rangle}_{=[\hat{\Psi}(x'), (\hat{a}_p^+)^n]\,|0\rangle} \tag{4.44}$$

It is $[\hat{\Psi}(x), (\hat{a}_p^+)^n] = \frac{1}{\sqrt{2\pi}}\, n \exp(ipx)\, (\hat{a}_p^+)^{n-1}$, where $[\hat{\Psi}(x), \hat{a}_p^+] = \frac{1}{\sqrt{2\pi}} \exp(ipx)$ has been used. Noting that $[\hat{a}_p, \hat{a}_p^+] = \delta(p - p')$ and thus $\langle 0|(\hat{a}_{p'})^{n-1}\, (\hat{a}_p^+)^{n-1}|0\rangle = (n-1)!\, \delta(p - p')$, one is finally lead to the result:

$$\langle n, p'|\hat{\Psi}^+(x)\hat{\Psi}(x')|n, p\rangle = \frac{n}{2\pi} \exp\big(i\, p(x' - x)\big)\, \delta(p - p') \tag{4.45}$$

Interacting bosons

An analytical expression for the matrix element $\langle n, p'|\hat{\Psi}^+(x)\hat{\Psi}(x')|n, p\rangle$ can also be calculated for the exact BETHE solution $|n, p\rangle^{(\mathrm{B})}$ from sect. 4.2. The rather lengthy calculations are presented in appendix B.4. The result (B.47) has a complicated structure of nested finite sum- and product-expressions. However, for small particle numbers n it is accessible to a direct numerical treatment with acceptable runtime behaviour.

To have an impression about its basic functional behaviour, plots of the modulus of $\langle n, p'|\hat{\Psi}^+(x)\hat{\Psi}(x')|n, p\rangle$ as function of x' for different values of the momentum $p - p'$, the particle number n and the nonlinearity coefficient κ are presented in fig. 4.4. One finds:

- The essential difference to the behaviour of a system of non-interacting bosons as treated above is revealed when focusing on the case $p \neq p'$: Whereas eq. (4.45) predicts a vanishing value of the matrix element for non-interacting bosons in this case, the p-off-diagonal elements have a finite

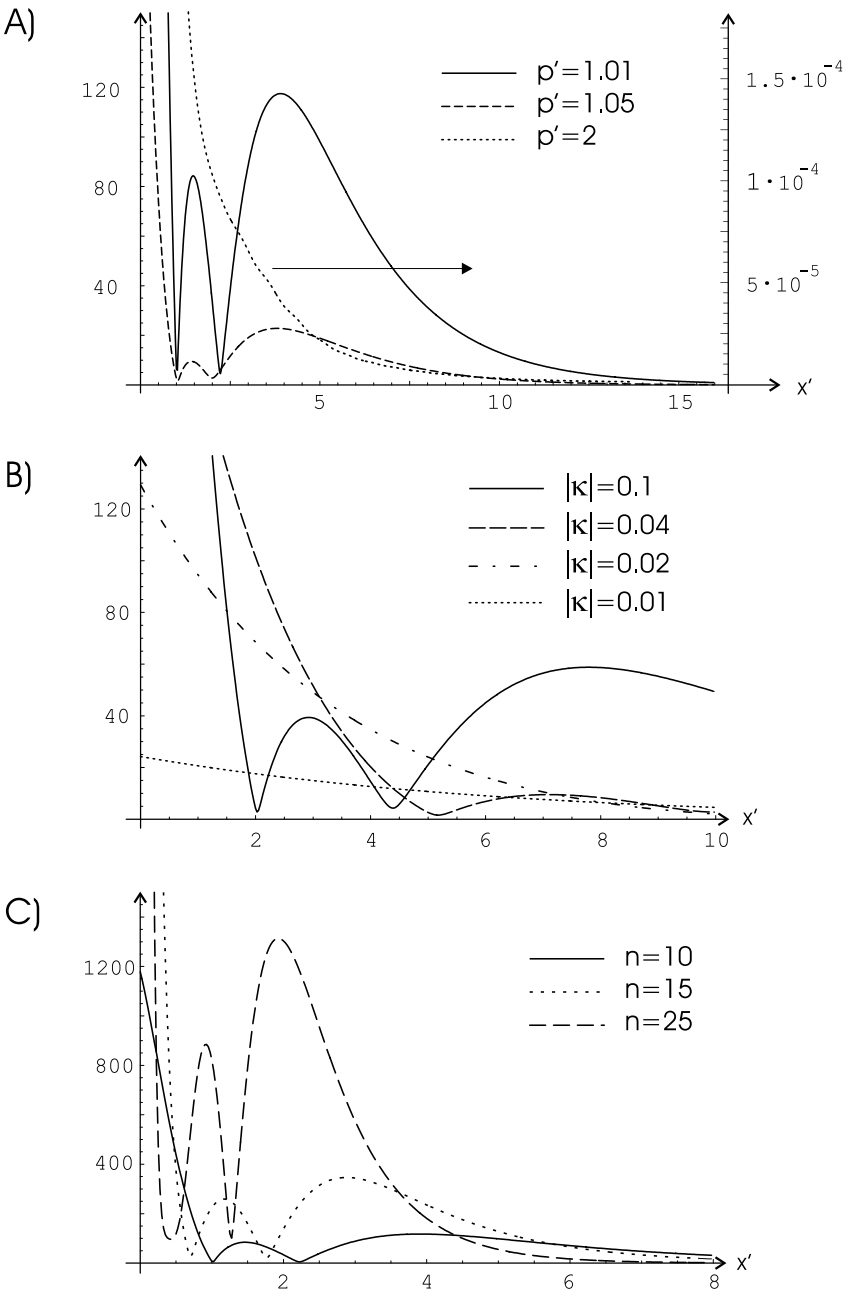

Figure 4.4: Plots of $|\langle n, p'|\hat{\Psi}^{+}(x)\hat{\Psi}(x')|n, p\rangle|$ as function of x' according to (B.47).
• A): Plots for different values of p', where $p = 1$, $n = 10$, $|\kappa| = 0.2$, and $x = 0$.
• B): Plots for different values of $|\kappa|$, where $n = 10$, $p = 1$, $p' = 1.01$ and $x = 0$.
• C): Plots for different values of n, where $|\kappa| = 0.2$, $p = 1$, $p' = 1.01$ and $x = 0$.
The calculations have been carried out using C/C++.

value for interacting bosons (cp. fig. 4.4 A)) and thus contribute to the integral (4.40), which can be interpreted as *interaction-induced correlations*. However, the value of the matrix element decreases rather fast for increasing $(p - p')$ as can be seen from fig. 4.4 A).

- The term 'interaction-induced correlations' is also justified by the dependence of the matrix element on the value of the nonlinearity coefficient κ (cp. fig. 4.4 B)): The bigger the interactions (expressed by a higher value of $|\kappa|$), the bigger is the value of the matix element (regarding the tendency at least; obviously the spatial dependence shows a more complicated structure in some regions).

- Fig. 4.4 C) depicts some spatial plots for different n: As could be expected[21], the values of the matrix element increase with increasing particle number n regarding the tendency.

First order correlation function So far only the matrix element of the BETHE states $\langle n, p'|\hat{\Psi}^+(x)\hat{\Psi}(x')|n, p\rangle$ has been focused on. However, for the calculation of the first order correlation function $g^{(1)}(x, x')$ one has to sum up over relevant values of n and perform a double integration over p and p'. We have tried to employ an approximate method ("method of stationary phase") to omit an integration; this, however, fails for the given problem (4.40). Having in mind the — especially for large n — considerable time of calculation just for single values of the matrix element, this is a massive numerical effort: Using N_p supporting points for each of the two integrals and summing over Δn particle numbers[22], $N_p^2 \cdot \Delta n$ matrix elements have to be calculated for each combination (x, x') — even for moderate values of N_p and Δn ($\lesssim 100$) this is numerically not accessible.

[21] As an example, for $p = p'$, $x = x'$ the matrix element formally is nothing else but the expectation value of the number operator $\langle n, p|\hat{\Psi}^+(x)\hat{\Psi}(x)|n, p\rangle$, which is proportional to the particle number, of course.

[22] For the Poissonian distribution (4.31) Δn is in the order of $\sqrt{n_0} := \sqrt{\langle n\rangle} = \alpha_0$.

Chapter 5

n-particle Schrödinger equation (1D) with realistic interactions: An approximative approach

In the previous chapter a one-dimensional system of n interacting bosons was discussed, where the interactions were given by the zero range pseudo potential ("δ-interactions"). It turned out that such a problem can be solved exactly by the BETHE ansatz.
The zero range pseudo potential has been introduced as a *model potential* for ultracold gases ($T \to 0$), where atomic interactions can be described sufficiently by s-wave scattering (sect. 2.2.2). However, for higher temperatures it is desirable to have a more realistic description of the interactions: Subsequently the n-particle SCHRÖDINGER equation with the δ-model potential substituted by a more realistic interaction potential will be considered, and an approximative ansatz for its solution will be presented for the case of dilute systems, where a restriction to binary interactions is sufficient (sect. 5.1). As done in the previous chapter for the BETHE states, the matrix elements of the field operator etc. will be focused on in sect. 5.2, where the emphasis will be laid in the investigation of the structure of the emerging expressions. As the latter turns out to be rather complex, a sophisticated computeralgebraic approach implementing the commutator algebra of the above model will be presented in sect. 5.3. Finally, in sect. 5.4 the problems emerging for a numerical implementation of the model will be discussed.

5.1 The model

The n-particle Hamiltonian, which the following discussion will be based on, is given by:

$$H_n = \sum_{i=1}^{n} \underbrace{\Big[-\frac{\hbar^2}{2m} \frac{\partial^2}{\partial x_i^2} \Big]}_{=: T_i} + \sum_{1 \le i < j \le n} \underbrace{V(|x_i - x_j|)}_{=: V_{i,j}} \tag{5.1}$$

The corresponding stationary n-particle SCHRÖDINGER equation is:

$$H_n \, f_n(x_1, \ldots, x_n) = E_n \, f_n(x_1, \ldots, x_n) \tag{5.2}$$

Analogously to eq. (2.33), which has been derived for the zero range pseudo potential, eqns. (5.1)f describe n untrapped ($\Leftrightarrow V_{\text{ext}} = 0$) particles interacting via a two-body interaction potential V. As bosons are considered, $f_n(x_1, \ldots, x_n)$ has to be a symmetric function of its arguments.

5.1.1 Dilute systems: Restriction to binary interactions

Essential simplifications arise from the assumption of diluteness of the system: For particle densities small enough the probability for *three* (or more) particles to have mutual distances in the order of the typical range of the interaction potential (or less) — the latter denoted by σ in the following — is completely negligible. Thus the model can be based on the assumption that only *binary interactions* play a role in this case.
Subsequently a rough estimate of the particle densities for which the restriction to binary interactions is a valid approximation will be given.

Considering a one-dimensional system of n particles, which are assumed to be confined to a region with an extend of $\sim L$, the (n-dimensional) volume $\mathcal{V}$ of the configuration space ($\{x_1, \ldots, x_n\} \in \mathbb{R}^n$) is $\mathcal{V} \sim L^n$. Moreover, it is evident that the probabilities for certain particle configurations are proportional to the volume of the corresponding subspaces of configuration space:

- The probability to find two particles having a distance $\lesssim \sigma$ regardless of the positions of the other $(n-2)$ particles is proportional to

$$\mathcal{V}_2 = \frac{n\,(n-1)}{2} \cdot L^{n-1} \cdot \sigma \tag{5.3}$$

  The factor $L^{n-1}\,\sigma$ expresses that $n-2$ particles have arbitrary positions (factor $\sim L^{n-2}$) and two particles have a distance $\lesssim \sigma$ with arbitrary center position (factor $\sim L\,\sigma$). The combinatorial prefactor is nothing else but the binomial coefficient $\binom{n}{2}$ giving the number of possible two-particle combinations out of n particles.

- The analogous quantity for three particles, i.e. the probability to find *three* particles having a mutual distance $\lesssim \sigma$ regardless of the positions of the other $(n-3)$ particles, is proportional to

$$\mathcal{V}_3 = \frac{n\,(n-1)\,(n-2)}{3!} \cdot L^{n-2} \cdot \sigma^2 \tag{5.4}$$

Obviously the restriction to binary interactions only as discussed above is possible for $\mathcal{V}_3/\mathcal{V}_2 \overset{!}{\ll} 1$. Using the relation $\rho = n/L$ for the particle density ρ this condition can be rewritten to

$$\rho \ll \frac{n}{n-2} \cdot \frac{3}{\sigma} \approx \frac{3}{\sigma} \tag{5.5}$$

This requirement for the restriction to binary interactions is plausible as it claims that *in average* (much) less than one particle can be found in a region with an extend of $\sim \sigma$, i.e. in the range of the interaction potential.

5.1.2 The model wave function

The wave function that will be investigated in the following sections is given by:

$$f_n^{(\text{binary})}(x_1, \ldots, x_n) = \begin{cases} Symm\big\{\chi(x_1, x_2) \cdots \chi(x_{n-1}, x_n)\big\} & \text{for } n \text{ even} \\ Symm\big\{\phi(x_1)\chi(x_2, x_3) \cdots \chi(x_{n-1}, x_n)\big\} & \text{for } n \text{ odd} \end{cases} \tag{5.6}$$

Here $Symm\{ \ldots \}$ denotes the operator of *explicit symmetrization* with respect to the variables $x_1, \ldots, x_i$ (see the example eq. (5.9) for $n = 4$).
$\chi(\cdot, \cdot)$ is the (exact) solution to the SCHRÖDINGER equation (5.2) for $n = 2$, i.e. $\chi(x_i, x_j) := f_2(x_i, x_j)$ is the normed, symmetric wave function describing two particles with interaction potential $V_{i,j}$:

$$\big[T_i + T_j + V_{i,j}\big]\, \chi(x_i, x_j) = E_2\, \chi(x_i, x_j) \tag{5.7a}$$

$$\iint dx_1 dx_2\; \chi^*(x_1, x_2)\chi(x_1, x_2) \overset{!}{=} 1 \qquad \textit{normalization} \tag{5.7b}$$

Analogously, the one-particle wave function ϕ has been introduced as $\phi(x_i) := f_1(x_i)$, which thus fulfills:

$$T_i\, \phi(x_i) = E_1\, \phi(x_i) \tag{5.8a}$$

$$\int dx\; \phi^*(x)\phi(x) \overset{!}{=} 1 \qquad \textit{normalization} \tag{5.8b}$$

Justification of the ansatz (5.6)

Solely regarding binary interactions is a valid approximation for dilute systems as discussed in sect. 5.1.1. This suggests that an ansatz for the n-particle wave function decomposes into a product of (at most) *two*-particle wave functions, i.e. three (or more)-particle wave functions need not be considered in an ansatz for this case.
Eq. (5.6) is only an approximation to the exact n-particle solution, of course.

The error that is made can be elucidated by considering the wave function for $n = 4$ as an example:

$$f_4^{(\text{binary})}(x_1, \ldots, x_4)$$
$$= \mathcal{N}_4 \cdot \Big(\chi(x_1, x_2)\chi(x_3, x_4) + \chi(x_1, x_3)\chi(x_2, x_4) + \chi(x_1, x_4)\chi(x_2, x_3) \Big) \quad (5.9)$$

Here the explicit symmetrization has already been carried out; $\mathcal{N}_4$ is a normalization constant.
The quality of $f_4^{(\text{binary})}$ as approximative eigenfunction of the Hamiltonian H_4 (eq. (5.1)) becomes obvious by considering the expression $H_4\, f_4^{(\text{binary})}$:[1]

$$\Big[\big(T_1 + T_2 + V_{1,2}\big) + \big(T_3 + T_4 + V_{3,4}\big) + V_{1,3} + V_{1,4} + V_{2,3} + V_{2,4} \Big]\ \chi(x_1, x_2)\chi(x_3, x_4)$$
$$= \Big[2E_2 + \underline{V_{1,3} + V_{1,4} + V_{2,3} + V_{2,4}} \Big]\ \chi(x_1, x_2)\chi(x_3, x_4)$$

This shows that $\chi(x_1, x_2)\chi(x_3, x_4)$ obviously is a good approximation to the exact eigenfunction, if the underlined contributions of the interaction potential vanish, which is fulfilled for

$$|x_3 - x_1|, |x_4 - x_1|, |x_3 - x_2|, |x_4 - x_2| \gg \sigma \quad (5.10)$$

This, of course, is nothing else but the condition for *solely binary* interactions between the particles 1-2, 3-4. Errors are evidently made, if not all conditions (5.10) are satisfied, i.e. if more than two particles have mutual distances $\lesssim \sigma$; however, as discussed in the previous section this is negligible in dilute systems.

5.1.3 The 2-particle wave function $\chi(x_i, x_j)$

The question arises what kind of 2-particle state is described by the function χ.

Remembering that for the zero range pseudo potential as model interaction potential the BETHE wave function eq. (4.19) represents a kind of "bound state" in the multidimensional configuration space (see p. 30), one might at first be lead to the presumption that χ analogously describes a two-particle bound state of the realistic interaction potential. This is investigated numerically in appendix C for a potential of LENNARD-JONES type, which is often used as a reasonable model for real interaction potentials of alkali atoms. Having assumed an effective extent of the potential in the order of $\sim$ 1nm, it has been found that the ground state of the relative motion of the two particles has a size of less than 0.1nm,

[1] Here only the effect of H_4 on the first addend of the wave function eq. (5.9) is explicitly presented; for the other addends one finds corresponding expressions (except for permutation of the indices).

which corresponds to a tightly bound molecular state. Apart from the fact that molecular states of alkali atoms are typically *untrapped*, the problem arises that the lenght scale given by such a bound state is *much too small* to allow modeling of a n-particle soliton state (typical size in the order of 10^{-5} m, see p. 36) based on such states. Incidentally, a two-particle BETHE state has a width which typically is in the mm-range[2] — and thus obviously represents anything else but a "bound state" in the usual sense.

Consequently, one is lead to χ representing a *two-particle scattering state* — the form of a corresponding scattering wave function will be presented subsequently. This presumption is substantiated further below on page 46, where it is shown that a two-particle BETHE state — i.e. the exact solution in the case of δ-interaction potential — can approximately be constructed by an appropriate superposition of scattering states, when assuming s-wave scattering — the latter limiting case is the validity condition for using the δ-model potential.

Two-particle scattering state Introducing new coordinates according to

$$R_{i,j} := \frac{1}{2}(r_i + r_j), \quad r_{i,j} := r_j - r_i \tag{5.11}$$

the two-particle SCHRÖDINGER equation (5.7a) separates into the two independent problems of center-of-mass and relative motion (see appendix C.1):

$$H = H_{\mathrm{cm}} + H_{\mathrm{rel}} := \Big[-\frac{\hbar^2}{4m}\,\partial^2_{R_{i,j}} \Big] + \Big[-\frac{\hbar^2}{2\mu}\,\partial^2_{r_{i,j}} + V(|r_{i,j}|) \Big] \tag{5.12}$$

$$\chi(x_i, x_j) \to \chi_{\mathrm{cm}}(R_{i,j}) \cdot \chi_{\mathrm{rel}}(r_{i,j}) \tag{5.13}$$

($\mu := m/2$: reduced mass of the relative problem)
The *center-of-mass problem* $H_{\mathrm{cm}}\,\chi_{\mathrm{cm}}(R_{i,j}) = E_{\mathrm{cm}}\,\chi_{\mathrm{cm}}(R_{i,j})$ has the usual plane wave solutions

$$\chi_{\mathrm{cm}}(R_{i,j}) \propto \exp\big(ik_{\mathrm{cm}}R_{i,j}\big), \tag{5.14}$$

where $k_{\mathrm{cm}} = \sqrt{4mE_{\mathrm{cm}}/\hbar^2}$ is the wave number of the center-of-mass motion.
The *relative problem* $H_{\mathrm{rel}}\,\chi_{\mathrm{rel}}(r_{i,j}) = E_{\mathrm{rel}}\,\chi_{\mathrm{rel}}(r_{i,j})$ is treated in appendix D in detail; there the scattering wave function is shown to have the asymptotic form (see eq. (D.25)):

$$\chi_{\mathrm{rel}}(r_{i,j}) = 2\exp\big(i\delta_0(k_{\mathrm{rel}})\big)\cos\big(k_{\mathrm{rel}}\,|r_{i,j}| + \delta_0(k_{\mathrm{rel}})\big), \tag{5.15}$$

where $k_{\mathrm{rel}} = \sqrt{2\mu E_{\mathrm{rel}}/\hbar^2}$ is the wave number of relative motion and δ_0 is the scattering phase shift, which generally shows a dependence on k_{rel}; however, in the limiting case of s-wave scattering δ_0 is assumed to be constant.

[2]The two-particle BETHE state is explicitly given by eq. (5.16) and obviously has a characteristic width of $\sim 1/|\kappa|$ in *scaled variables*. Using the definition of κ in eq. (4.1) and rescaling according to (4.2a), one finds for the unscaled width: $\Delta x^{(\mathrm{B})} \sim \hbar/(4am\omega_\perp)$. Taking the values of ^7Li as a basis (given on p. 35 in the context of eq. (4.38)), one finds a value in the range of mm for $\Delta x^{(\mathrm{B})}$.

Two-particle scattering states: Approximative construction of Bethe-eigenstates

The two-particle BETHE solution is given by (see eq. (4.19) for $n = 2$):

$$f_2^{(\mathrm{B})}(x_1, x_2) = \sqrt{\frac{|\kappa|}{4\pi}} \exp\big(i\,p\,(x_1 + x_2)\big) \exp\Big(-\frac{|\kappa|}{4}|x_1 - x_2|\Big) \tag{5.16}$$

Subsequently it will be shown that — in the limiting case of s-wave scattering — such a wave function can essentially be constructed by an appropriate superposition of 2-particle scattering states according to

$$\begin{aligned}\chi(x_1, x_2) &:= f_2^{(scatt)}(x_1, x_2) \\ &= \int dk_{\mathrm{cm}}\; g_{\mathrm{cm}}(k_{\mathrm{cm}})\, \chi_{\mathrm{cm}}(x_1, x_2) \cdot \int dk_{\mathrm{rel}}\; g_{\mathrm{rel}}(k_{\mathrm{rel}})\, \chi_{\mathrm{rel}}(x_1, x_2),\end{aligned} \tag{5.17}$$

where the distribution functions $g_{\mathrm{cm}} = g_{\mathrm{cm}}(k_{\mathrm{cm}})$ and $g_{\mathrm{rel}} = g_{\mathrm{rel}}(k_{\mathrm{rel}})$ have to be chosen appropriately.

Center-of-mass motion Choosing $g_{\mathrm{cm}}(k_{\mathrm{cm}}) = \delta(k_{\mathrm{cm}} - k_{\mathrm{cm},0})$ one is lead to

$$\int dk_{\mathrm{cm}}\; g_{\mathrm{cm}}(k_{\mathrm{cm}})\, \chi_{\mathrm{cm}}(x_1, x_2) = \exp\big(i\,k_{\mathrm{cm},0}\,(x_1 + x_2)\big), \tag{5.18}$$

where (5.14) and (5.11) have been used. This essentially reproduces the first *exp*-factor in (5.16) ($\hbar$ set to "1").

Relative motion Focusing on the second integral in eq. (5.17), i.e. the superposition of scattering states χ_{rel} as given by eq. (5.15), one has to specify the functional dependency $\delta_0 = \delta_0(k_{\mathrm{rel}})$ of the scattering phase for concrete calculations. In appendix D.2.1 this is calculated for a square-well model potential, which for small values of k_{rel} shows a linear dependence (see eq. (D.24a)):

$$\delta_0(k_{\mathrm{rel}}) = \frac{\pi}{2} - \tau_0\, k_{\mathrm{rel}} \tag{5.19}$$

As mentioned above, for the zero-range model potential the limiting case of s-wave scattering is relevant, i.e. $\delta_0 = \text{const.} \Leftrightarrow \tau_0 = 0$. However, to see effects of a small k_{rel}-dependence, first the more general linear dependence eq. (5.19) will be regarded: Using this and (5.11) in (5.15) and employing the relation $\cos(x) = \big(\exp(ix) + \exp(-ix)\big)/2$ yields:

$$\chi_{\mathrm{rel}}(x_1, x_2) = -\exp(-2i\tau_0 k_{\mathrm{rel}}) \exp\big(ik_{\mathrm{rel}}|x_1 - x_2|\big) + \exp\big(-ik_{\mathrm{rel}}|x_1 - x_2|\big) \tag{5.20}$$

Choosing a LORENTZ distribution of width $\sim c$ centered around a nonvanishing value $k_{\mathrm{rel},0}$ according to

$$g_{\mathrm{rel}}^{(\mathrm{L})}(k_{\mathrm{rel}}) = \frac{1}{\pi}\,\frac{c}{c^2 + (k_{\mathrm{rel}} - k_{\mathrm{rel},0})^2} \tag{5.21}$$

and using the relation

$$\int_{-\infty}^{\infty} dk\; g_{\mathrm{rel}}^{(\mathrm{L})}(k)\exp(ikx) = \exp(-c\,|x|)\;\exp(ik_{\mathrm{rel},0}\,x) \tag{5.22}$$

one is finally lead to the following expression for the second integral in eq. (5.17):

$$\begin{aligned}
&\int dk_{\mathrm{rel}}\; g_{\mathrm{rel}}(k_{\mathrm{rel}})\,\chi_{\mathrm{rel}}(x_1,x_2) \\
&\qquad = -\exp\Big(-c\,\big|-2\tau_0+|x_2-x_1|\big|\Big)\;\exp\big(ik_{\mathrm{rel},0}\,(-2\tau_0+|x_2-x_1|)\big) \\
&\qquad\quad + \exp\big(-c\,|x_2-x_1|\big)\;\exp\big(-ik_{\mathrm{rel},0}\,|x_2-x_1|\big)
\end{aligned} \tag{5.23}$$

This is the result assuming a linear dependence of the scattering phase. However, in the limiting case of s-wave scattering ($\tau_0 = 0$) one finds:

$$\int dk_{\mathrm{rel}}\; g_{\mathrm{rel}}(k_{\mathrm{rel}})\,\chi_{\mathrm{rel}}(x_1,x_2) = \exp\big(-c\,|x_2-x_1|\big)\cdot\sin\big(k_{\mathrm{rel},0}\,|x_2-x_1|\big) \tag{5.24}$$

Essentially (except of the *sin*-term), this is the second *exp*-factor in the BETHE solution (5.16) (for $c = |\kappa|/4$).

5.2 The structure of some relevant quantities

As an application of the model given by the wave function $f^{(\mathrm{binary})}$ from eq. (5.6) quantities like the normalization of the states and the matrix elements $\langle n|\hat{\Psi}(x)|n+1\rangle$, $\langle n|\hat{\Psi}^+(x)\hat{\Psi}(x')|n\rangle$ will be focused on in this section. Here the particle number eigenstates in FOCK representation are given by (cp. the corresponding expression (4.22)):[3]

$$|n\rangle^{(\mathrm{binary})} = \frac{1}{\sqrt{n!}}\int_{-\infty}^{\infty}\cdots\int_{-\infty}^{\infty} dx_1\cdots dx_n\; f_n^{(\mathrm{binary})}(x_1,\ldots,x_n)\hat{\Psi}^+(x_1)\cdots\hat{\Psi}^+(x_n)\,|0\rangle \tag{5.25}$$

It will turn out that all the resulting expressions are build up of a few types of what we call *chain integrals*. In this section these types of chain integrals will be introduced, and the structure of the abovementioned quantities will be described.

[3]For notational convenience "$|n\rangle^{(\mathrm{binary})}$" will be simply denoted by "$|n\rangle$" on the following pages.

5.2.1 Normalization of the states: $\langle n|n\rangle$

One finds:[4]

$$\langle n|n\rangle = \int_{-\infty}^{\infty}\cdots\int_{-\infty}^{\infty} dx_1\cdots dx_n\; f_n^*(x_1,\ldots,x_n) f_n(x_1,\ldots,x_n) \tag{5.26}$$

As it depends on n being even or odd, whether the n-particle wave function contains the one-particle wave function $\phi(\cdot)$, these two cases have to be distinguished:

• **even** n

Due to the explicit symmetrization of the n-particle wave function eq. (5.6) the integrand $f_n^*(\cdots)\cdot f_n(\cdots)$ in (5.26) consists of numerous addends[5] with different combinations of the integration variables x_i.
As an example for $n=6$ one of these addends is given by:

$$\begin{aligned}&\chi^*(x_1,x_2)\chi^*(x_3,x_4)\chi^*(x_5,x_6)\cdot\chi(x_1,x_2)\chi(x_3,x_5)\chi(x_4,x_6)\\ =&\underbrace{\chi^*(x_1,x_2)\chi(x_1,x_2)}_{\overset{(5.7b)}{\rightsquigarrow}\,1}\cdot\underbrace{\chi(x_3,x_5)\chi^*(x_5,x_6)\chi(x_6,x_4)\chi^*(x_4,x_3)}_{\rightsquigarrow\, I_{\chi\chi^*,\,4}},\end{aligned}$$

where the symmetry property of the function χ has been used. Carrying out the integration according to (5.26), the first expression underbraced can be simplified using the normalization condition for $\chi(\cdot,\cdot)$, and for the second one the following abbreviation is introduced:[6]

$$I_{\chi\chi^*,\,m} := \int\cdots\int dx_1\cdots dx_m\;\chi(x_1,x_2)\chi^*(x_2,x_3)\cdots\chi(x_{m-1},x_m)\chi^*(x_m,x_1), \tag{5.27}$$

where m is even. This integral is of so-called *chain integral* type — a name that is chosen for obvious reasons due to the special structure of the integrand: Adjacent $\chi(\cdot,\cdot)$ functions have common arguments and form a "chain". Thus the multiple integral does not separate into sub-integrals, but is a real n-fold integral.

The example above is only one of the addends emerging for $f_n^*(\cdots)\cdot f_n(\cdots)$. Unfortunately, the combinatorics arising in this context is quite complicated: For example, as mentioned in footnote 5, for $n=6$ ($n=8$) the wave function f_n consists of 15 (105) addends of the form $\chi(\cdot,\cdot)\cdots\chi(\cdot,\cdot)$ resulting in 15^2 (105^2)

[4] A derivation of eq. (5.26) — starting from the expression (5.25) for $|n\rangle$ — can be found in appendix B.1.

[5] For even n the number of different addends emerging for $Symm\{\chi(x_1,x_2)\cdots\chi(x_{n-1},x_n)\}$ is $n!/\big(2^{n/2}\,(n/2)!\big)$. [$n!$ possible permutations of n variables; $n/2$ *symmetric* χ functions ($\rightarrow$ factor $2^{n/2}$); factor $(n/2)!$ due to commutativity of the product of $(n/2)$ χ-functions]

[6] Note that formally the normalization condition eq. (5.7b) for $\chi(\cdot,\cdot)$ can be formulated using the chain integral eq. (5.27): $I_{\chi\chi^*,\,2}=1$.

addends for $f_n^*(\cdots)\cdot f_n(\cdots)$ (!). However, the value of an integral does not depend on the names of the integration variables — thus adequately renaming the integration (dummy-) variables for each of these addends, it can be easily shown that all these expressions are build up of chain integrals of the type (5.27). Using f_n in a form analogous to eq. (5.9), one finds for the mentioned examples:

$$\langle 6|6\rangle = |\mathcal{N}_6|^2 \left(15 + 90\, I_{\chi\chi^*;\,4} + 120\, I_{\chi\chi^*;\,6}\right)$$

$$\langle 8|8\rangle = |\mathcal{N}_8|^2 \left(105 + 1260\, I_{\chi\chi^*;\,4} + 1260\, (I_{\chi\chi^*;\,4})^2 + 3360\, I_{\chi\chi^*;\,6} + 5040\, I_{\chi\chi^*;\,8}\right)$$

Due to the complicated combinatorics computeralgebraic methods using the software *Mathematica* have been developed, which are described in detail in sect. 5.3. The above expressions have been calculated using this software.
From these examples it is obvious that $\langle n|n\rangle$ is a sum containing chain integrals of the type $I_{\chi\chi^*;\,m}$, where m can have all even values $m \le n$.

• **odd** n

As a difference to the previous case the n-particle wave function contains the single particle wave function $\phi(\cdot)$ for odd n.
Two examples for $n = 5$ should be sufficient to illustrate the structure of the emerging addends, when calculating the integrand $f_n^*(\cdots)\cdot f_n(\cdots)$:

$$\begin{aligned}
&\phi(x_2)\chi^*(x_1,x_3)\chi^*(x_4,x_5)\cdot\phi(x_2)\chi(x_1,x_4)\chi(x_3,x_5)\\
=&\underbrace{\phi^*(x_2)\phi(x_2)}_{\overset{(5.8b)}{\rightsquigarrow}\,1}\cdot\underbrace{\chi(x_1,x_4)\chi^*(x_4,x_5)\chi(x_5,x_3)\chi^*(x_3,x_1)}_{\rightsquigarrow\, I_{\chi\chi^*;\,4}}
\end{aligned}$$

Thus this type of combination does not give anything new.
However, a new type of chain integral arises, if the two ϕ-functions have different arguments:

$$\begin{aligned}
&\phi^*(x_2)\chi^*(x_1,x_3)\chi^*(x_4,x_5)\cdot\phi(x_3)\chi(x_1,x_2)\chi(x_4,x_5)\\
=&\underbrace{\phi^*(x_2)\chi(x_2,x_1)\chi^*(x_1,x_3)\phi(x_3)}_{\rightsquigarrow\, I_{\phi^*\chi\chi^*\phi,\,3}}\cdot\underbrace{\chi^*(x_4,x_5)\chi(x_4,x_5)}_{\overset{(5.7b)}{\rightsquigarrow}\,1}
\end{aligned}$$

Here the following chain integral has been introduced:

$$I_{\phi^*\chi\chi^*\phi,\,m} := \int\cdots\int dx_1\cdots dx_m$$

$$\phi^*(x_1)\chi(x_1,x_2)\chi^*(x_2,x_3)\cdots\chi(x_{m-2},x_{m-1})\chi^*(x_{m-1},x_m)\phi(x_m), \quad (5.28)$$

where m is odd.

As in the previous case of even n one is confronted with a rather complicated combinatorics[7] when calculating the integral (5.26) for odd n. To have an idea of the structure of the resulting expressions, "$\langle 7|7\rangle$" is subsequently given as an example:[8]

$$\langle 7|7\rangle = |\mathcal{N}_7|^2 \big(105 + 630\, I_{\phi^*\chi\chi^*\phi,\,3} + 2520\, I_{\phi^*\chi\chi^*\phi,\,5} + 5040\, I_{\phi^*\chi\chi^*\phi,\,7} + 630\, I_{\chi\chi^*,\,4} + 1260\, I_{\chi\chi^*,\,4} \cdot I_{\phi^*\chi\chi^*\phi,\,3} + 840\, I_{\chi\chi^*,\,6}\big)$$

Obviously both types of chain integrals occur, where m can have all values $m \leq n$.

5.2.2 Matrix element: $\langle n|\hat{\Psi}(x)|n+1\rangle$

It can be shown that the matrix element of the field operator can be expressed as (see appendix B.2, eq. (B.9)):

$$\langle n|\hat{\Psi}(x)|n+1\rangle = \sqrt{n+1} \int_{-\infty}^{\infty} \cdots \int_{-\infty}^{\infty} dx_1 \cdots dx_n \; f_n^*(x_1, \ldots, x_n) f_{n+1}(x_1, \ldots, x_n, x) \tag{5.29}$$

• **even** n

As the matrix element eq. (5.29) is dependent on x, it is not surprising that a new type of chain integral, which also shows a dependence on an external variable, has to be introduced:

$$I_{\chi\chi^*\phi,\,m}(x) := \int \cdots \int dx_1 \cdots dx_m \; \chi(x, x_1)\chi^*(x_1, x_2) \cdots \chi(x_{m-2}, x_{m-1})\chi^*(x_{m-1}, x_m)\phi(x_m), \tag{5.30}$$

where m is even.

The typical structure of the emerging expressions can be seen in the following example:[8]

$$\langle 6|\hat{\Psi}(x)|7\rangle = \sqrt{7}\,\mathcal{N}_6^*\,\mathcal{N}_7 \big(90\, I_{\chi\chi^*\phi,\,2}(x) + 360\, I_{\chi\chi^*\phi,\,4}(x) + 720\, I_{\chi\chi^*\phi,\,6}(x) + 180\, I_{\chi\chi^*\phi,\,2}(x) \cdot I_{\chi\chi^*,\,4} + 15\,\phi(x) + 90\,\phi(x) \cdot I_{\chi\chi^*,\,4} + 120\,\phi(x) \cdot I_{\chi\chi^*,\,6}\big)$$

Obviously both chain integrals of the type eq. (5.27) and the type eq. (5.30) emerge in this case with m taking all possible values $m \leq n$.

[7] The number of different addends emerging for $Symm\{\phi(x_1)\chi(x_2, x_3) \cdots \chi(x_{n-1}, x_n)\}$ is $n!/\big(2^{(n-1)/2}\,((n-1)/2)!\big)$ (see also footnote 5).

[8] This has been calculated using the computeralgebraic methods described in section 5.3.

• **odd** n

Compared to the previous case of even n, here a slightly different chain integral has to be introduced:

$$I_{\chi\chi^*\chi\phi^*;\,m}(x) := \int\cdots\int dx_1\cdots dx_m$$
$$\chi(x,x_1)\chi^*(x_1,x_2)\chi(x_2,x_3)\cdots\chi^*(x_{m-2},x_{m-1})\chi(x_{m-1},x_m)\phi^*(x_m), \quad (5.31)$$

where m is odd.

Again the matrix element of the field operator is build up of chain integrals (in this case of type eq. (5.27) and (5.31)) with m taking all possible values $m \leq n$, compare:[8]

$$\begin{aligned}\langle 7|\hat{\Psi}(x)|8\rangle = 2\sqrt{2}\,\mathcal{N}_7^*\,\mathcal{N}_8\,\big(&105\,I_{\chi\chi^*\chi\phi^*;\,1}(x) + 630\,I_{\chi\chi^*\chi\phi^*;\,3}(x) + 2520\,I_{\chi\chi^*\chi\phi^*;\,5}(x)\\ &+ 5040\,I_{\chi\chi^*\chi\phi^*;\,7}(x) + 630\,I_{\chi\chi^*\chi\phi^*;\,1}(x)\cdot I_{\chi\chi^*;\,4}\\ &+ 1260\,I_{\chi\chi^*\chi\phi^*;\,3}(x)\cdot I_{\chi\chi^*;\,4} + 840\,I_{\chi\chi^*\chi\phi^*;\,1}(x)\cdot I_{\chi\chi^*;\,6}\big)\end{aligned}$$

5.2.3 Matrix element: $\langle n|\hat{\Psi}^+(x)\hat{\Psi}(x')|n\rangle$

This matrix element can be calculated according to the following relation (see appendix B.4, eq. (B.28)):

$$\langle n|\hat{\Psi}^+(x)\hat{\Psi}(x')|n\rangle$$
$$= n\int_{-\infty}^{\infty}\cdots\int_{-\infty}^{\infty} dx_1\cdots dx_{n-1}\; f_n^*(x_1,\ldots,x_{n-1},x)f_n(x_1,\ldots,x_{n-1},x') \quad (5.32)$$

• **even** n

As (5.32) is dependent on two variables x, x', the following type of chain integral arises:

$$\tilde{I}_{\chi\chi^*;\,m}(x,x') :=$$
$$\int\cdots\int dx_1\cdots dx_m\;\chi(x,x_1)\chi^*(x_1,x_2)\cdots\chi(x_{m-1},x_m)\chi^*(x_m,x'), \quad (5.33)$$

where m is odd. Note that this chain integral is related to $I_{\chi\chi^*;\,m}$ from eq. (5.27) by the relation $I_{\chi\chi^*;\,m} = \int dy\;\tilde{I}_{\chi\chi^*;\,m-1}(y,y)$.

One finds that the matrix element eq. (5.32) only contains the chain integrals eq. (5.27) and eq. (5.33) (in the form $\tilde{I}_{\chi\chi^*,\,m}(x',x)$), where m can have all values $m \leq n$, compare:[8]

$$\begin{aligned}\langle 8|\hat{\Psi}^+(x)\hat{\Psi}(x')|8\rangle = 8\,|\mathcal{N}_8|^2\,\big(&105\,\tilde{I}_{\chi\chi^*,\,1}(x',x) + 630\,\tilde{I}_{\chi\chi^*,\,3}(x',x) + 2520\,\tilde{I}_{\chi\chi^*,\,5}(x',x)\\ &+ 5040\,\tilde{I}_{\chi\chi^*,\,7}(x',x) + 630\,\tilde{I}_{\chi\chi^*,\,1}(x',x)\cdot I_{\chi\chi^*,\,4}\\ &+ 1260\,\tilde{I}_{\chi\chi^*,\,3}(x',x)\cdot I_{\chi\chi^*,\,4} + 840\,\tilde{I}_{\chi\chi^*,\,1}(x',x)\cdot I_{\chi\chi^*,\,6}\big)\end{aligned}$$

• **odd** n

Two additional chain integral types arise in this case, which are, however, closely related to known chain integrals:

$$\begin{aligned}I_{\phi^*\chi\chi^*,\,m}(x) &:= \int\cdots\int dx_1\cdots dx_m\\ &\qquad \phi^*(x_1)\chi(x_1,x_2)\chi^*(x_2,x_3)\cdots\chi(x_{m-1},x_m)\chi^*(x_m,x) \quad (5.34)\\ &\overset{(5.30)}{\equiv} I^*_{\chi\chi^*\phi,\,m}(x),\end{aligned}$$

where m is even; and ...

$$\begin{aligned}I_{\phi\chi^*\chi\chi^*,\,m}(x) &:= \int\cdots\int dx_1\cdots dx_m\\ &\qquad \phi(x_1)\chi^*(x_1,x_2)\chi(x_2,x_3)\chi^*(x_3,x_4)\cdots\chi(x_{m-1},x_m)\chi^*(x_m,x) \quad (5.35)\\ &\overset{(5.31)}{\equiv} I^*_{\chi\chi^*\chi\phi^*,\,m}(x),\end{aligned}$$

where m is odd.

As the subsequent example[8] shows, the matrix element $\langle n|\hat{\Psi}^+(x)\hat{\Psi}(x')|n\rangle$ generally is build up of *all* types of chain integrals introduced on the previous pages, if n is odd:

$$\begin{aligned}&\langle 5|\hat{\Psi}^+(x)\hat{\Psi}(x')|5\rangle\\ &= 5\,|\mathcal{N}_5|^2\,\big(12\,\tilde{I}_{\chi\chi^*,\,1}(x',x) + 24\,\tilde{I}_{\chi\chi^*,\,3}(x',x) + 24\,I_{\chi\chi^*\phi,\,2}(x')\cdot I_{\phi^*\chi\chi^*,\,2}(x)\\ &\quad + 24\,\tilde{I}_{\chi\chi^*,\,1}(x',x)\cdot I_{\phi^*\chi\chi^*\phi,\,3} + 12\,I_{\chi\chi^*\chi\phi^*,\,1}(x')\cdot I_{\phi\chi^*\chi\chi^*,\,1}(x)\\ &\quad + 24\,I_{\chi\chi^*\chi\phi^*,\,3}(x')\cdot I_{\phi\chi^*\chi\chi^*,\,1}(x) + 24\,I_{\chi\chi^*\chi\phi^*,\,1}(x')\cdot I_{\phi\chi^*\chi\chi^*,\,3}(x)\\ &\quad + 12\,\phi(x')\cdot I_{\phi^*\chi\chi^*,\,2}(x) + 24\,\phi(x')\cdot I_{\phi^*\chi\chi^*,\,4}(x) + 12\,\phi^*(x)\cdot I_{\chi\chi^*\phi,\,2}(x')\\ &\quad + 24\,\phi^*(x)\cdot I_{\chi\chi^*\phi,\,4}(x') + 3\,\phi^*(x)\cdot\phi(x') + 6\,\phi^*(x)\cdot\phi(x')\cdot I_{\chi\chi^*,\,4}\big)\end{aligned}$$

5.3 Computeralgebraic implementation of a commutator-algebra

In quantum field theory one is often faced with the problem of handling expressions of operators, which obey a noncommutative algebra. A typical example is the calculation of the normal-ordering of an operator-valued expression or — related to this — the calculation of matrix elements and expectation values of operator-valued functions. Computeralgebra software can be a powerful tool for algebraic structural manipulation here.

In this section *Mathematica*[9]-code developed for handling the expressions focused on in the previous section 5.2 will be presented. However, we consider the structure of the developed code as general enough to allow a rather easy adaption to other, related problems.

5.3.1 The commutator algebra of the model

Introducing a *one-particle creation operator* — creating a particle with the wave function $\phi(x)$ — according to

$$\hat{a}^+ = \int_{-\infty}^{\infty} dx_1 \;\; \phi(x_1)\hat{\Psi}^+(x_1) \tag{5.36}$$

and a *two-particle creation operator* — creating two particles with the (symmetric) two-particle wave function $\chi(x_1, x_2)$ $\big(= \chi(x_2, x_1)\big)$ — according to[10]

$$\hat{S}^+ = \iint_{-\infty}^{\infty} dx_1 dx_2 \;\; \chi(x_1, x_2)\hat{\Psi}^+(x_1)\hat{\Psi}^+(x_2), \tag{5.37}$$

the particle-number eigenstates $|n\rangle^{(\text{binary})}$ from eq. (5.25) can be equivalently written as:

$$|n\rangle = \begin{cases} [\hat{S}^+]^{n/2}\,|0\rangle & \text{for } n \text{ even} \\ \hat{a}^+[\hat{S}^+]^{(n-1)/2}\,|0\rangle & \text{for } n \text{ odd} \end{cases}, \tag{5.38}$$

[9][39]. For reasons of space no detailed introduction into the syntax of Mathematica can be given here; however, Mathematica has a very good online-help system, including an interactive version of the standard reference [40]. The interested reader is also referred to the lecture notes [41] of a Mathematica-course held by the author of this work.

[10] Note that the usual definition of a two particle operator differs from (5.37) by a factor $1/\sqrt{2}$, which assures the correct normalization of $\langle n|n\rangle$ to "1". Introducing this factor in eq. (5.37) would change some of the commutation relations (5.42) by a factor $1/\sqrt{2}$ resp. 1/2. This, however, would require some extensions in the Mathematica-code, which have significant negative effects on the runtime performance of the code (see footnote 14) — hence these changes have not been implemented. Due to this the results provided by the code presented in this section are correct only except for a factor.

Taking this representation of the FOCK states $|n\rangle$ as a basis, the expressions focused on in the previous section are given by

- $$\langle n|n\rangle = \begin{cases} \langle 0|\,[\hat{S}]^{n/2}[\hat{S}^+]^{n/2}\,|0\rangle & \text{for } n \text{ even} \\ \langle 0|\,[\hat{S}]^{(n-1)/2}\hat{a}\,\hat{a}^+[\hat{S}^+]^{(n-1)/2}\,|0\rangle & \text{for } n \text{ odd} \end{cases} \tag{5.39}$$

- $$\langle n|\hat{\Psi}(x)|n+1\rangle = \begin{cases} \langle 0|\,[\hat{S}]^{n/2}\hat{\Psi}(x)\,\hat{a}^+[\hat{S}^+]^{n/2}\,|0\rangle & \text{for } n \text{ even} \\ \langle 0|\,[\hat{S}]^{(n-1)/2}\hat{a}\,\hat{\Psi}(x)[\hat{S}^+]^{(n+1)/2}\,|0\rangle & \text{for } n \text{ odd} \end{cases} \tag{5.40}$$

- $$\langle n|\hat{\Psi}^+(x)\hat{\Psi}(x')|n\rangle = \begin{cases} \langle 0|\,[\hat{S}]^{n/2}\hat{\Psi}^+(x)\hat{\Psi}(x')[\hat{S}^+]^{n/2}\,|0\rangle & \text{for } n \text{ even} \\ \langle 0|\,[\hat{S}]^{(n-1)/2}\hat{a}\,\hat{\Psi}^+(x)\hat{\Psi}(x')\,\hat{a}^+[\hat{S}^+]^{(n-1)/2}\,|0\rangle & \text{for } n \text{ odd} \end{cases} \tag{5.41}$$

Such expressions are evaluated by rewriting the operators enclosed in the vacuum states into *normal-ordered form*[11] using the following commutation relations:

$$\left[\hat{\Psi}(x_1),\hat{\Psi}^+(x_2)\right] = \delta(x_1-x_2) \tag{5.42a}$$

$$\left[\hat{a},\hat{a}^+\right] = 1 \tag{5.42b}$$

$$\left[\hat{S},\hat{S}^+\right] = 2 + 4\iiint dy_1dy_2dy_3\ \ \chi^*(y_1,y_2)\chi(y_1,y_3)\hat{\Psi}^+(y_3)\hat{\Psi}(y_2) \tag{5.42c}$$

$$\left[\hat{\Psi}(x_1),\hat{a}^+\right] = \phi(x_1) \tag{5.42d}$$

$$\left[\hat{\Psi}(x_1),\hat{S}^+\right] = 2\int dy\ \ \chi(y,x_1)\hat{\Psi}^+(y) \tag{5.42e}$$

$$\left[\hat{a},\hat{S}^+\right] = 2\iint dy_1dy_2\ \ \phi^*(y_1)\chi(y_1,y_2)\hat{\Psi}^+(y_2) \tag{5.42f}$$

These expressions elementarily follow from (5.36) and (5.37) using (2.10).

5.3.2 Realization using *Mathematica*

The key-idea is to formulate all (needed) mathematical structural operations comprised by the algebra and other mathematical objects as Mathematica-*(transformation) rules*, which are syntactically denoted by "`->`" or[12] "`:>`". If the left-hand side of a rule "`expr1 -> expr2`" resp. "`expr1 :> expr2`" is formulated as a so-called Mathematica-*pattern* — syntactically denoted by underscore characters

[11] An operator valued expression is said to be *normal-ordered*, if all creation operators are positioned to the left of the annihilation operators.

[12] The second form is a so-called *delayed* rule; the significance of the difference will become obvious below (footnote 18).

"_" (designation in Mathematica: "blank") — the rule will apply to a whole class of (sub-)expressions that are of the specified form. It turns out that repeated application of a set of such rules leads to the intended reformulation and simplification of the original expression.

The rules

The rules needed for handling the occurring expressions have been grouped according to their semantic meaning; in the following the rules will be presented and some syntactical details will be commented.

• General rules for NonCommutativeMultiply-expressions

Using the ordinary multiplication operator "*" (for convenience this can be abbreviated simply by using a space character: `a*b` $\hat{=}$ `a b`) Mathematica implicitly assumes commutativity[13]: `a b` $\hat{=}$ `b a`. Moreover, properties like associativity and distributivity are accounted for automatically.

For the non-commutative composition of two objects Mathematica provides the operator "**". However, only associativity is implemented by default for this Mathematica-operator — distributivity with respect to addition (line 2f) and general properties of multiplication of c-valued expressions (esp. integer-valued: lines 4ff)[14] have to be explicitly defined:

```
NCMrulesgeneral = {
  a_**(b_+c_)         -> a**b + a**c,
  (a_+b_)**c_         -> a**c + b**c,
4 a_Integer**b_       -> a b,
  a_**b_Integer       -> a b,
  a_**(b_Integer c_) -> b a**c,
  (a b_Integer)**c_  -> b a**c};
```

[13] Internally this is implemented by "Times" (this is the internal representation of "*") having the attribute "Orderless" as can be seen evaluating "Attributes[Times]".

[14] As discussed in footnote 10 the introduction of a factor $1/\sqrt{2}$ would lead to corresponding factors in some of the commutation relations. This requires an extension of the rules "NCMrulesgeneral" according to

```
    ..., a_Power**b_ -> a b, a_**b_Power -> a b,
         a_**(b_Power c_) -> b a**c, (a b_Power)**c_ -> b a**c, ...,
```

as "$\sqrt{2}$" is not of integer type but of type "Power" in Mathematica. Unfortunately, this leads to significantly worse runtime performance of the code as has been tested. The reason is that the rules "NCMrulesgeneral" are used in a (kind of) "inner loop" (see the function "ΨaSalgebra[...]" on p. 62) and thus are internally tested and (if necessary) applied *very* often by Mathematica.

• **Commutativity properties of $\phi(\cdot)$, $\chi(\cdot,\cdot)$ and the δ-function**

Like integer-valued expressions (lines 4-7) also the DIRAC delta "function"[15] — "$\delta(x-y)$" is represented in the following code by a two-argument function "δ[x, y]"— and the wave functions ϕ and χ (complex conjugation is denoted by a suffix "c": "ϕc", "χc") are c-valued with respect to non-commutative multiplication, which is implemented by:

```
δmult = {
  δ[x1_, x2_]**a_       -> δ[x1, x2] a,
  a_**δ[x1_, x2_]       -> δ[x1, x2] a,
  a_**(b_ δ[x1_, x2_])  -> δ[x1, x2] a**b,
  (a_ δ[x1_, x2_])**b_  -> δ[x1, x2] a**b};

φχmult = {
  φ[x1_]**a_            -> φ[x1] a,
  a_**φ[x1_]            -> φ[x1] a,
  a_**(b_ φ[x1_])       -> φ[x1] a**b,
  (a_ φ[x1_])**b_       -> φ[x1] a**b,
  φc[x1_]**a_           -> φc[x1] a,
  a_**φc[x1_]           -> φc[x1] a,
  a_**(b_ φc[x1_])      -> φc[x1] a**b,
  (a_ φc[x1_])**b_      -> φc[x1] a**b,
  χ[x1_, x2_]**a_       -> χ[x1, x2] a,
  a_**χ[x1_, x2_]       -> χ[x1, x2] a,
  a_**(b_ χ[x1_, x2_])  -> χ[x1, x2] a**b,
  (a_ χ[x1_, x2_])**b_  -> χ[x1, x2] a**b,
  χc[x1_, x2_]**a_      -> χc[x1, x2] a,
  a_**χc[x1_, x2_]      -> χc[x1, x2] a,
  a_**(b_ χc[x1_, x2_]) -> χc[x1, x2] a**b,
  (a_ χc[x1_, x2_])**b_ -> χc[x1, x2] a**b};
```

Annotations At first glance it might not look very elegant that the — from a *mathematical* point of view — *same* rules have to be explicitly formulated for integers, δ, ϕ, ϕc, χ and χc. One might have the idea to reduce the above list of rules by condensing the $\phi/\phi c$- (one-argument expressions) and $\delta/\chi/\chi c$-rules (two-argument expressions) like in the following example:

$$\left.\begin{matrix}\text{line 15}\\ \text{line 19}\end{matrix}\right\rangle \rightsquigarrow \texttt{phi\_[x1\_]**a\_ -> phi[x1] a}$$

Here not only the function's argument is formulated as a pattern, but also the name of the function itself. As intended, this rule definition covers both ϕ and ϕc as function names; the problem is that *all* one-argument expressions would be affected by this rule — i.e. also the *operators* $\hat{\Psi}(x)$ resp. $\hat{\Psi}^{+}(x)$ ("Ψop[x]", "Ψopad[x]"), which would lead to wrong results, of course.[16]

[15] Its properties as a distribution are implemented below (see p. 58).

[16] As in this specific example no *operators* having *two* arguments are involved, the rule-definitions for the two-argument functions χ and χc indeed could be condensed correspondingly; however, for reasons of code-uniformity and -extendability this has been refrained from.

• **Implementation of the commutation-relations (5.42) of $\hat{\Psi}$, $\hat{a}$ and $\hat{S}$**

As stated above, the basic aim persued is to obtain *normal ordering* of a given operator expression meaning that the position of *all* creation operators is in front of the annihilation operators. Using Mathematica this can simply be achieved by (explicitly) formulating a rule for any possible combination of two operators out of the given set of occurring operators (i.e. $\{\hat{\Psi}, \hat{\Psi}^+, \hat{a}, \hat{a}^+, \hat{S}, \hat{S}^+\}$ in this example[17]) with the rules being of the form:

□op**△opad -> △opad**□op + ...

Here the "..." indicate the particular expression for the value of the commutator. In detail, for the "$\hat{\Psi}/\hat{a}/\hat{S}$"-algebra this means:

```
ΨaScommutat = {
  Ψop[x1_]**Ψopad[x2_] -> Ψopad[x2]**Ψop[x1] + δ[x1, x2],
  Ψop[x1_]**aopad      -> aopad**Ψop[x1] + ϕ[x1],
34  Ψop[x1_]**Sopad      :> Sopad**Ψop[x1]
    + Module[{y}, 2 χ[y, x1] Ψopad[y]]
  aop**Ψopad[x1_]      -> Ψopad[x1]**aop + ϕc[x1],
  aop**aopad           -> aopad**aop + 1,
38  aop**Sopad           :> Sopad**aop
    + Module[{y1, y2}, 2 ϕc[y1] χ[y1, y2] Ψopad[y2]],
  Sop**Ψopad[x1_]      :> Ψopad[x1]**Sop
    + Module[{y}, 2 χc[y, x1] Ψop[y]],
42  Sop**aopad           :> aopad**Sop
    + Module[{y1, y2}, 2 ϕ[y1] χc[y1, y2] Ψop[y2]],
  Sop**Sopad           :> Sopad**Sop + 2
    + Module[{y1, y2, y3}, 4 χc[y1, y2] χ[y1, y3] Ψopad[y3]**Ψop[y2]]};
```

Annotations The implementation of the expressions containing integrals probably could have been realized "directly" using the internal "`Integral[...]`" Mathematica function. However, the advantage of improved readability of the code would have been bought at the expense of a more complex handling of the emerging Mathematica-expressions and thus by extended duration of calculations.

In the above code this has been bypassed by using so-called *modules*. Generally speaking, the `Module` command provides a kind of local environment typically used for the realization of "subroutines".
The first argument of `Module` is the list of *local variables* to be used in the subroutine; everytime the module is called Mathematica automatically creates new symbols having the name of the local variables followed by a suffix "`$...`", where "..." denotes an integer value specific for every new call of the module — in this way it is guaranteed that no conflicts between names of variables arise.
The list of local variables is followed by the actual subroutine's code; by standard the last command or expression thereof is interpreted as the return value that is exported to

[17] In the Mathematica code *creation (i.e. adjoint) operators* are denoted by the suffix "`opad`", whereas *annihilation operators* have "`op`" as suffix.

the calling code-level. All local variables appearing in this last command or expression are also exported and thus are available further on.

Noting that — from a structural point of view — (mathematical) integration variables are nothing else but "local" ("dummy") variables, the use of `Module` for automatically creating such integration dummy variables becomes obvious: Everytime one of the above rules containing a `Module`-command is applied, new unique integration variables are created[18]; even though integration is not *explicitly* indicated by a corresponding symbol ("$\int$" or the like), *indirectly* the user (or a parsing mechanism; see below) can unambiguously infer the integrals from the naming "...`$`..." of the integration variables.

• Implementation of properties of the δ-distribution

The essential property of the DIRAC delta distribution becomes evident by regarding its action on a test-function:

$$\int_{-\infty}^{\infty} dx\, \delta(x-y)\, f(x) = f(y) \tag{5.43}$$

δ`[x, y]` is the Mathematica representation of the delta distribution in the presented code, and the property (5.43) has been implemented by:

```
SetAttributes[δ, Orderless];

δeliminate = {δ[x1_, x2_] func_[x3___, x1_, x4___] :> func[x3, x2, x4]
49   /;((x1 =!= x)&&(x1 =!= xp))};
```

Annotations The rule in line 48 is the central command in this code segment: "`func`" represents a test function with *arbitrary* name — indicated by the single blank in "`func_`" — and *arbitrary* number of arguments: In Mathematica *two blanks* "`__`" denote a pattern that consists of any nonvanishing number of expressions (separated by commas); using *three blanks* "`___`", the case of matching zero expressions is also included. Thus the pattern "`func_[x3___, x1_, x4___]`" in line 48 effectively expresses that "`x1_`" can have arbitrary position as argument of "`func`". Consequently the above rule applies whenever an argument of a function matches an argument of a δ`[·, ·]`-expression; the *condition* in line 49 — in Mathematica conditions under which rules or patterns should be applied are formulated using "`/;`"[19] — assures that such an 'integration' (5.43) is only 'carried out', if this coinciding argument is *not*[20] one of

[18] Note the use of the operator "`:>`" ("`RuleDelayed`") instead of "`->`", which causes an evaluation of the whole rule-expression *everytime* the rule is applied (using "`->`", the `Module`-expressions would only be evaluated once, namely when evaluating the corresponding rule definition). This obviously is indispensable for the creation of unique integration variable-symbols for *every* commutating action carried out.

[19] Mind that the "...`Delayed`" version of the rule operator ("`:>`") has to be used here: Testing of the condition can only be carried out with the *current* values of the patterns for each application of the rule.

[20] "`=!=`" is the "`UnsameQ`"-operator, which yields "`True`" as result, if its arguments are *not* (exactly) matching each other.

the "non-dummy (-integration)" variables x *or*[21] x' ("`x`"; "`xp`" ('x prime')).

As $\delta(-x) = \delta(x)$, the action of δ`[·, ·]` may not depend on the order of the arguments; the "`SetAttributes[·, Orderless]`"-command provides a comfortable possibility to implement such a behaviour.

• Annihilation operators acting on the vacuum $|0\rangle$

Requiring the possibility of calculating expectation values $\langle 0|\cdots|0\rangle$, the specific action of creation-/annihilation-operators on the vacuum-bra $\langle 0|$ resp. -ket $|0\rangle$ (represented as "`zerobra`" resp. "`zeroket`") has to be implemented:

```
zerorules = {
  Ψop[x_]**zeroket   -> 0,
  aop**zeroket       -> 0,
53  Sop**zeroket       -> 0,
  zerobra**Ψopad[x_] -> 0,
  zerobra**aopad     -> 0,
  zerobra**Sopad     -> 0,
57  zerobra**zeroket   -> 1};
```

Annotations In addition to the action of the corresponding operators on the vacuum states (lines 51-56), the normalization condition for the vacuum state has been formulated in line 57 for convenience.

It is worth mentioning that the above rules have significant positive effect on the speed of calculations: As soon as a creation (annihilation) operator happens to directly act on a $\langle 0|$ ($|0\rangle$) from the right (left) after applying one of the commutating rules, it is clear that the whole corresponding addend — and *all* addends that would evolve by repeated application of the commutation relations! — vanish; thus the enhancement of speed results from preventing Mathematica from superfluously calculating expressions giving "0" anyhow.

• Pattern recognition of chain integrals

When applying the rules `ΨaScommutat` as defined in line 31-45 (i.e. the commutation relations of the $\hat{\Psi}/\hat{a}/\hat{S}$-algebra) to expressions of the type (5.39)-(5.41), the integrands of the emerging integrals typically consist of products of a huge number of $\phi^{(*)}(\cdot)$- and $\chi^{(*)}(\cdot,\cdot)$-functions, which all can be identified as being of *chain integral type* as introduced in sect. 5.2.
It is desirable to implement a kind of "pattern recognition" mechanism in Mathematica, which automatically identifies such chain integrals and replaces the corresponding lenthy and thus confusing expressions by convenient mnemonics. This can be realized by defining the rules presented below in line 61-114, where the following table facilitates the orientation in the code:

[21] To avoid a misunderstanding: "`&&`" is the operator of *logical "and"*.

lines ...	62	64-74	76f	79	81-83
implementation of eq. ...	(5.8b)	(5.27)	(5.33)	(5.7b)[6]	(5.28)
lines ...	85f	88-98	100-102	104-114	
implementation of eq. ...	(5.30)	(5.31)	(5.34)	(5.35)	

It follows the corresponding Mathematica code:

```
SetAttributes[χ, Orderless];
SetAttributes[χc, Orderless];

chainintegrals = {
  ϕc[x1_] ϕ[x1_] :> 1 /;((x1 =!= x)&&(x1 =!= xp)),

  χ[x1_, x2_] χc[x2_, x3_] :> chainχχc[x1, x3, 1]
    /;((x2 =!= x)&&(x2 =!= xp)),
  chainχχc[x1_, x2_ , n_Integer] chainχχc[x2_, x3_, m_Integer] :>
    chainχχc[x1, x3, n+m+1]
    /;((x2 =!= x)&&(x2 =!= xp)),
  χ[x1_, x2_] chainχχc[x3_, x2_, n_Integer] χc[x3_, x4_] :>
    chainχχc[x1, x4, n+2]
    /;((x2 =!= x)&&(x2 =!= xp)&&(x3 =!= x)&&(x3 =!= xp)),
  chainχχc[x1_, x1_, n_Integer] :>
    chainχχc[n+1]
    /;((x1 =!= x)&&(x1 =!= xp)),

  chainχχc[x1_, x2_, n_Integer] :> chainXχχcX[n, x1, x2]
    /;(((x1 === x)||(x1 === xp))&&((x2 === x)||(x2 === xp))),

  chainχχc[2] -> 1,

  ϕc[x1_] chainχχc[x1_, x2_, n_Integer] ϕ[x2_] :>
    chainϕcχχcϕ[n+2]
    /;((x1 =!= x)&&(x1 =!= xp)&&(x2 =!= x)&&(x2 =!= xp)),

  chainχχc[x1_, x2_, n_Integer] ϕ[x2_] :> chainXχχcϕ[n+1, x1]
    /;(((x1 === x)||(x1 === xp))&&(x2 =!= x)&&(x2 =!= xp)),

  χ[x1_, x2_] ϕc[x2_] :> chainXχχcχϕc[1, x1]
    /;(((x1 === x)||(x1 === xp))&&(x2 =!= x)&&(x2 =!= xp)),
  chainχχc[x1_, x2_, n_Integer] χ[x2_, x3_] ϕc[x3_] :>
    chainXχχcχϕc[n+2, x1]
    /;(((x1 === x)||(x1 === xp))&&(x2 =!= x)&&(x2 =!= xp)
    &&(x3 =!= x)&&(x3 =!= xp)),
  chainχχc[x1_, x2_, n_Integer] χ[x2_, x3_]
    chainχχc[x4_, x3_, m_Integer] ϕc[x4_] :>
      chainXχχcχϕc[n+m+3, x1]
      /;(((x1 === x)||(x1 === xp))&&(x2 =!= x)&&(x2 =!= xp)
      &&(x3 =!= x)&&(x3 =!= xp)&&(x4 =!= x)&&(x4 =!= xp)),
```

```
    ϕc[x1_] chainχχc[x1_, x2_, n_Integer] :>
101   chainϕcχχcX[n+1, x2]
      /;(((x2 === x)||(x2 === xp))&&(x1 =!= x)&&(x1 =!= xp)),

    ϕ[x1_] χc[x1_, x2_] :> chainϕχcχχcX[1, x2]
105   /;(((x2 === x)||(x2 === xp))&&(x1 =!= x) && (x1 =!= xp)),
    ϕ[x1_] χc[x1_, x2_] chainχχc[x2_, x3_, n_Integer] :>
      chainϕχcχχcX[n+2, x3]
      /;(((x3 === x)||(x3 === xp))
109   &&(x1 =!= x)&&(x1 =!= xp)&&(x2 =!= x)&&(x2 =!= xp)),
    ϕ[x1_] chainχχc[x2_, x1_, n_Integer]
      χc[x2_, x3_] chainχχc[x3_, x4_, m_Integer] :>
        chainϕχcχχcX[n+m+3, x4]
113     /;(((x4 === x)||(x4 === xp))&&(x1 =!= x)&&(x1 =!= xp)
        &&(x2 =!= x)&&(x2 =!= xp)&&(x3 =!= x)&&(x3 =!= xp))};
```

The abbreviations for the chain integrals follow the scheme "`chain...[···]`", where the order n of the multiple integral appears as an argument. A "`X`" in the name indicates a dependence of the integral on a spatial variable, which then appears as an additional argument.

Annotations Using the "`SetAttributes[·, Orderless]`"-command for "χ" and "χ`c`" (line 58f), one can tell Mathematica, that all possible permutations of the arguments of these functions are tried for pattern matching of rules which contain these functions.[22] Obviously, this is a comfortable way to implement the symmetry of "χ" and "χ`c`" with respect to its arguments.

Representative for all other types of chain integrals, the rules in line 64-77 for the recognition of chain integrals of the type $\tilde{I}_{\chi\chi^*;\,n}(x, x')$ (eq. (5.33)) and $I_{\chi\chi^*;\,n}$ (eq. (5.27)) are subsequently explained:

- **(A):** The fundamental rule in this context is the one in line 64f: Whenever in a product two functions "χ" and "χ`c`" have one argument coinciding, this has to be interpreted as "integration" over this argument as described on p. 57; thus this rule yields "`chainχχc[x1, x3, 1]`", which is nothing else but the chain integral $\tilde{I}_{\chi\chi^*;\,1}(x1, x3)$ from eq. (5.33). Note the condition ("`/. ...`") in line 65, which assures that "`x2`" is really a integration(-dummy) variable (see the corresponding discussion for the rule "δ`eliminate`" on page 58).

- **(B):** The rule in line 66-68 is the implementation of the following relation:

$$\int dx_2\; \tilde{I}_{\chi\chi^*;\,n}(x_1, x_2) \cdot \tilde{I}_{\chi\chi^*;\,m}(x_2, x_3) \equiv \tilde{I}_{\chi\chi^*;\,n+m+1}(x_1, x_3)$$

- **(C):** The rule in line 69-71 is necessary to handle a special case: For example, given the expression "χ`[x1, x2]` χ`[x5, x3]` χ^*`[x5, x2]` χ^*`[x3, x4]`",

[22] As an example: If the symbol "χ" is assigned the attribute "`Orderless`" the pattern "χ`[x_, y_]` ϕ`[y_]`" matches both the expression "χ`[x, y]` ϕ`[y]`" and "χ`[y, x]` ϕ`[y]`". Also see the annotations about "δ" on page 58.

the rule (A) from above *could* first yield "`chain[x1, x5, 1] chain[x5, x4, 1]`" and rule (B) finally "`chain[x1, x4, 3]`". However, the 'problem' is that rule (A) *could as well* yield "χ`[x1, x2] chain[x3, x2, 1]` χ^*`[x3, x4]`" first, which shows the necessity of rule (C).

- **(D):** The rule in line 72-74 finally "closes the chain":

$$\int dx_1 \, \tilde{I}_{\chi\chi^*,\, n-1}(x_1, x_1) = I_{\chi\chi^*,\, n}$$

with $I_{\chi\chi^*,\, n}$ as given by eq. (5.27).

- **(E):** The rule in line 76f finally handles the case that the first two arguments in an expression "`chain[x1, x2, n]`" are either x *or*[23] x' *both*, i.e. "non-dummy (-integration)" variables. The result "`chainX`$\chi\chi$`cX[n, x1, x2]`" denotes a chain integral of the type eq. (5.33).

Calculation of operator-normal ordering and expectation values

For convenience of simple application of the above rules a short function has been formulated:

```
ΨaSalgebra[expr_] := Module[{},
  (Expand[expr//.Flatten[{ΨaScommutat, NCMrulesgeneral,
    φχmult, δmult, zerorules}]]//.δeliminate)//.chainintegrals
118 ];
```

Annotations In Mathematica rules are applied to expressions by the operators "`/.`" ("ReplaceAll") or "`//.`" ("`ReplaceRepeated`"). The difference between these two Mathematica-operators is, that using "`/.`" replacements in a given expression are only carried out *once* wheras "`//.`" causes a *repeated application* of the rules until the resulting expression does not change anymore.

For the above problem "`//.`" is the adequate operator for obvious reasons. The first rules to be applied are given by the list enclosed by the "`Flatten`" command, which is needed solely for syntactical reasons[24]. Essentially, the arising expression already is the aspired final result — if one were not interested in removing the δ`[·, ·]`-expressions and parsing the chain integrals. However, before applying these rules it has to be guaranteed by using "`Expand`" that the whole expression is completely factored out with respect to normal (commutative) multiplication.[25]

[23] "`||`" is the operator of *logical "or"*.

[24] "`//.`" is acting as described only if its right-argument is a single, non-nested list; "`Flatten`" does nothing else but uniting a nested list structure to a single list.

[25] This could be effected equivalently by appling the rule "`a_*(b_+c_) -> a b + a c`".

Examples

Two examples should be sufficient for illustrating the use of the above code:

Calculation of normal ordering

The normal ordered form of $\hat{a}^+\hat{\Psi}^+(x)\hat{S}$ can be calculated by

```
ΨaSalgebra[aop**Ψop[x]**Sopad]
```

This results in the following Mathematica output[26]:

```
2 chainXχχcχϕc[1, x] + Sopad**aop**Ψop[x] +
2 Ψopad[y$22]**aop χ[x, y$22] +
2 Ψopad[y2$23]**Ψop[x] ϕc[y1$23] χ[y1$23, y2$23]
```

Calculation of expectation values resp. matrix elements

The expectation value of $\hat{\Psi}^+(x)\hat{\Psi}(x')$ for a three particle FOCK state is to be calculated ("$\langle 3|\hat{\Psi}^+(x)\hat{\Psi}(x')|3\rangle$"):

```
ΨaSalgebra[
  zerobra**Sop**aop**Ψopad[x]**Ψop[xp]**aopad**Sopad**zeroket]
```

Mathematica gives:

```
4 chainXχχcX[1, xp, x] + 4 chainXχχcχϕc[1, xp] chainϕχcχχcX[1, x] +
4 chainϕcχχcX[2, x] ϕ[xp] + 4 chainXχχcϕ[2, xp] ϕc[x] +
2 ϕ[xp] ϕc[x]
```

5.3.3 Limitations

Implementing adapted versions of the above code, many standard problems concerning operator normal-ordering can in principle be trusted to a computer performing the typically lenghty and monotonic calculations.

However, the probably most significant limitation here is the bad *runtime performance* of such calculations for expressions build up of more than a few operators[27] due to the exploding number of commutating-operations to be carried out. Moreover, once more it has to be emphasized that the computations performed using the above code are mere *structural manipulations* not making use of certain general facts and findings[28]; this implies that Mathematica does not

[26] As a matter of course, the names of the local variables' suffixes "`$...`" (see the discussion on page 57) vary from evaluation to evaluation of the expression.

[27] For the above example the calculation of expressions consisting of more than ≈ 20 operators (corresponding to FOCK states $|n\rangle$ with $n \approx 10$) is not accessible with acceptable runtime using a contemporary PC.

[28] As an example "$\langle n = 100|n' = 101\rangle = \langle 0|\hat{a}\ldots\hat{a}\hat{a}^+\ldots\hat{a}^+|0\rangle = 0$" is obvious even without any explicit calculation. However, such a general fact is not automatically recognized by the above code leading to effectively 'infinite' time needed for such a trivial problem.

provide *general mathematical rules* here — i.e. expressions like $\langle n|\hat{\Psi}(x)|n+1\rangle$ cannot be calculated for symbolic n. Nevertheless, the *explicit* calculation of results for only small values of n can be quite supportive for the user to obtain an idea of the structure of the arising expressions, of course; induction (or the like) may then be employed for a generalization of the results.

5.4 Discussion of the applicability of the model

Aiming at the investigation of solitonic states emerging in the model introduced in sect. 5.1, a superposition of the FOCK states $|n\rangle^{(\text{binary})}$ (eq. (5.25) resp. (5.38)) according to

$$|\psi\rangle^{(\text{binary})} = \sum_n a_n \, |n\rangle^{(\text{binary})} \tag{5.44}$$

has to be focused on.[29]

Like in chapter 4 for the BETHE solutions, the calculation of the expectation value of the field operator $\langle\psi|\hat{\Psi}(x)|\psi\rangle$ (sect. 4.2.1) and of correlation functions such as $g^{(1)}(x,x') \propto \langle\psi|\hat{\Psi}^+(x)\hat{\Psi}(x')|\psi\rangle$ (sect. 4.3) is desirable also for $|\psi\rangle =: |\psi\rangle^{(\text{binary})}$:

$$\langle\psi|\hat{\Psi}(x)|\psi\rangle = \sum_n a_n^* a_{n+1} \, \underline{\langle n|\hat{\Psi}(x)|n+1\rangle} \tag{5.45}$$

$$\langle\psi|\hat{\Psi}^+(x)\hat{\Psi}(x')|\psi\rangle = \sum_n |a_n|^2 \, \underline{\langle n|\hat{\Psi}^+(x)\hat{\Psi}(x')|n\rangle} \tag{5.46}$$

So far only the *structure* of the underlined matrix elements has been investigated: It was shown in sect. 5.2 that the resulting expressions are made up of a few types of chain integrals. However, the combinatorics arising turned out to be quite complicated — only small particle numbers n are accessible with the methods presented in the previous sections 5.2 and 5.3.
But even without the latter problem one would be faced with the difficulty of evaluating the chain integrals: For given value of n, corresponding chain integrals of *all* orders $m \leq n$ contribute to a particular matrix element (see sect. 5.2). Even for moderate values of n this is a considerable challenge:

- A *direct* numerical treatment, i.e. directly applying algorithms for numerical integration, is not possible as a chain integral of order m is a genuine multiple integral of m-th order, which cannot be separated into sub-integrals.

- An analytical treatment of the chain integrals has been tried: Both the

[29] See the analogous discussion for the BETHE states in sect. 4.2.1, which led to eq. (4.28).

one-particle wave function $\phi(\cdot)$ (cp. eq. (5.8a)) and the asymptotic form[30] of the two-particle wave function $\chi(\cdot,\cdot)$ (eq. (5.14), (5.15)) can be rewritten in terms of simple *exp*-functions. However, it is $\chi_{\mathrm{rel}}(r_i, r_j) = \chi_{\mathrm{rel}}(|r_i - r_j|)$ (cp. eq. (5.15)) and thus the region of integration has to be restricted to a simplex region for analytical evaluation as described in appendix B.1.1, B.2.1. This significantly complicates an analytical treatment as relations such as $\int_{-\infty}^{\infty} dx\ \exp(ikx) = 2\pi\,\delta(k)$ cannot be employed for simplification of the expressions due to the finite integration limits in 'simplex integrals'.[31]

5.5 Summary

The approximative model introduced in this chapter for a more realistic description of particle interactions for the limiting case of dilute gases turns out to be intractable for concrete calculations both numerically and analytically as discussed in the previous section.
However, the computeralgebraic methods developed for implementing the commutator-algebra of this model (sect. 5.3) can be regarded as a noteworthy 'spin-off' here, which should also be useful for related problems emerging in the framework of quantum field theory.

[30] Using the asymptotic form of the two-particle wave function $\chi(x_i, x_j)$ — which is valid for $|r_i - r_j| \gg \sigma$ (σ: effective extent of the interaction potential) — is a good approximation: Evaluating a multiple integral of n-th order, errors are made only in a small subspace $\sim \sigma^n$ of configuration space.

[31] However, an analogous relation exists for the case of semi-infinite region of integration: $\int_0^{\infty} dx\ \exp(ikx) = \pi\,\delta(k) + i/k \cdot \mathcal{P}$ [Here $\mathcal{P}$ denotes taking the principal value, when integrating over k]. Nevertheless, as has been tried, this relation does not lead to significant simplification of the 'simplex integrals'.

Chapter 6

Conclusion

In this thesis we focused on the the discussion of quantum-field theoretical models of solitons in Bose-Einstein condensates beyond the usual mean-field approaches.

In chapter 2 we have introduced the theory of Bose-Einstein condensation. In systems of ultracold, dilute gases particle interactions can be approximately described by s-wave scattering, which allows the introduction of the zero-range pseudo potential as model potential having the s-wave scattering length as only parameter. This leads to essential simplifications in the description of the system: In the Heisenberg picture a mean field approach leads to the fundamental Gross-Pitaevskii equation for the condensate's macroscpoic wave function. The nonlinear term in this equation arises from the particle interactions, and it is shown in chapter 3 that the Gross-Pitaevskii equation supports both dark and bright solitonic solutions.

In the Schrödinger picture the system is described by a n-particle Schrödinger equation with the wave function explicitly depending on the n position variables of the particles. Again, in this equation the mutual interactions of the n particles are explicitly given by the abovementioned zero-range pseudo potential in the ultracold, dilute limit. In chapter 4 the 1D version of this equation has been discussed for the case of attractive interactions: Considering the expectation value of the field operator, both a mean-field Hartree approach and the exact so-called Bethe ansatz have been shown to provide solutions of bright-soliton form for large particle numbers. Focusing on the exact Bethe solution, the soliton state arises as a superposition of eigenstates of the particle number and the total momentum operator, which has as a consequence both phase diffusion and dispersion effects. The latter leads to broadening of the soliton as genuine quantum field effect, which should be observable in experiments as has been estimated.
Moreover, certain matrix elements, which emerge when considering two point correlation functions for the soliton state, have been calculated for the Bethe states, thereby revealing interaction induced correlations. However, it turns out that for Bethe solitons quantities like the expectation value of the field operator and the two-point correlation functions are numerically intractable for large particle

numbers.

In chapter 5 the n-particle Schrödinger equation with the zero-range pseudo potential substituted by a more general potential is considered. This is intended to provide a more realistic description of particle interactions beyond the above-mentioned limiting case of $T \to 0$. Considering systems of dilute gases it has been shown that the restriction to binary interactions is a valid approximation. Consequently, a corresponding ansatz for the n-particle wave function separates into a product of (at most) *two*-particle wave functions. Initially it has been hoped to obtain an approximate framework that way, which is — in contrast to the Bethe model from above — applicable also in the case of large particle numbers. However, it turns out that the emerging expressions are intractable both analytically and numerically even for moderate particle numbers. In this context computer-algebraic methods for handling the commutator-algebra of this model have been developed, which are regarded to be useful also for related problems emerging in quantum field theory.

Summarizing, when describing systems of interacting particles with quantum field theoretical methods beyond a mean field/Hartree approach the concrete calculation of relevant quantities is promising at most for small particle numbers. In the case of high particle numbers one is typically confronted with an immense expenditure of calculations.

Appendix A

Inverse scattering method

A standard method of solving nonlinear partial differential equations (PDEs) is the "inverse scattering method". First applied to the so-called KORTEWEG-DE-VRIES-*(KdV-)-equation* $\partial_t u(x,t) = 6u(x,t)\partial_x u(x,t) - \partial_x^3 u(x,t)$ (KRUSKAL ET AL., [42]), the application to other nonlinear PDEs like the *nonlinear* SCHRÖDINGER-*equation (NLSE)*[1] $i\partial_t u(x,t) = -\partial_x^2 u(x,t) - \kappa|u(x,t)|^2 u(x,t)$ (ZAKHAROV, SHABAT, [18]) was successful.
The following is intended to give an overview over the principles of this method; for reasons of space the interested reader will be referred to literature for details of the calculations.

A.1 The principle

The basic idea of the inverse scattering method is to find the time-evolution $u = u(x,t)$ for a given initial condition $u_0 = u(x,0)$ *not* by solving the nonlinear partial differential equation (PDE) itself, but instead by searching for an appropriate *generalized "spectral"-transformation*, for which the spectral components of $u(x,t)$ obey simple time evolution equations; if this — crucial step — is successful, the solution $u = u(x,t)$ can be obtained from the spectral components by an inverse spectral transformation at time t.[2]

For the mentioned *KdV-equation* one is lead to the proper generalized spectral transformation by examining the quantum mechanical *scattering spectrum*, i.e. one has to study the eigenfunctions ψ and -energies λ of bound and free states for the scattering problem $[-\partial_x^2 + u(x,0)]\psi = \lambda\psi$ — thus the initial state $u(x,0)$ serves as a 'scattering potential' so to say. The equation for time-evolution of

[1] with $\kappa > 0$; cp. eq. (3.8) with permutation of the roles of the position- and time-variables.

[2] An analogue to this is the FOURIER-transform method for *linear* PDEs, by which a PDE is transformed into an algebraic equation for the FOURIER-(/"spectral-") components of the solution; using this equation, for a given FOURIER-spectrum of $u(x,0)$ the solution $u(x,t)$ can be obtained by inverse FOURIER-transform (cp. eg. [14] (chap. 4.3.7)).

the eigenfunctions then reduces to a *linear* PDE, that can be solved relatively easily[3]. The solution $u = u(x,t)$ is then obtained by using the scattering-data at time t for deducing the "scattering potential" $u(x,t)$; for this *"inverse scattering problem"* (this is the origin of the method's name) adequate equations can be found in the literature (eg. [43] (chap. 4.6)).
The proper spectral transformation for the *nonlinear Schrödinger equation* — in contrast to the KdV-equation — does not lead to a quantum mechanical scattering problem, but to another eigenvalue problem ([18]).[4] However, the basic principle of the method is the same.

A.2 The Lax-formalism

The abstract-formal formulation of the inverse scattering method, which reveals its general principles, was succesfully done by LAX in 1968 ([44]; cf. also [43] (chap. 5) and [18]); a short review hereof will be given in the following.

Every nonlinear PDE can be represented as

$$\partial_t u = \hat{S}[u] \tag{A.1}$$

with a nonlinear operator $\hat{S}$ and a function $u = u(x,t)$.

Examples: It is $\hat{S}[u] = 6u\partial_x u - \partial_x^3 u$ for the KdV-equation and

$$\hat{S}[u] = i\partial_x^2 u + i\kappa|u|^2 u \tag{A.2}$$

for the NLSE.

If eq. (A.1) can be equivalently formulated in the form

$$\partial_t \hat{L} = [\hat{L}, \hat{A}] := \hat{L}\hat{A} - \hat{A}\hat{L} \tag{A.3}$$

with a linear, Hermitian (/self-adjoint/symmetric) operator $\hat{L}$ and a linear, antihermitian operator $\hat{A}$, the inverse scattering method is applicable for the given $\hat{S}$ in principle. Finding such operators $\hat{L}$ and $\hat{A}$ is the crucial problem of the method. Moreover, it is $\hat{L} = \hat{L}[u]$ and $\hat{A} = \hat{A}[u]$, of course.

Examples: In the case of the KdV-equation (A.3) is equivalent to (A.1), if $\hat{L} = -\partial_x^2 + u$ (as mentioned above this is the operator of a scattering problem in the true sense) and $\hat{A} = 4\partial_x^3 - 6u\partial_x - 3(\partial_x u) - 4i\sqrt{\lambda^3}$.[5]

[3] For the inverse scattering problem of the KdV equation one not even has to explicitly solve for the time-dependence of the states, but only for some characteristic quantities (reflection-, transmission-coefficients etc., cp. [43] (chap. 4.5)).

[4] Strictly speaking, the name "inverse *scattering* method" is suitable only for the treatment of the KdV-equation, but nevertheless also established itself for other nonlinear PDEs.

[5] This can be checked elementarily; explicit calculations can be found eg. in [43] (p. 81).

For the NLSE one has the following matrix-valued differential operators (see [18], eq. (5) ib.):

$$\hat{L} = i \begin{bmatrix} 1+p & 0 \\ 0 & 1-p \end{bmatrix} \partial_x + \begin{bmatrix} 0 & u^* \\ u & 0 \end{bmatrix} \tag{A.4a}$$

$$\hat{A} = -ip \begin{bmatrix} 1 & 0 \\ 0 & 1 \end{bmatrix} \partial_x^2 + \begin{bmatrix} i|u|^2/(1+p) & -u^*_{|x} \\ u_{|x} & -i|u|^2/(1-p) \end{bmatrix} \tag{A.4b}$$

Without loss of generality the parameter p ($0 < |p| \leq 1$) has been introduced by $\kappa = 2/(1-p^2)$. Moreover, a special notation for denoting partial differentiation has been used: $\partial_x(\dots) =: (\dots)_{|x}$.
Using these operators, elementary calculations yield for eq. (A.3) [notation $\partial_t(\dots) =: (\dots)_{|t}$]:

$$\partial_t \hat{L} = \begin{bmatrix} 0 & u^*_{|t} \\ u_{|t} & 0 \end{bmatrix} = \begin{bmatrix} 0 & -i\, u^*_{|x\,|x} - i\, \frac{2}{1-p^2}\, |u|^2 u^* \\ i\, u_{|x\,|x} + i\, \frac{2}{1-p^2}\, |u|^2 u & 0 \end{bmatrix} = [\hat{L}, \hat{A}] \tag{A.5}$$

Considering the elements of this matrix equation, this is indeed equivalent to eq. (A.1) with $\hat{S}$ from (A.2).

The generalized "scattering problem" now can be formulated as

$$\hat{L}\psi = \lambda\psi \tag{A.6}$$

It can be shown — and that is essential — that the *eigenvalue-spectrum* of the operator $\hat{L}$ — though $\hat{L}$ itself is time-dependent via $u = u(x,t)$ — is time-*in*dependent:

$$\partial_t \lambda = 0 \tag{A.7}$$

and that the time-evolution of the eigenstates $\psi = \psi(t)$ hence is very simple:

$$\partial_t \psi = -\hat{A}\psi \tag{A.8}$$

proof: To see this, (A.6) is differentiated and rewritten:

$$\begin{aligned} \hat{L}_{|t}\psi + \hat{L}\psi_{|t} = \lambda_{|t}\psi + \lambda\psi_{|t} \Longleftrightarrow \lambda_{|t}\psi &\overset{(A.3)}{=} (\hat{L}-\lambda)\psi_{|t} + (\hat{L}\hat{A} - \hat{A}\hat{L})\psi \\ &\overset{(A.6)}{=} (\hat{L}-\lambda)\psi_{|t} + \hat{L}\hat{A}\psi - \hat{A}\lambda\psi \\ &= (\hat{L}-\lambda)(\psi_{|t} + \hat{A}\psi) \end{aligned} \tag{A.9}$$

Taking the *inner product* (notation: $(\dots,\dots)$) with ψ and making use of the hermiticity of $\hat{L}$ ("$(*)$") indeed (A.7) is reproduced because of ψ being normed ($(\psi,\psi) = 1$):

$$\lambda_{|t}(\psi,\psi) = (\psi, (\hat{L}-\lambda)(\psi_{|t} + \hat{A}\psi)) \overset{(*)}{=} ((\hat{L}-\lambda)\psi, \psi_{|t} + \hat{A}\psi) \overset{(A.6)}{=} (0, \psi_{|t} + \hat{A}\psi) = 0$$

Using this in (A.9) provides:

$$(\hat{L} - \lambda)(\psi_{|t} + \hat{A}\psi) = 0$$

This means that the expression $\psi_{|t} + \hat{A}\psi$ is an eigenfunction of $\hat{L}$ with λ as eigenvalue; thus $\psi_{|t} + \hat{A}\psi = \alpha\psi$ with α as proportionality constant. Except for an additive constant[6] α this is (A.8) indeed: $\psi_{|t} = (-\hat{A} + \alpha)\psi$. □

To sum up, the strategy of finding a solution to (A.1) for a given initial condition $u_0 = u(x, 0)$ is to solve the $\hat{L}$-eigenvalue equation (A.6) with $u = u_0$, then to use the rather simple equation (A.8) for determining the time-dependence of ψ and to finally focus on the "inverse scattering problem", i.e. to calculate $u(x, t)$ using the information given by the eigenfunctions ψ at time t — general methods have been developed therefor.[7]

Finally a remarkable correlation between the properties of the eigenvalue-spectrum and the soliton solutions should be mentioned: It turns out that the discrete part of the eigenvalue spektrum ("bound states") of (A.6) has influence on the character of the soliton solutions, wheras the continuous part corresponds to "dispersive waves" ('background'): Starting with an initial function $u_0 = u(x, 0)$ in general a kind of 'superposition' of a soliton solution and dispersive waves will be observable, where the dispersive wave-background spreads out over the whole space and vanishes for $t \to \infty$ — only a soliton solution will survive; quite remarkable, this soliton is of N-th order, exactly if (A.6) has N discrete eigenvalues for $u = u_0$. If u_0 already is an exact soliton-solution, no dispersive waves at all show, of course.[8]

[6] The additive constant α disappears for a rescaling according to $\psi \to e^{\alpha t}\psi$.

[7] Without going into details it has to be remarked that in concrete calculations an explicit solution for $\psi = \psi(t)$ using (A.8) is not necessary, as only derived quantities (generalized reflection-/transmission-coefficients etc.) enter the "inverse scattering-formula" (cp. footnote 3).

[8] This case is also reflected in the properties of the eigenvalue spectrum of (A.6): For example, an exact soliton solution as initial condition $u = u_0$ corresponds to a "reflectionless potential" in the NLSE, cp. p. 19.

Appendix B

Calculations to chapter 4; Applying "simplex integration"

In this chapter some explicit calculations to chapter 4 are carried out — both complementing the corresponding (rather terse) calculations presented in the paper of Lai and Haus [33] and extending it by a method for the calculation of correlation functions. Here special emphasis of the description will be placed on "simplex integration" as a method to avoid trouble caused by integrands containing absolute values "$|\dots|$".

B.1 Normalization of the states $|n,p\rangle$: $\langle n',p'|n,p\rangle$

It is $\langle n',p'|n,p\rangle \propto \delta_{n,n'}$, as states of different particle number involve an unequal number of (creation/annihilation) operators. Thus it is sufficient to regard:

$$\langle n,p'|n,p\rangle \overset{(4.22a)}{=} \frac{1}{n!}\int_{-\infty}^{\infty}\cdots\int_{-\infty}^{\infty} dx_1'\cdots dx_n' dx_1\cdots dx_n$$
$$\cdot f^*_{n,p'}(x_1',\dots,x_n') f_{n,p}(x_1,\dots,x_n)\ \underline{\langle 0|\hat\Psi(x_n')\cdots\hat\Psi(x_1')\hat\Psi^+(x_1)\cdots\hat\Psi^+(x_n)|0\rangle} \tag{B.1}$$

Before explicitly calculating the integral the underlined operator expression has to be evaluated. As $\hat\Psi(\cdot)|0\rangle = 0$, it can be equivalently written by introducing commutators in the following way:

$$\langle 0|\left[\hat\Psi(x_n'),\dots\left[\hat\Psi(x_2'),\left[\hat\Psi(x_1'),\hat\Psi^+(x_1)\cdots\hat\Psi^+(x_n)\right]\right]\right]|0\rangle \tag{B.2}$$

Repeated application of the relation $\big[\hat{A},\hat{B}\hat{C}\big] = \big[\hat{A},\hat{B}\big]\hat{C} + \hat{B}\big[\hat{A},\hat{C}\big]$ yields:

$$\begin{aligned}
&\Big[\hat{\Psi}(x_1'), \hat{\Psi}^+(x_1)\cdots\hat{\Psi}^+(x_n)\Big] \\
&\qquad \overset{(2.10a)}{=} \sum_{i_1=1}^{n} \delta(x_1' - x_{i_1})\, \hat{\Psi}^+(x_1)\cdots\hat{\Psi}^+(x_{i_1-1})\hat{\Psi}^+(x_{i_1+1})\cdots\hat{\Psi}^+(x_n) \\
&\qquad \equiv \sum_{i_1=1}^{n} \delta(x_1' - x_{i_1}) \prod_{\substack{j=1\\ j\neq i_1}}^{n} \hat{\Psi}^+(x_j) \qquad \text{(B.3)}
\end{aligned}$$

Repeated use of this relation one finally obtains for (B.2):

$$\begin{aligned}
&\langle 0|\hat{\Psi}(x_n')\cdots\hat{\Psi}(x_1')\hat{\Psi}^+(x_1)\cdots\hat{\Psi}^+(x_n)|0\rangle \\
&\qquad = \sum_{i_1=1}^{n}\sum_{\substack{i_2=1\\ i_2\neq i_1}}^{n} \cdots \sum_{\substack{i_n=1\\ i_n\neq\{i_1,i_2,\ldots,i_{n-1}\}}}^{n} \delta(x_1' - x_{i_1})\cdots\delta(x_n' - x_{i_n}) \\
&\qquad = \sum_{\{\mathcal{P}\}} \delta(x_1' - x_{\mathcal{P}(1)})\cdots\delta(x_n' - x_{\mathcal{P}(n)}) \qquad \text{(B.4)}
\end{aligned}$$

Here the notation in the last line denotes a sum over all possible, i.e. $n!$ permutations of $[1,\ldots,n]$ as described in the context of (4.16).

Using (B.4) in eq. (B.1), the sum over $n!$ permutations turns out to yield the same value for each addent, as $f_{n,p}$ is a symmetric function of its arguments. Thus:

$$\langle n,p'|n,p\rangle = \frac{1}{n!}\, n! \int_{-\infty}^{\infty}\cdots\int_{-\infty}^{\infty} dx_1\cdots dx_n\; f^*_{n,p'}(x_1,\ldots,x_n) f_{n,p}(x_1,\ldots,x_n) \qquad \text{(B.5)}$$

B.1.1 Integration over a simplex region

Generally, if the integration region of an integral is the whole $\mathbb{R}^n$ and the integrand is *symmetric* in the integration variables ("symmetric integral with symmetric integrand"), the value of the integral can equivalently be obtained by restricting the integration region to a so-called *simplex region* $x_{\mathcal{P}(1)} \leq x_{\mathcal{P}(2)} \leq \cdots x_{\mathcal{P}(n)}$ and multiplying the resulting value by "$n!$", which is the number of such simplex subregions of the $\mathbb{R}^n$.

This fact is obviously helpful for the above integral (B.5): Inserting $f_{n,p}$ from (4.19), the integrand contains the expression $\sum_{1\leq i<j\leq n}|x_j - x_i|$. Obviously, restricting the integration region to the simplex $x_1 \leq \cdots \leq x_n$ has the advantage

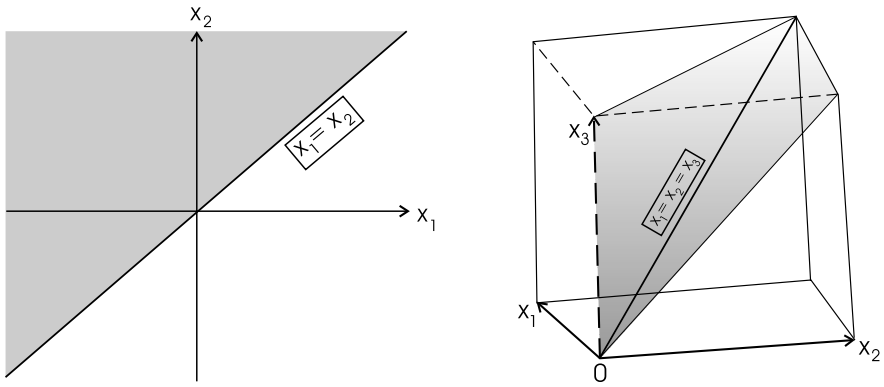

Figure B.1: Illustration of the simplex region $x_1 \leq x_2$ of the $\mathbb{R}^2$ (left) and the three dimensional simplex $x_1 \leq x_2 \leq x_3$ of the $\mathbb{R}^3$ (right).

of getting rid of the *abs*-function:

$$\langle n, p'|n, p\rangle = \mathcal{N}_n^2\, n! \int_{-\infty}^{\infty} dx_n \int_{-\infty}^{x_n} dx_{n-1} \ldots \int_{-\infty}^{x_2} dx_1 \cdot \exp\left(\sum_{j=1}^{n} \Big[\underbrace{\left(\tfrac{|\kappa|}{2}(n-2j+1) + i(p-p')\right)}_{=:\, l(j)} x_j \Big] \right) \tag{B.6}$$

where (4.18) has been used for $f_{n,p}$.
The integrations in (B.6) can be carried out elementarily[1]:

$$\langle n, p'|n, p\rangle = \mathcal{N}_n^2\, n! \int_{-\infty}^{\infty} dx_n \, \frac{\exp\left[\left(\sum_{j=1}^{n} l(j)\right) x_n\right]}{\prod_{r=1}^{n-1}\left(\sum_{j=1}^{r} l(j)\right)} \tag{B.7a}$$

$$\overset{[39]}{=} \mathcal{N}_n^2\, n! \int_{-\infty}^{\infty} dx_n \, \frac{\exp\left[(in(p-p'))\, x_n\right]}{\prod_{r=1}^{n-1}\left(r\left[\frac{|\kappa|}{2}(n-r) + i(p-p')\right]\right)} \tag{B.7b}$$

Using the relations $\int_{-\infty}^{\infty} dx \exp(in(p-p')x) = \frac{2\pi}{n}\delta(p-p')$ and $\prod_{r=1}^{n-1}[r(n-r)] = [(n-1)!]^2$, the value (4.26) of the normalization factor is obtained finally. □

[1] The integrals vanish at the lower boundaries "$-\infty$", as $\Re\left(\sum_{j=1}^{k} l(j)\right) \geq 0$ for $k \leq n$.

B.2 Matrix element $\langle n, p'|\hat{\Psi}(x)|n+1, p\rangle$

Inserting the representation (4.22a) of the states $|n, p\rangle$ in $\langle n, p'|\hat{\Psi}(x)|n+1, p\rangle$, the following operator expression is produced:

$$\langle 0|\hat{\Psi}(x'_n)\cdots\hat{\Psi}(x'_1)\hat{\Psi}(x)\hat{\Psi}^+(x_1)\cdots\hat{\Psi}^+(x_{n+1})|0\rangle$$
$$= \sum_{\{\mathcal{P}\}} \delta(x'_1 - x_{\mathcal{P}(1)})\cdots\delta(x'_n - x_{\mathcal{P}(n)})\delta(x - x_{\mathcal{P}(n+1)}), \quad \text{(B.8)}$$

The second line is proven in a similar way to the corresponding operator expression (B.4) in the previous section. Note that $\sum_{\{\mathcal{P}\}}$ is a sum over $(n+1)!$ permutations here.
Making use of the symmetry of the many-particle wave function, this gives

$$\langle n, p'|\hat{\Psi}(x)|n+1, p\rangle$$
$$= \frac{(n+1)!}{\sqrt{n!(n+1)!}} \int_{-\infty}^{\infty}\cdots\int_{-\infty}^{\infty} dx_1\cdots dx_n\ f^*_{n,p'}(x_1,\ldots,x_n) f_{n+1,p}(x_1,\ldots,x_n,x)$$
$$\overset{(4.19)}{=} \sqrt{n+1}\mathcal{N}_n\mathcal{N}_{n+1}\exp(ipx)$$
$$\cdot \underline{\int_{-\infty}^{\infty}\cdots\int_{-\infty}^{\infty} dx_1\cdots dx_n\ \exp\left(i(p-p')\sum_{j=1}^{n} x_j - \frac{|\kappa|}{2}\sum_{1\le i<j\le n}|x_j - x_i|\right)}$$
$$\underline{\cdot\exp\left(-\frac{|\kappa|}{4}\sum_{j=1}^{n}|x - x_j|\right)} \quad \text{(B.9)}$$

B.2.1 Simplex integration: Subdivision of the simplex region (one external variable)

In contrast to the situation in the preceding section a simple restriction of the integration region to a simplex is not sufficient for handling the integral in (B.9): In the expression $\sum_{j=1}^{n}|x - x_i|$ the argument of the *abs* function has no definite sign for integration over a *whole* simplex. However, subdividing the simplex $-\infty \le x_1 \le \cdots \le x_n \le \infty$ into (n+1) regions according to

$$\bigcup_{m=0}^{n}\{-\infty \le x_1 \le \cdots x_m \le x \le x_{m+1} \le \cdots x_n \le \infty\} \quad \text{(B.10)}$$

assures that $(x - x_i)$ has a definite sign in each of these regions. Fig. B.2 depicts the situation for the simple case of two-dimensional integration.

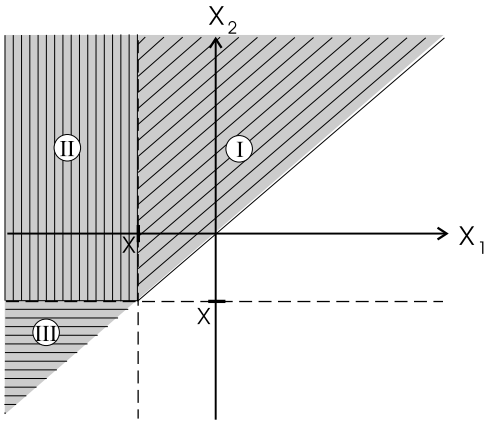

◯	m	2D simplex subregion
I	0	$x \le x_1 \le x_2 \le \infty$
II	1	$-\infty \le x_1 \le x \le x_2 \le \infty$
III	2	$-\infty \le x_1 \le x_2 \le x$

Figure B.2: Subdivision of a two-dimensional simplex (one external variable "x") according to (B.10).

Applying this subdivision, the integral in (B.9) (underlined) can be rewritten as $n!$ times the following "simplex integral":

$$\sum_{m=0}^{n} \int_{-\infty}^{x} dx_m \int_{-\infty}^{x_m} dx_{m-1} \ldots \int_{-\infty}^{x_2} dx_1 \int_{x}^{\infty} dx_{m+1} \int_{x_{m+1}}^{\infty} dx_{m+2} \ldots \int_{x_{n-1}}^{\infty} dx_n$$

$$\exp\Bigg(\sum_{j=1}^{n} \Big[\Big(\frac{|\kappa|}{2}(n-2j+1) + i(p-p') \Big) x_j \Big] \Bigg)$$

$$\cdot \exp\Bigg(-\frac{|\kappa|}{4} \Big[\underbrace{\sum_{j=1}^{m}(x-x_j) + \sum_{j=m+1}^{n}(x_j-x)}_{=[m-(n-m)]x-\sum_{j=1}^{m}x_j+\sum_{j=m+1}^{n}x_j} \Big] \Bigg)$$

$$= \sum_{m=0}^{n} \exp\Big(-\frac{|\kappa|}{4}(2m-n)\,x \Big) \cdot \mathcal{I}_1^m(x) \cdot \mathcal{I}_{m+1}^n(x), \tag{B.11}$$

where the integration separates into two subintegrals, which are given by[2]:

$$\mathcal{I}_1^m(x) = \int_{-\infty}^{x} dx_m \int_{-\infty}^{x_m} dx_{m-1} \ldots \int_{-\infty}^{x_2} dx_1 \exp\Big(\sum_{j=1}^{m} l_1(j) x_j \Big)$$

$$= \exp\Big[\Big(\sum_{j=1}^{m} l_1(j) \Big) x \Big] \Big/ \prod_{r=1}^{m} \Big(\sum_{j=1}^{r} l_1(j) \Big) \tag{B.12a}$$

[2]The calculations leading to (B.12a) and (B.12b) are completely analogous to those carried out in the context of (B.7a).

$$\mathcal{I}^n_{m+1}(x) = \int_x^\infty dx_{m+1} \int_{x_{m+1}}^\infty dx_{m+2} \ldots \int_{x_{n-1}}^\infty dx_n \exp\Big(\sum_{j=m+1}^{n} l_2(j) x_j\Big)$$

$$= (-1)^{n-m} \exp\left[\Big(\sum_{j=m+1}^{n} l_2(j)\Big) x\right] \Big/ \prod_{r=1}^{n-m} \Big(\sum_{j=n-(r-1)}^{n} l_2(j)\Big) \qquad \text{(B.12b)}$$

Here the abbreviations $l_1(j) = \frac{|\kappa|}{2}(n-2j+3/2)+i(p-p')$ and $l_2(j) = \frac{|\kappa|}{2}(n-2j+1/2)+i(p-p')$ have been introduced. Carrying out the sums explicitly (using eg. [39]) one obtains:

$$\mathcal{I}^m_1(x) = \frac{\exp\left[mx\left(\frac{|\kappa|}{2}(n-m+\frac{1}{2})+i(p-p')\right)\right]}{\prod_{r=1}^{m}\left(r\left[\frac{|\kappa|}{2}(n-r+\frac{1}{2})+i(p-p')\right]\right)} \qquad \text{(B.13a)}$$

$$\mathcal{I}^n_{m+1}(x) = (-1)^{n-m} \frac{\exp\left[(n-m)x\left(-\frac{|\kappa|}{2}(m+\frac{1}{2})+i(p-p')\right)\right]}{\prod_{r=1}^{n-m}\left(r\left[-\frac{|\kappa|}{2}(n-r+\frac{1}{2})+i(p-p')\right]\right)} \qquad \text{(B.13b)}$$

Using (B.11) with (B.13) for the calculation of $\langle n, p'|\hat{\Psi}(x)|n+1, p\rangle$ as given by (B.9), the result can be rewritten[3] to (4.27a) finally. □

B.2.2 Approximations for large particle number n

The *exact* result (4.27a) can be simplified for the case of large particle numbers as will be discussed in the following.

Consider the subsequent subexpression of (4.27a):

$$\prod_{r=1}^{n}\left[\frac{1}{(2r-1)^2+\frac{16}{|\kappa|^2}(p-p')^2}\right] \cdot \underbrace{2^{2n}\, n!(n-1)!}_{=(2^n n!)^2/n}$$

Rearranging the products this can be rewritten to:

$$\frac{1}{n}\prod_{r=1}^{\infty}\left[\frac{(2r-1)^2}{(2r-1)^2+\frac{16}{|\kappa|^2}(p-p')^2}\right] \cdot \left(\frac{2^n\, n!}{\prod_{r=1}^{n}[2r-1]}\right)^2 \cdot \prod_{r=n+1}^{\infty}\left[1+\frac{\frac{16}{|\kappa|^2}(p-p')^2}{(2r-1)^2}\right] \qquad \text{(B.14)}$$

[3]The explicit calculations can be found in the paper of Lai and Haus [33]. It was decided in this section only to focus on the aspects of simplex integration in more detail.

n	(lhs of (B.16))/$\sqrt{n\pi}$	lhs of (B.17) with $a = 5$
1	1.12838	49.538
5	1.02527	3.3175
10	1.01257	1.8555
20	1.00627	1.3656
50	1.00250	1.1331
100	1.00125	1.0645
200	1.00063	1.0317
500	1.00025	1.0126
1000	1.00013	1.0063

Table B.1: For the judgement of the quality of the approximative relations (B.16), (B.17). *(calculated using [39])*

This representation allows the application of the following three relations:

- $$\prod_{r=1}^{\infty} \frac{(2r-1)^2}{(2r-1)^2+a^2} \overset{\text{eg. [39]}}{=} \operatorname{sech}(\tfrac{1}{2}\pi a) \quad \textit{product representation of sech} \tag{B.15}$$
- $$\frac{(2n)!!}{(2n-1)!!} := \frac{2^n n!}{\prod_{r=1}^{n}(2r-1)} \xrightarrow{n\to\infty} \sqrt{n\pi} \quad \textit{(Wallis formula)} \tag{B.16}$$
- $$\prod_{r=n+1}^{\infty} \left(1 + \frac{a^2}{(2r-1)^2}\right) \xrightarrow{n\to\infty} 1 \tag{B.17}$$

Using these relations for (B.14) with $a = \frac{4}{|\kappa|}(p - p')$, the approximative result (4.27b) for the matrix element is obtained. □

Quality of the approximations

The error that is made by substituting the left-hand sides of (B.16)f with the approximative right-hand sides depends on the value of n and becomes less serious for large n as can be seen from table B.1:

- Obviously the Wallis formula (B.16) is a very good approximation even for very small values of n.
- For (B.17) a typical value[4] of $a = 5$ has been chosen. Unfortunately, this approximation is not as good as the previously discussed one: Relative errors of $\lesssim 5\%$ are made only, if $n \gtrsim 130$.

[4]This value is "typical" with regard to the later use of $\langle n, p'|\hat{\Psi}(x)|n+1, p\rangle$ for the calculation of the expectation value $\langle\psi|\hat{\Psi}(x)|\psi\rangle$ according to (B.18): As is clear from the discussion of (B.24)f, the region of integration of $p_1 \propto (p - p')$ actually does not excess values $(p - p') \lesssim |\kappa|$, if (B.24) is fulfilled. Thus $a = 5$ is a reasonable assumption for this special application of the matrix element.

B.3 Expectation value $\langle\psi|\hat{\Psi}(x)|\psi\rangle$

The expression to be calculated is:

$$\langle\psi|\hat{\Psi}(x)|\psi\rangle(t) \overset{(4.28)}{=} \sum_{n=0}^{\infty} a_n^* a_{n+1} \underline{\iint_{-\infty}^{\infty} dp\, dp'\; g_n^*(p') g_{n+1}(p)\, \langle n, p'|\hat{\Psi}(x)|n+1, p\rangle(t)}, \tag{B.18}$$

where $\langle n', p'|\hat{\Psi}(x)|n, p\rangle \propto \delta_{n,n'+1}$ has already been used for removing one summation.
Using (4.32) for the momentum distribution, (4.27b) for the matrix element[5] and (4.24), (4.20) for the time dependence of the latter, the integral (underlined) in (B.18) can be rewritten to

$$\begin{aligned}\iint dp\, dp'\; \frac{1}{(\Delta p)\sqrt{\pi}} \exp\left(-\frac{(p'-p_0)^2+(p-p_0)^2}{2(\Delta p)^2}\right) \exp\left(i[np'-(n+1)p]\, x_0\right) \\ \cdot \sqrt{\frac{n(n+1)}{2|\kappa|}} \exp\left(i\frac{|\kappa|^2}{16} n(n+1)\, t\right) \exp\left(-i[(n+1)p^2 - np'^2]\, t\right) \\ \cdot \exp\left(i[(n+1)p - np']\, x\right) \operatorname{sech}\left(\frac{2\pi}{|\kappa|}(p-p')\right)\end{aligned} \tag{B.19}$$

The argument of the *sech* function implies a transformation of the momentum variables according to

$$p_1 = \tfrac{1}{2}(p-p') \tag{B.20}$$

$$p_2 = \tfrac{1}{2}(p+p') \tag{B.21}$$

$$\frac{\partial(p,p')}{\partial(p_1,p_2)} = 2 \quad \textit{(functional determinant)} \tag{B.22}$$

This yields for (B.19):

$$\begin{aligned}&\frac{2}{(\Delta p)\sqrt{\pi}} \sqrt{\frac{n(n+1)}{2|\kappa|}} \exp\left(i\frac{|\kappa|^2}{16} n(n+1)\, t\right) \\ &\cdot \int_{-\infty}^{\infty} dp_2 \exp\left(-\frac{(p_2-p_0)^2}{(\Delta p)^2}\right) \exp\left(i[p_2(x-x_0) - p_2^2 t]\right) \\ &\cdot \int_{-\infty}^{\infty} dp_1 \exp\left(\underline{-\frac{p_1^2}{(\Delta p)^2}} + ip_1\left[2(n+\tfrac{1}{2})(x-x_0-2p_2 t)\right] \underline{-ip_1^2\, t}\right) \operatorname{sech}\left(\frac{4\pi}{|\kappa|} p_1\right)\end{aligned} \tag{B.23}$$

[5]Note that (4.27b) is an approximation not valid for small values of n, which causes an error in the summation of (B.18).

The underlined expressions in the integral over p_1 are negligible under the following conditions:

- *Gaussian* $\exp\left(-p_1^2/(\Delta p)^2\right)$*:* If

$$\Delta p \gg |\kappa| \tag{B.24}$$

  (i.e. the Gaussian is much broader than the *sech* function), the Gaussian is virtually constant (and has the value ≈ 1) in the region of integration, in which the integrand gives essential contribution to the value of the integral.

- *Phase factor* $\exp(-ip_1^2\,t)$*:* For times short enough, i.e.

$$\left[\min(\Delta p, |\kappa|)\right]^2 t \overset{(B.24)}{=} |\kappa|^2\, t \ll 1, \tag{B.25}$$

  higher order dispersion effects caused by this phase factor can be neglected. (B.25) results from the fact the region of integration is effectively given by the width of the *sech*, if (B.24) is fulfilled.

Under these conditions the integral over p_1 essentially represents a Fourier transform of the *sech* function: $\int_{-\infty}^{\infty} dp\ \exp(ipy)\ \mathrm{sech}(cp) = \frac{\pi}{c}\,\mathrm{sech}\left(\frac{\pi}{2c}\,y\right)$. This yields:

$$\begin{aligned}\langle\psi|\hat{\Psi}(x)|\psi\rangle(t) \approx \sum_{n=0}^{\infty} a_n^* a_{n+1} \frac{1}{(\Delta p)\sqrt{\pi}} \sqrt{\frac{n(n+1)}{8}}\,\sqrt{|\kappa|}\,\exp\left(i\frac{|\kappa|^2}{16}n(n+1)\,t\right)\\ \cdot \int_{-\infty}^{\infty} dp_2 \exp\left(-\frac{(p_2-p_0)^2}{(\Delta p)^2}\right)\exp\left(ip_2(x-x_0)-p_2^2 t\right)\\ \cdot \mathrm{sech}\left(\frac{|\kappa|}{4}(n+\tfrac{1}{2})(x-x_0-2p_2 t)\right)\end{aligned} \tag{B.26}$$

Dropping the subscript on p_2 and inserting the Poissonian distribution (4.31) for a_n, (4.33) is obtained finally. □

B.4 Matrix element $\langle n, p'|\hat{\Psi}^+(x)\hat{\Psi}(x')|n, p\rangle$

The operator expression emerging for $\langle n, p'|\hat{\Psi}^+(x)\hat{\Psi}(x')|n, p\rangle$ yields:

$$\begin{aligned}&\langle 0|\hat{\Psi}(x'_n)\cdots\hat{\Psi}(x'_1)\hat{\Psi}^+(x)\underbrace{\hat{\Psi}(x')\hat{\Psi}^+(x_1)\cdots\hat{\Psi}^+(x_n)}_{\overset{(B.3)}{=}\sum_{i=1}^{n}\delta(x'-x_i)\ \prod_{j=1,j\neq i}^{n}\hat{\Psi}^+(x_j)}|0\rangle\\ &\qquad = \sum_{i=1}^{n}\delta(x'-x_i)\cdot\sum_{\{\mathcal{P}\}}\delta(\widetilde{x}_1-x'_{\mathcal{P}(1)})\cdots\delta(\widetilde{x}_n-x'_{\mathcal{P}(n)})\end{aligned} \tag{B.27}$$

After applying (B.3) for the underbraced subexpression as hinted, the resulting expression $\propto \langle 0|\hat{\Psi}(x'_n)\cdots\hat{\Psi}(x'_1)\hat{\Psi}^+(x)\prod_{j=1,j\neq i}^{n}\hat{\Psi}^+(x_j)|0\rangle$ can be rewritten using (B.4), which yields the second line. Here the new variables $[\widetilde{x}_1,\ldots,\widetilde{x}_n] := [x_1,\ldots,x_{i-1},x,x_{i+1},\ldots,x_n]$ (i.e. the variable x_i is replaced by x) have been introduced for notational convenience.
Due to the symmetry of the many-particle wave function the $n\cdot n!$ addends resulting from (B.27) give the same value when using it in $\langle n, p'|\hat{\Psi}^+(x)\hat{\Psi}(x')|n+1, p\rangle$; one thus finds:

$$
\begin{aligned}
&\langle n, p'|\hat{\Psi}^+(x)\hat{\Psi}(x')|n, p\rangle \\
&\quad = n\int_{-\infty}^{\infty}\cdots\int_{-\infty}^{\infty} dx_1\cdots dx_{n-1}\; f^*_{n,p'}(x_1,\ldots,x_{n-1},x)f_{n,p}(x_1,\ldots,x_{n-1},x') \\
&\quad \overset{(4.19)}{=} n\,\mathcal{N}_n^2\exp\big(i(px'-p'x)\big) \\
&\qquad \cdot\int_{-\infty}^{\infty}\cdots\int_{-\infty}^{\infty} dx_1\cdots dx_{n-1}\;\exp\left(i(p-p')\sum_{j=1}^{n-1}x_j - \frac{|\kappa|}{2}\sum_{1\le i<j\le n-1}|x_j-x_i|\right) \\
&\qquad\qquad \cdot\exp\left(-\frac{|\kappa|}{4}\sum_{j=1}^{n-1}\big[|x-x_j|+|x'-x_j|\big]\right)
\end{aligned}
\tag{B.28}
$$

B.4.1 Simplex integration: Subdivision of the simplex region (two external variables)

Similar to the situation described in section B.2.1 one is faced with the need of finding a proper subdivision of the simplex region to avoid the *abs* functions in the integrand of (B.28). Assuming $x \le x'$ without loss of generality[6], for the simplex $-\infty \le x_1 \le \cdots \le x_{n-1} \le \infty$ this is achieved by the a subdivision according to:[7]

$$
\bigcup_{\substack{k,m=0\\ k\le m}}^{n-1}\{-\infty\le x_1\le\cdots x_k\le x\le x_{k+1}\le\cdots\le x_m\le x'\le x_{m+1}\le\cdots x_{n-1}\le\infty\}
\tag{B.29}
$$

Integrating over a symmetric integrand this subdivision results into the following

[6] It can be shown that the matrix element $\langle n, p'|\hat{\Psi}^+(x)\hat{\Psi}(x')|n, p\rangle$ actually is dependent on $|x-x'|$ only, as the BETHE states are solutions to a free space problem.

[7] For $k = m$ (B.29) has to be read as $\{-\infty \le x_1 \le \cdots x_k \le x \le x' \le x_{k+1} \le \cdots x_{n-1} \le \infty\}$.

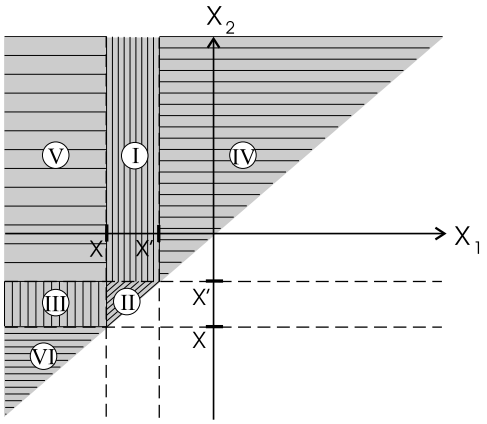

◯	(k,m)	2D simplex subregion
I	$(0,1)$	$x \le x_1 \le x' \le x_2 \le \infty$
II	$(0,2)$	$x \le x_1 \le x_2 \le x'$
III	$(1,2)$	$-\infty \le x_1 \le x \le x_2 \le x'$
IV	$(0,0)$	$x' \le x_1 \le x_2 \le \infty$
V	$(1,1)$	$-\infty \le x_1 \le x$ $\wedge\, x' \le x_2 \le \infty$
VI	$(2,2)$	$-\infty \le x_1 \le x_2 \le \infty$

Figure B.3: Subdivision of a two-dimensional simplex (two external variables "x, x'") according to (B.29).

expression for the "simplex integral"[8]:

$$\int_{-\infty}^{\infty}\cdots\int_{-\infty}^{\infty} dx_1\cdots dx_{n-1}\Big(\dots\Big)$$

$$= (n-1)!\sum_{\substack{k,m=0\\ k\le m}}^{n-1}\int_{-\infty}^{x} dx_k\int_{-\infty}^{x_k} dx_{k-1}\dots\int_{-\infty}^{x_2} dx_1\int_{x}^{x'} dx_m\int_{x}^{x_m} dx_{m-1}\dots\int_{x}^{x_{k+2}} dx_{k+1}$$

$$\cdot\int_{x'}^{\infty} dx_{m+1}\int_{x_{m+1}}^{\infty} dx_{m+2}\dots\int_{x_{n-2}}^{\infty} dx_{n-1}\Big(\dots\Big) \qquad \text{(B.30)}$$

Applying this subdivision of the simplex region, it is assured that the arguments of the *abs*-expressions in (B.28) have a definite sign in each subregion and thus can be rewritten in a similar way as hinted in (B.11). Performing simple calculations, the integral in (B.28) (underlined) can be rewritten as:

$$(n-1)!\sum_{\substack{k,m=0\\ k\le m}}^{n-1}\exp\left(-\frac{|\kappa|}{4}\Big[-x(n-2k-1)-x'(n-2m-1)\Big]\right)$$

$$\cdot\,\mathfrak{I}_1^k(x)\cdot\mathfrak{I}_{k+1}^m(x,x')\cdot\mathfrak{I}_{m+1}^{n-1}(x'), \qquad \text{(B.31)}$$

[8]Following footnote 7, for the case $k = m$ the "simplex integral" (B.30) has to be read as "$\int_x^{x'} dx_m \int_x^{x_m} dx_{m-1}\dots\int_x^{x_{k+2}} dx_{k+1}$" being omitted.

where the integration separates into three subintegrals, which are given by:

- $$\mathcal{I}_1^k(x) = \int_{-\infty}^{x} dx_k \int_{-\infty}^{x_k} dx_{k-1} \ldots \int_{-\infty}^{x_2} dx_1 \cdot \exp\left(\sum_{j=1}^{k} \Big[\underbrace{\Big(\frac{|\kappa|}{2}(n-2j+1) + i(p-p') \Big)}_{=:\, l_A(j)} x_j \Big] \right) \quad \text{(B.32a)}$$

- $$\mathcal{I}_{k+1}^m(x, x') = \int_{x}^{x'} dx_m \int_{x}^{x_m} dx_{m-1} \ldots \int_{x}^{x_{k+2}} dx_{k+1} \cdot \exp\left(\sum_{j=k+1}^{m} \Big[\underbrace{\Big(\frac{|\kappa|}{2}(n-2j) + i(p-p') \Big)}_{=:\, l_B(j)} x_j \Big] \right) \quad \text{(B.32b)}$$

- $$\mathcal{I}_{m+1}^{n-1}(x') = \int_{x'}^{\infty} dx_{m+1} \int_{x_{m+1}}^{\infty} dx_{m+2} \ldots \int_{x_{n-2}}^{\infty} dx_{n-1} \cdot \exp\left(\sum_{j=m+1}^{n-1} \Big[\underbrace{\Big(\frac{|\kappa|}{2}(n-2j-1) + i(p-p') \Big)}_{=:\, l_C(j)} x_j \Big] \right) \quad \text{(B.32c)}$$

These integrals are calculated in the following.

The integrals $I_1^k(x)$ and $\mathcal{I}_{m+1}^{n-1}(x')$

These two integrals are essentially of the same type as the integrals (B.12a) and (B.12b), which emerged in the context of the calculation of $\langle n, p'|\hat{\Psi}(x)|n+1, p\rangle$ in section B.2. Analogous calculations lead to the subsequent results:

$$\mathcal{I}_1^k(x) = \frac{\exp\left[kx \left(\frac{|\kappa|}{2}(n-k) + i(p-p') \right) \right]}{k! \left[\frac{|\kappa|}{2} \right]^k \prod_{r=1}^{k} \left[(n-r) + \frac{2i}{|\kappa|}(p-p') \right]} \quad \text{(B.33)}$$

$$\mathcal{I}_{m+1}^{n-1}(x') = \frac{\exp\left[(n-m-1)x' \left(-\frac{|\kappa|}{2}(m+1) + i(p-p') \right) \right]}{(n-m-1)! \left[\frac{|\kappa|}{2} \right]^{n-m-1} \prod_{r=1}^{n-m-1} \left[(n-r) - \frac{2i}{|\kappa|}(p-p') \right]} \quad \text{(B.34)}$$

The integral $\mathfrak{I}^m_{k+1}(x, x')$

Carrying out the substitutions $y_i = x_i - x$ for the integration variables and performing the renaming $y_i \to y_{i-k}$ ($i \in \{k+1, \ldots, m\}$), the integral (B.32b) is transformed to a standard representation[9]:

$$C \cdot \int_0^y dy_N \int_0^{y_N} dy_{N-1} \ldots \int_0^{y_2} dy_1 \exp\left(\sum_{j=1}^{N} [\underbrace{l_B(j+k)}_{=:\, l(j)} y_j] \right) =: C \cdot \mathfrak{I}_N(y), \qquad \text{(B.35)}$$

where it has been introduced $y := x' - x$, $N := m - k$ and

$$C \;:=\; \exp\Big(\sum_{j=k+1}^{m} l_B(j) x \Big) \qquad \text{(B.36)}$$

$$\overset{[39]}{=} \exp\left((m-k)x \left[\frac{|\kappa|}{2}(n-m-k-1) + i(p-p') \right] \right) \qquad \text{(B.37)}$$

Unlike the integrals (B.32a), (B.32c), which vanish at one of its limits, (B.32b) and its standard form (B.35) do not. This complicates a direct integration for the case of general k, m — thus another method for its calculation is desirable.

Derivation of a recursion relation As only *exp*-functions are involved one can easily find that $\mathfrak{I}_N(y)$ is of the following general form:

$$\mathfrak{I}_N(y) := f_{N,1}\, e^{[l(1)+\cdots+l(N)]\, y} + f_{N,2}\, e^{[l(2)+\cdots+l(N)]\, y} + \cdots + f_{N,N}\, e^{[l(N)]\, y} + g_N$$

$$\equiv \sum_{j=1}^{N} \left[f_{N,j} \cdot \exp\Big(\sum_{r=j}^{N} l(r)\, y \Big) \right] + g_N, \qquad \text{(B.38)}$$

This ansatz defines the $f_{N,j}$ ($j \in \{1, \ldots, N\}$) as coefficients of the *exp*-terms and g_N as an integration constant.

Taking the derivative provides a *recursion relation* for the $\mathfrak{I}_N$:

$$\frac{\partial \mathfrak{I}_N(y)}{\partial y} = \exp\big(l(N)\, y\big) \cdot \mathfrak{I}_{N-1}(y) \qquad \text{(B.39)}$$

Inserting the ansatz (B.38) into (B.39) one is lead to the following recursion relations for the coefficients in (B.38):

$$f_{N-1,j} = f_{N,j} \cdot \sum_{r=j}^{N} l(r) \quad \overset{\sum_{r=j}^{N} l(r) \neq 0}{\Rightarrow} \quad f_{N,j} = \frac{f_{N-1,j}}{\sum_{r=j}^{N} l(r)} \quad \text{for } j = \{1, \ldots, N-1\} \qquad \text{(B.40a)}$$

$$g_{N-1} = f_{N,N} \cdot l(N) \quad \overset{l(N) \neq 0}{\Rightarrow} \quad f_{N,N} = \frac{g_{N-1}}{l(N)} \qquad \text{(B.40b)}$$

[9] (B.32b) is advantageous for exlicit calculations, as the lower limits of the integrations have the value "0".

Solution Explicit calculation of the integrals $\mathfrak{I}_N(y)$ using [39] suggests the subsequent representation of the integration constants:[10]

$$g_N = \frac{(-1)^N}{\prod_{t=1}^{N}\left[\sum_{r=t}^{N} l(r)\right]} \tag{B.41}$$

Taking the g_N as given, the recursion relations (B.40) can be employed for the calculation of the coefficients $f_{N,j}$ with $j = N$:

$$f_{N,N} \overset{(B.40b)}{=} \frac{g_{N-1}}{l(N)} = \frac{(-1)^{N-1}}{l(N)} \cdot \frac{1}{\prod_{t=1}^{N-1}\left[\sum_{r=t}^{N-1} l(r)\right]} \tag{B.42}$$

and with $1 \leq j < N$:

$$\begin{aligned} f_{N,j} &\overset{(B.40a)}{=} \frac{f_{N-1,j}}{\sum_{r=j}^{N} l(r)} \overset{(B.40a)}{=} \frac{1}{\sum_{r=j}^{N} l(r)} \cdot \frac{f_{N-2,j}}{\sum_{r=j}^{N-1} l(r)} \\ &\overset{(B.40a)}{=} \dots \overset{(B.40a)}{=} \frac{f_{j,j}}{\prod_{t=1}^{N-j}\left[\sum_{r=j}^{N+1-t} l(r)\right]} \\ &\overset{(B.42)}{=} \frac{(-1)^{j-1}}{l(j)} \cdot \frac{1}{\underline{\prod_{t=1}^{N-j}\left[\sum_{r=j}^{N+1-t} l(r)\right]} \cdot \prod_{t=1}^{j-1}\left[\sum_{r=t}^{j-1} l(r)\right]} \end{aligned} \tag{B.43}$$

Following the convention that products like the one underlined in (B.43) simply give a factor "1" as contribution by definition, if the upper limit is smaller than the lower limit, one notes that the validity of (B.43) can formally be extended to the case $j = N$.
Inserting (B.41) and (B.43) into the general ansatz (B.38) and reintroducing $l(l) \to l_B(j + k)$ (cp. (B.35)) one is finally lead to:

[10] A rigorous proof using *induction* or the like is omitted here. However, g_N has been introduced as an integration constant in eq. (B.38) and consequently is determined by $\mathfrak{I}_N(0) = 0$ (see eq. (B.35)). Thus the g_N have to fulfill the relation

$$g_N \overset{!}{=} -\sum_{i=1}^{N} f_{N,j},$$

which follows from eq. (B.38)) for $y = 0$. Inserting the expressions (B.41) for g_N and (B.43) for $f_{N,j}$, this relation has been extensively checked heuristically for different concrete values of N with [39].

$$\mathfrak{I}_N(y) =$$

$$\sum_{j=1}^{N}\left[\frac{(-1)^{j-1}\,\exp\Big[\overbrace{\Big(\sum_{r=j}^{N} l_B(r+k)\Big)}^{=:\mathfrak{S}(j,N)}\,y\Big]}{l_B(j+k)\Big[\prod_{t=1}^{N-j}\underbrace{\Big(\sum_{r=j}^{N+1-t} l_B(r+k)\Big)}_{=:\mathfrak{S}(j,N+1-t)}\Big]\Big[\prod_{t=1}^{j-1}\underbrace{\Big(\sum_{r=t}^{j-1} l_B(r+k)\Big)}_{=:\mathfrak{S}(t,j-1)}\Big]}\right]$$

$$+\frac{(-1)^N}{\prod_{t=1}^{N}\underbrace{\Big(\sum_{r=t}^{N} l_B(r+k)\Big)}_{=:\mathfrak{S}(t,N)}} \tag{B.44}$$

Here the abbreviation $\mathfrak{S}(a,b)$ has been introduced to denote the sum

$$\mathfrak{S}(a,b) = \sum_{r=a}^{b} l_B(r+k) \tag{B.45}$$

$$= (b-a+1)\left[\frac{|\kappa|}{2}(n-2k-a-b)+i(p-p')\right], \tag{B.46}$$

where (B.46) is the result, if $l_B(j)$ from (B.32b) is inserted in (B.45).

Final result

Summarizing all the previous results [i.e. (B.31) in (B.28) with $I_1^k(x)$ given by (B.33), $\mathfrak{I}_{m+1}^{n-1}(x')$ given by (B.34) and $\mathfrak{I}_{k+1}^{m}(x,x')$ given by (B.35); $\mathcal{N}_n$ from (4.26)], the final result can be rewritten to:

$$\langle n,p'|\hat{\Psi}^{+}(x)\hat{\Psi}(x')|n,p\rangle = \frac{n!(n-1)!}{2\pi}\exp\Big(i(px'-p'x)\Big)$$

$$\cdot\sum_{\substack{k,m=0\\ k\le m}}^{n-1}\Bigg[\frac{1}{k!(n-m-1)!\left[\frac{|\kappa|}{2}\right]^{k-m}}$$

$$\cdot\frac{\mathfrak{I}_{m-k}(x'-x)}{\Big[\prod_{r=1}^{k}\Big((n-r)+\frac{2i}{|\kappa|}(p-p')\Big)\Big]\Big[\prod_{r=1}^{n-m-1}\Big((n-r)-\frac{2i}{|\kappa|}(p-p')\Big)\Big]}$$

$$\cdot\exp\Big(-\frac{|\kappa|}{4}(x'-x)\left[2m(n-m-1)+(n-1)\right]$$

$$+i(p-p')\left[mx+(n-m-1)x'\right]\Big)\Bigg], \tag{B.47}$$

where $\mathfrak{I}_{m-k}(x'-x)$ is given by (B.44).

B.5 Matrix element $\langle n,p'|\hat{\Psi}^+(x)\hat{\Psi}^+(x')\hat{\Psi}(x')\hat{\Psi}(x)|n,p\rangle$

Similar methods as those that lead to (B.28) in the previous section can also be used for evaluating the matrix element $\langle n, p'|\hat{\Psi}^+(x)\hat{\Psi}^+(x')\hat{\Psi}(x')\hat{\Psi}(x)|n, p\rangle$. This expression emerges in the context of the two-point spatial correlation function of second order as defined on p. 37. The corresponding result here is:

$$\begin{aligned}
&\langle n, p'|\hat{\Psi}^+(x)\hat{\Psi}^+(x')\hat{\Psi}(x')\hat{\Psi}(x)|n, p\rangle \\
&\quad = n(n-1) \\
&\qquad \cdot \int_{-\infty}^{\infty}\cdots\int_{-\infty}^{\infty} dx_1\cdots dx_{n-2}\; f^*_{n,p'}(x_1,\ldots,x_{n-2},x,x') f_{n,p}(x_1,\ldots,x_{n-2},x,x') \\
&\overset{(4.19)}{=} n(n-1)\,\mathcal{N}_n^2 \exp\big(i(p-p')\,(x+x')\big)\,\exp\Big(-\frac{|\kappa|}{2}\,|x'-x|\Big) \\
&\qquad \cdot \int_{-\infty}^{\infty}\cdots\int_{-\infty}^{\infty} dx_1\cdots dx_{n-2}\;\exp\left(i(p-p')\sum_{j=1}^{n-2}x_j - \frac{|\kappa|}{2}\sum_{1\le i<j\le n-2}|x_j-x_i|\right) \\
&\qquad\qquad \cdot \exp\left(-\frac{|\kappa|}{2}\sum_{j=1}^{n-2}\big[|x-x_j|+|x'-x_j|\big]\right) \qquad \text{(B.48)}
\end{aligned}$$

Except for some factors and the fact that the integration extends only over $n-2$ variables, this expression is essentially the same as (B.28) for the matrix element $\langle n, p'|\hat{\Psi}^+(x)\hat{\Psi}(x')|n, p\rangle$. Thus it can be calculated completely analogously. Omitting details of the derivation, the final result turns out to be of the following form:

$$\begin{aligned}
&\langle n, p'|\hat{\Psi}^+(x)\hat{\Psi}^+(x')\hat{\Psi}(x')\hat{\Psi}(x)|n, p\rangle = \frac{n!(n-1)!}{2\pi} \\
&\quad \cdot \sum_{\substack{k,m=0\\ k\le m}}^{n-2}\Bigg[\frac{1}{k!(n-m-2)!\,\big[\frac{|\kappa|}{2}\big]^{k-m-1}} \\
&\qquad \cdot \frac{\mathcal{I}_{m-k}(x'-x)}{\Big[\prod_{r=1}^{k}\Big((n-r)+\frac{2i}{|\kappa|}(p-p')\Big)\Big]\Big[\prod_{r=1}^{n-m-2}\Big((n-r)-\frac{2i}{|\kappa|}(p-p')\Big)\Big]} \\
&\qquad \cdot \exp\Big(-\frac{|\kappa|}{2}(x'-x)\,[m(n-m-2)+(n-1)] \\
&\qquad\qquad + i(p-p')\,[(m+1)x+(n-m-1)x']\Big)\Bigg] \qquad \text{(B.49)}
\end{aligned}$$

$\mathfrak{I}_N(y)$ (third line of (B.49)) is given by (B.44) again, though $l_B(j)$ is a slightly different function here:

$$l_B := \frac{|\kappa|}{2}(n-2j-1) + i(p-p') \tag{B.50}$$

Thus, also the concrete form of the sum expression $\mathfrak{S}(a,b)$ (generally given by (B.45)) changes:

$$\mathfrak{S}(a,b) = (b-a+1)\left[\frac{|\kappa|}{2}(n-2k-a-b-1) + i(p-p')\right], \tag{B.51}$$

Appendix C

Bound states of realistic interaction potentials

In chapter 4 a n-particle system with the zero-range pseudo potential as *model potential* for atomic interactions has been discussed: In such a system the BETHE ansatz provides exact solutions (see eq. (4.19)), which can be regarded as a kind of "bound states" of the zero-range pseudo potential in the multidimensional configuration space. It is interesting to compare this result with *real* bound states of *realistic interaction potentials* — this comparison is discussed in detail in sect. 5.1.3.

In this appendix a numerical approach ('method of imaginary-time propagation') for the calculation of a 1D two-particle bound state (ground state) is presented[1], where the so-called LENNARD-JONES potential serves as model potential for the atomic interactions; following [8] (p. 26f) this potential provides a good parametrization for real interatomic potentials of alkali atoms and is widely used as model potential due to its simplicity.

C.1 The Lennard-Jones model potential

The LENNARD-JONES potential

$$V_{\mathrm{LJ}}(r) = 4\epsilon \left[\left(\frac{\sigma}{r}\right)^{12} - \left(\frac{\sigma}{r}\right)^{6} \right] \tag{C.1}$$

is parametrized by two parameters: "ϵ" specifies the depth of the minimum and "σ" determines the position of the minimum and the typical width of the potential (see fig. C.1).

The Hamiltonian describing two particles with mass m each in an external harmonic potential (trap frequency ω) and with LENNARD-JONES interaction

[1] As a slight generalization the presence of an additional external trapping potential will be discussed.

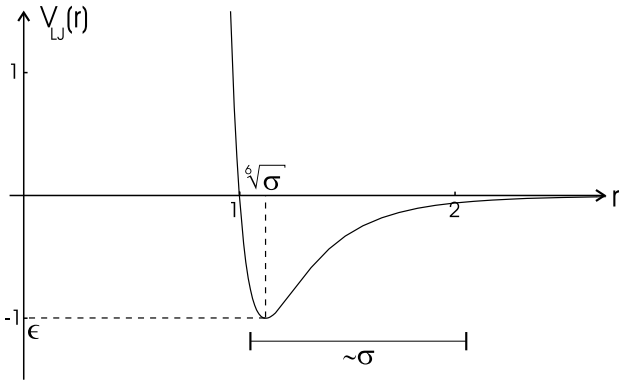

Figure C.1: LENNARD-JONES potential (C.1) for $\epsilon = 1 = \sigma$.

potential is:

$$\hat{H} = -\frac{\hbar^2}{2m}(\partial_{x_1}^2 + \partial_{x_2}^2) + \frac{m\omega^2}{2}(x_1^2 + x_2^2) + V_{\mathrm{LJ}}(|x_1 - x_2|) \tag{C.2}$$

Changing to center-of-mass/relative ("cm/rel") coordinates

$$R := \frac{1}{2}(x_1 + x_2), \quad r := x_1 - x_2, \tag{C.3}$$

(C.2) separates:

$$\begin{aligned} \hat{H} &= \hat{H}_{\mathrm{cm}} + \hat{H}_{\mathrm{rel}} \\ &:= \left[-\frac{1}{2}\frac{\hbar^2}{2m}\partial_R^2 + 2\frac{m\omega^2}{2}R^2\right] + \left[-2\frac{\hbar^2}{2m}\partial_r^2 + \frac{1}{2}\frac{m\omega^2}{2}r^2 + V_{\mathrm{LJ}}(r)\right] \end{aligned} \tag{C.4}$$

Center-of-mass motion Substituting $R = R_0\,\overline{R}$ with $R_0 = \sqrt{\hbar/(2m\omega)}$, the scaled center-of-mass Hamiltonian becomes $\hat{\overline{H}}_{\mathrm{cm}} = \frac{\hbar\omega}{2}\left(\partial_{\overline{R}}^2 + \overline{R}^2\right)$, which describes a simple harmonic oscillator problem with solutions analytically known from standard quantum mechanics ($\propto$ HERMITE polynomials times $\exp(-x^2/2)$).

The problem of relative motion remains to be solved; in the following the numerical implementation used for calculating the ground-state will be outlined.

C.2 Relative motion: Numerical implementation

As can be seen from (C.4) two potentials enter $\hat{H}_{\mathrm{rel}}$:

- A harmonic part with an *oscillator length* $r_{\mathrm{HO}} = \sqrt{2\hbar/(m\omega)}$ as typical length scale.

- The LENNARD-JONES part with the width σ as typical length scale.

σ is of the order of nm or less, whereas r_{HO} is in the μm-range for traps in typical experiments. Expecting the ground state of the relative problem to have negative energy, it will essentially be the ground state of the LENNARD-JONES part and thus have an extent of the order of σ.
Consequently, for numerical convenience a rescaling to dimensionless units according to $\overline{r} = r/r_0$ with $r_0 = \sigma$ is advisable and leads to[2]:

$$\hat{\overline{H}}_{\mathrm{rel}} = \frac{\hbar^2}{m\sigma^2}\left[-\partial_{\overline{r}}^2 + \underbrace{\frac{m^2\omega^2\sigma^4}{4\hbar^2}}_{\approx 3.5\cdot 10^{-15}}\overline{r}^2 + \overbrace{\underbrace{\frac{4\epsilon m\sigma^2}{\hbar^2}}_{\approx 1.6\cdot 10^{5}}\left(\frac{1}{\overline{r}^{12}} - \frac{1}{\overline{r}^{6}}\right)}^{:=\overline{V}_{\mathrm{LJ}}(\overline{r})}\right] \tag{C.5}$$

This clearly shows that for the problem of relative motion — at least from a *numerical* point of view — the harmonic oscillator part is completely negligible, if one is interested only in the ground state. The harmonic part only affects the behaviour of the solution for $r \to \infty$, but, however, in a numerically irrelevant way.
Thus the Hamiltonian that will be investigated numerically in the following is given by:

$$\hat{\overline{H}}_{\mathrm{rel}} = \frac{\hbar^2}{m\sigma^2}\left[-\partial_{\overline{r}}^2 + \overline{V}_{\mathrm{LJ}}(\overline{r})\right] \tag{C.6}$$

C.2.1 The method of imaginary-time propagation for calculation of the ground state

Applying the method of *imaginary-time propagation* for a given Hamiltonian $\hat{H}$ to a — more or less arbitrary[3] — start wave function $\psi_0(\mathbf{r})$, the algorithm drives the wave function into the ground state of that Hamiltonian.

The principle The formal expansion of the initial wave function in the complete set of $\hat{H}$-eigenfuctions $\{\phi_i\}$ is:

$$\psi_0(\mathbf{r}) = \sum_i a_i\phi_i(\mathbf{r}) \tag{C.7}$$

Taking ψ_0 as wave function at time $t = 0$, the quantum mechanical time evolution is performed by the operator $\hat{U}$, which is acting as:

$$\psi(\mathbf{r},t) = \hat{U}(t)\psi_0(\mathbf{r}) = e^{-\frac{i}{\hbar}\hat{H}t}\sum_i a_i\phi_i(\mathbf{r}) = \sum_i a_i e^{-\frac{i}{\hbar}E_i t}\phi_i(\mathbf{r}) \tag{C.8}$$

[2]The given numerical values result from taking the parameters for ^{133}Cs as a basis: $m = 2.22\cdot 10^{-25}\,\mathrm{kg}$; $\epsilon \approx 525\mathrm{K}\cdot k_{\mathrm{B}} \approx 7.25\cdot 10^{-21}\,\mathrm{J}$, $\sigma \approx 0.53\mathrm{nm}$ (from [8], fig. 7 ib); $\omega \sim 200\mathrm{Hz}$ (typical value).

[3]As will subsequently become clear the only constraint on the start wave function ψ_0 is a nonvanishing overlap with the ground state wave function (cp. footnote 4).

where the $\{E_i\}$ are the eigenenergies of $\hat{H}$.

The idea the name of the method originates from is to perform "time evolution" in the imaginary regime: $t := -iT$ ($T \in \mathbb{R}$):

$$\psi(\mathbf{r}, T) = \sum_i a_i e^{-E_i T/\hbar} \phi_i(\mathbf{r}) \tag{C.9}$$

Obviously, "imaginary time evolution" is realized by exponential damping-factors, where high energy components are damped faster than low energy components and the ground state is damped least.
To avoid that *all* components are damped for $T \to \infty$ — which would be the result of a naive, direct implementation of (C.9) — one has to *renormalize* the wave function after each time step ΔT giving the following expression after n time steps:

$$\psi(\mathbf{r}, n\,\Delta T) = \sum_i \frac{a_i e^{-E_i n\,\Delta T/\hbar}}{\sqrt{\sum_j |a_j|^2 e^{-2E_j n\,\Delta T/\hbar}}} \phi_i(\mathbf{r}) \tag{C.10}$$

As $E_0 = \min\{E_i\}$, the denominator — i.e. the renormalizing factor — behaves like $\sqrt{|a_0|^2 e^{-2E_0 n\,\Delta T/\hbar}} = |a_0| \exp(-E_0 n\,\Delta T/\hbar)$ for $n \to \infty$ and hence:

$$\lim_{n\to\infty} \psi(\mathbf{r}, n\,\Delta T) = \frac{a_0}{|a_0|} \phi_0(\mathbf{r}) \tag{C.11}$$

Thus, the method converges any initial wave function ψ_0 to the ground state indeed.[4]

Details of the implementation The structure of the algorithm is depicted in fig. C.2. The method has been implemented for the 1D-Hamiltonian[5] (C.6) using *C/C++*.
Some annotations concerning the implementation:

- The *convergence* of the algorithm and especially its speed depend on the choice of the initial wave function (one should choose ψ_0 similar to the expected form of the ground state) and the time step value ΔT (see below). Problems involving divergences are problematic; in this case searching for a transformation which causes the divergence to disappear is advisable.

- The "imaginary time-evolution operator"[6] $\exp(-\hat{H}\Delta T)$ has been implemented using its first order expansion:

$$\exp(-\hat{H}\Delta T) \approx \hat{1} - \hat{H}\Delta T \tag{C.12}$$

[4]However, ψ_0 has to have at least a small overlap with ϕ_0 (i.e. $a_0 \neq 0$), of course.

[5]The principle of the method is independent of the underlying problem's dimensionality, of course.

[6]The factor $\hbar$ — solely being a reminiscence to the quantum mechanical origin of the method's idea — can be omitted in numerical implementations as it obviously does not have any effect on the method's converging to the ground state (cp. (C.9)ff).

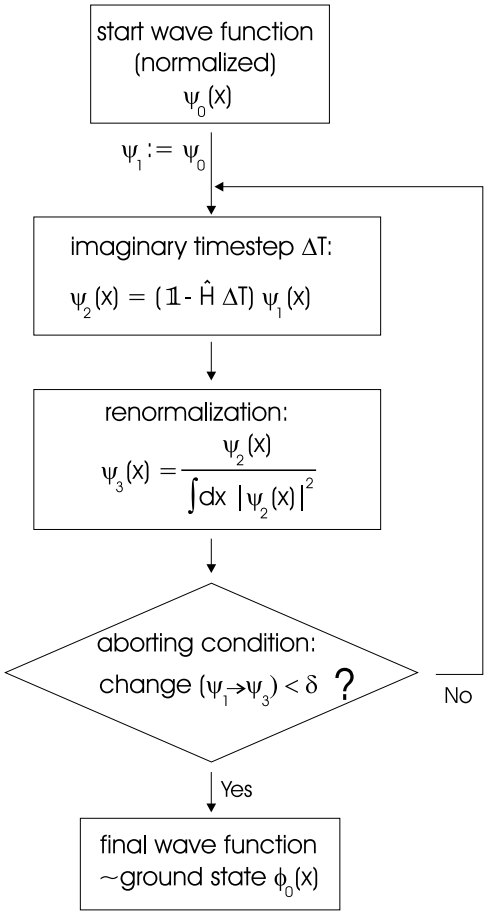

Figure C.2: Structure of the imaginary-time propagation algorithm.

Using $\partial_x^2\psi \stackrel{\wedge}{=} (\psi_{k+1} - 2\psi_k + \psi_{k-1})/\Delta x^2$ as discrete realization of the second derivative[7], the matrix representation of the Hamiltonian $\hat{H} \propto -\partial_x^2 + V(x)$ (cp. eq. (C.6)) becomes tridiagonal[8]:

$$(H)_{n,m} = \left[\frac{2}{\Delta x^2} + V(x_n)\right]\delta_{n,m} + \left[-\frac{1}{\Delta x^2}\right]\delta_{n,m+1} + \left[-\frac{1}{\Delta x^2}\right]\delta_{n,m-1} \quad \text{(C.13)}$$

As can be seen from the latter equation, (C.12) being a valid approximation imposes the following conditions on the parameters ΔT and Δx:

- $\Delta T/\Delta x^2 \ll 1$
- $\max(\{V(x_n)\})\,\Delta T \ll 1$

[7]Here ψ_k is an abbreviation for $\psi(x_k)$, which is the value of the wave function at the discrete supporting point x_k.

[8]$\delta_{n,m}$ denotes the KRONECKER delta here.

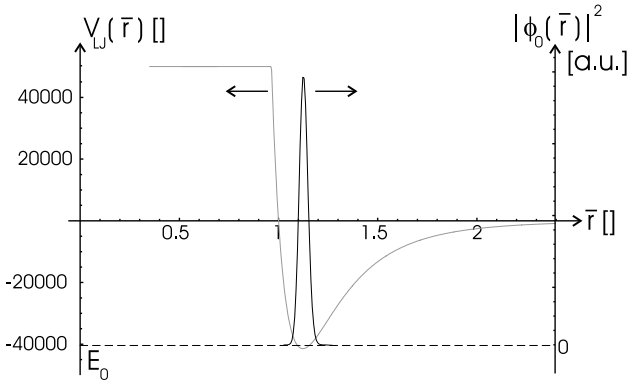

Figure C.3: Ground state wave function ϕ_0 (solid line) of the (scaled) Hamiltonian $\hat{H} = \partial_{\overline{r}}^2 + V_{\mathrm{LJ}}(\overline{r})$; note that for the numerical implementation of V_{LJ} (grey line) a (maximal) cutting value has been used. Numerical result for the ground state energy: $E_0 = -4.03 \cdot 10^4$; compare this with the minimal value of V_{LJ}: $-4.14 \cdot 10^4$ (scaled values).

- As *aborting condition for convergence* the following criterion has been used[9]: $\frac{1}{K}\sum_k |\psi_{3_k} - \psi_{1_k}|/|\psi_{3_k}| < \delta$, i.e. convergence has been assumed, if the *relative change* of the wave function after one cycle of the algorithm fell below a certain minimal value δ. A value of $\delta = 10^{-8}$ has been used for the calculations that led to fig. C.3.

C.2.2 Results

The method of imaginary time evolution has been applied to the (scaled) Hamiltonian (C.6) using the (scaled) LENNARD-JONES potential $\overline{V}_{\mathrm{LJ}}$ as given in (C.5): Starting with a Gaussian centered around the minimum of $\overline{V}_{\mathrm{LJ}}$ as initial wave function, the algorithm provides the ground-state wave function ϕ_0 as depicted in figure C.3.

As this typical example of ^{133}Cs shows, the ground state energy of two interacting alkali atoms typically is very small corresponding to a tightly bound molecular state scaling in the sub-nm-range (cp. fig. C.3: $\overline{r} = 1 \mathrel{\hat{=}} 0.53\mathrm{nm}$).

[9] K denotes the number of discrete supporting points; ψ_1 and ψ_3 are introduced in fig. C.2.

Appendix D

1D scattering theory

Scattering theory is one of the classic disciplines of quantum mechanics, and approaches to three-dimensional problems can be found in every standard textbook: For *centrosymmetric* scattering potentials ($V(\mathbf{r}) = V(r)$) it is convenient to regard the expansion in eigenfunctions of the angular-momentum operator (surface spherical harmonics). Applying this method — known as *partial-wave method* — the calculation of all essential quantities like the scattering amplitude or cross-sections can be reduced to finding the *scattering phase* resp. *phase shift* associated with each of the partial waves.

Although it is not the usual approach, an analogous "partial-wave expansion" can also be applied to one-dimensional problems of scattering of a particle from a potential ([45], [46]), if the scattering potential is a symmetric one ([47]). As an example, the latter also holds for *two-body scattering*, which in relative coordinates reduces to a problem of scattering from a potential (see sect. 5.1.3, p. 45).

Subsequently, first the general framework of one-dimensional partial-wave expansion and phase shift analysis will be presented before applying it to the abovementioned problem of two-body scattering with a square well potential as a simple model potential.

D.1 Partial-wave expansion in 1D

Given the one-dimensional SCHRÖDINGER equation

$$\hat{H}\psi(x) = \left[-\frac{\hbar^2}{2m}\frac{\partial^2}{\partial x^2} + V(x)\right]\psi(x) = E\psi(x) \tag{D.1}$$

with the (real) scattering potential $V(x)$ being restricted to a finite region[1] $|x| < b$ a scattering problem emerges for $E > 0$.

[1] This is assumed for convenience as only the asymptotic behaviour of the wavefunction will be focused on in the following ; however, it is not a necessary restriction (cp. footnote 10 on p. 9).

If the scattering potential is symmetric $V(-x) = V(x)$ it can be easily shown that the *parity operator* $\hat{P}$ defined by his action on functions $\hat{P}\,\psi(x) = \psi(-x)$ commutes with the above Hamiltonian:

$$\left[\hat{H}, \hat{P}\right] = 0 \tag{D.2}$$

Due to this a representation of the wave function in terms of parity eigenfunctions appears as favourable[2]:

$$\psi(x) = \sum_{i=0,1} \psi_i(x) = \sum_{i=0,1} \sigma^i \psi_i(|x|) \tag{D.3}$$

Here $\psi_{0/1}(x)$ is the even/odd eigenfunction of the parity operator $\hat{P}$ ($\hat{P}\psi_{0/1}(x) = \pm\hat{P}\psi_{0/1}$), and $\sigma = x/|x|$. (D.3) already is the desired *partial-wave expansion*[3] for one-dimensional scattering problems[4].

Subsequently it will be shown that in the asymptotic region the partial-wave expansion of $\psi(x)$ is given by

$$\boxed{\psi(x) = \frac{1}{\sqrt{2}}\left[C_0\phi_0(|x|) + C_1\phi_1(|x|)\right]} \tag{D.4}$$

with coefficients $C_0, C_1 \in \mathbb{C}$; here the ϕ_i are parity eigenfunctions, which are of the following asymptotic form for $|x| \to \infty$:

$$\boxed{\phi_i(x) = \begin{cases} 2e^{i\delta_0}\cos(k|x| + \delta_0) & \text{for } i = 0 \\ \sigma\, 2e^{i\delta_1}\sin(k|x| + \delta_1) & \text{for } i = 1 \end{cases}} \tag{D.5}$$

As usual $k = \sqrt{2mE/\hbar^2}$, and the δ_i are the corresponding partial-wave *phase shifts*. This reveals the advantage of this approach: In the asymptotic region the effect of the scattering potential enters the wave function (D.4) only by the two parameters δ_i; the C_i are determined solely by the boundary conditions.
The derivation of (D.4) and (D.5) is presented in the folowing section.

[2]Of course *every* function can be expanded in its even and odd part according to (D.3), but the representation (D.4) with the decoupled parity eigenfunctions $\phi_{0,1}$ (D.5) is valid only for symmetric V, i.e. if (D.2) is fulfilled. However, for nonsymmetric V these functions become coupled (cf. [46]).

[3]"Parity-wave expansion" obviously would be a more appropriate term in 1D.

[4]Mind the analogy to 3D: For centrosymmetric problems ($V(\mathbf{r}) = V(r)$) one finds $\left[\hat{H}, \hat{L}^2\right] = 0 = \left[\hat{H}, \hat{L}_z\right]$ with $\hat{L}$ denoting the angular momentum operator. Thus the general form of the partial-wave expansion in 3D is $\psi(\mathbf{r}) = \sum_l \sum_{m=-l}^{l} R(r)\, Y_{l,m}(\theta, \phi)$ with $Y_{l,m}(\theta, \phi)$ denoting the eigenfunctions of $\hat{L}^2$ and $\hat{L}_z$ ("surface spherical harmonics").

Asymptotic behaviour: Derivation of (D.4), (D.5)

For $|x| \to \infty$ the wave function becomes that of a free particle; assuming plane wave form

$$\psi(x) = \begin{cases} Ae^{ikx} + B'e^{-ikx} & \text{for } x \to -\infty \\ A'e^{ikx} + Be^{-ikx} & \text{for } x \to \infty \end{cases} \tag{D.6}$$

one can distinguish the *incoming* and *outgoing parts*:

$$\begin{aligned} \phi_{\text{in}}(x) &= A\,\Theta(-x)\,e^{ikx} + B\,\Theta(x)\,e^{-ikx} \\ \phi_{\text{out}}(x) &= A'\,\Theta(x)\,e^{ikx} + B'\,\Theta(-x)\,e^{-ikx} \end{aligned} \tag{D.7}$$

Here $\Theta(x)$ denotes the HEAVISIDE unit step function.
As known from general scattering theory the so-called *S-matrix* $\hat{S}$ relates ϕ_{in} and ϕ_{out}:

$$\begin{pmatrix} A' \\ B' \end{pmatrix} = \begin{pmatrix} S_{aa} & S_{ab} \\ S_{ba} & S_{bb} \end{pmatrix} . \begin{pmatrix} A \\ B \end{pmatrix} \tag{D.8}$$

The four elements of the S-matrix are complex-valued; however, general assumptions put certain constraints on these eight parameters (cf. [46]):

- Probability conservation $|A|^2 + |B|^2 = 1$ (and similarly for the primed coefficients) leads to unitarity of the S-matrix:

$$\hat{S}.\hat{S}^\dagger = 1 \tag{D.9}$$

- For real potential $V(x) \in \mathbb{R}$ the function $\psi^*(x)$, which can be obtained from $\psi(x)$ by the substitutions $A \leftrightarrow B'^*$ and $B \leftrightarrow A'^*$, is also a solution to (D.1). Making use of (D.9), it can be shown that this leads to

$$S_{aa} = S_{bb} \tag{D.10}$$

- Similarly, for symmetric potential $V(-x) = V(x)$ the function $\psi(-x)$, which can be obtained from $\psi(x)$ by the substitutions $A \leftrightarrow B$ and $A' \leftrightarrow B'$, is another solution to (D.1). This gives the additional constraint

$$S_{ab} = S_{ba} \tag{D.11}$$

Being interested in a representation of $\psi(x)$ in terms of partial waves the next aim will be to find a corresponding transformation of the S-matrix. Noting that the former, i.e. (D.3), is formally given by

$$\begin{aligned} \psi(x) &= \overbrace{\left[\tfrac{1}{2}(\psi(x) + \psi(-x))\right]}^{\overset{(D.3)}{=:}\ \psi_0(x)} + \overbrace{\left[\tfrac{1}{2}(\psi(x) - \psi(-x))\right]}^{\overset{(D.3)}{=:}\ \psi_1(x)} \\ &= \Big[\underbrace{\tfrac{A+B}{2}}_{:\propto C_0} e^{-ik|x|} + \underbrace{\tfrac{A'+B'}{2}}_{:\propto C'_0} e^{ik|x|}\Big] + \Big[\sigma\Big(\underbrace{\tfrac{B-A}{2}}_{:\propto C_1} e^{-ik|x|} + \underbrace{\tfrac{A'-B'}{2}}_{:\propto C'_1} e^{ik|x|}\Big)\Big], \end{aligned} \tag{D.12}$$

where (D.6) has been used, the following linear transformation is implied[5]:

$$\begin{pmatrix} C_0 \\ C_1 \end{pmatrix} = \frac{1}{\sqrt{2}} \begin{pmatrix} 1 & 1 \\ i & -i \end{pmatrix} \cdot \begin{pmatrix} A \\ B \end{pmatrix} \tag{D.13}$$

and similarly for C_0', C_1'. (D.13) in (D.7) yields:

$$\begin{aligned} \phi_{\text{in}}(x) &= \phi_{\text{in},0}(x) + \phi_{\text{in},1}(x) = \tfrac{1}{\sqrt{2}}(C_0 + iC_1\sigma)e^{-ik|x|} \\ \phi_{\text{out}}(x) &= \phi_{\text{out},0}(x) + \phi_{\text{out},1}(x) = \tfrac{1}{\sqrt{2}}(C_0' - iC_1'\sigma)e^{ik|x|} \end{aligned} \tag{D.14}$$

Thus C_0 (C_1) is the amplitude of the incoming even (odd) partial wave and correspondingly C_0' (C_1') is the amplitude of the outgoing even (odd) partial wave.
The S-matrix in partial-wave representation is defined by

$$\begin{pmatrix} C_0' \\ C_1' \end{pmatrix} = \begin{pmatrix} \mathcal{S}_{00} & \mathcal{S}_{01} \\ \mathcal{S}_{10} & \mathcal{S}_{11} \end{pmatrix} \cdot \begin{pmatrix} C_0 \\ C_1 \end{pmatrix} \tag{D.15}$$

Using (D.8), (D.13) one obtains:

$$\mathcal{S} = \begin{pmatrix} \mathcal{S}_{00} & \mathcal{S}_{01} \\ \mathcal{S}_{10} & \mathcal{S}_{11} \end{pmatrix} = \frac{1}{2} \begin{pmatrix} S_{aa} + S_{bb} + S_{ab} + S_{ba} & i(S_{bb} - S_{aa} + S_{ab} - S_{ba}) \\ i(S_{aa} - S_{bb} + S_{ab} - S_{ba}) & S_{aa} + S_{bb} - S_{ab} - S_{ba} \end{pmatrix} \tag{D.16}$$

As the potential is assumed real and symmetric, (D.10) and (D.11) show that $\mathcal{S}$ is diagonal and can be written as

$$\mathcal{S} = \begin{pmatrix} e^{2i\delta_0} & 0 \\ 0 & e^{2i\delta_1} \end{pmatrix} \tag{D.17}$$

due to its unitarity.[6]

Collecting these results, (D.12) becomes:

$$\psi(x) = \left[\tfrac{C_0}{\sqrt{2}}\left(e^{-ik|x|} + e^{2i\delta_0}e^{ik|x|}\right)\right] + \left[i\sigma\,\tfrac{C_1}{\sqrt{2}}\left(e^{-ik|x|} - e^{2i\delta_1}e^{ik|x|}\right)\right] \tag{D.18}$$

This is nothing else but the partial-wave representation (D.4), (D.5) □

[5]The factor "i" in the second row of the transformation matrix is chosen for convenience; without it, $\phi_1(x)$ in (D.5) would carry an additional factor "i".

[6]The factor "2" is introduced for convenience; without it, the phases in (D.5) would carry a corresponding factor.

D.2 An example: Scattering from a square-well

Due to its simplicity the square-well potential

$$V(x) = \begin{cases} -V_0 \ (<0) & \text{for } |x| \le a \\ 0 & \text{for } |x| > a \end{cases} \tag{D.19}$$

is a standard model potential, which has the advantage that analytic expressions for the scattering phase shifts can be derived; this is presented in the following subsection.

D.2.1 Phase shifts

As $V(x)$ is piecewise constant, the general partial-wave representations of the *interior* and the *exterior* solution are of similar form with $\psi_{\text{ext}}(x)$ being the asymptotic solution (D.4), which carries the phase shifts as defined in (D.5):

$$\psi_{\text{ext}}(x) = \tilde{C}_0 \cos(k|x| + \delta_0) + \sigma\, \tilde{C}_1 \sin(k|x| + \delta_1) \qquad (|x| > a) \tag{D.20}$$

$$\psi_{\text{int}}(x) = D_0 \cos(\beta|x|) + \sigma\, D_1 \sin(\beta|x|) \qquad (|x| < a) \tag{D.21}$$

Here $\beta = \sqrt{2m(E+V_0)}/\hbar$ and $k = \sqrt{2mE}/\hbar$ denote the wave numbers in the interior/exterior of the square-well potential.
The (finite) discontinuity of V provides fitting conditions at $x = \pm a$:

- *Continuity of ψ:*

$$\begin{aligned} \tilde{C}_0 \cos(ka + \delta_0) &= D_0 \cos(\beta a) \\ \tilde{C}_1 \sin(ka + \delta_1) &= D_1 \sin(\beta a) \end{aligned} \tag{D.22}$$

- *Continuity of $\partial_x \psi$:*

$$\begin{aligned} \tilde{C}_0 k \sin(ka + \delta_0) &= D_0 \beta \sin(\beta a) \\ \tilde{C}_1 k \cos(ka + \delta_1) &= D_1 \beta \cos(\beta a) \end{aligned} \tag{D.23}$$

Division of the corresponding equations of (D.22) and (D.23) and subsequently solving for the phases finally yields:

$$\delta_0 \;=\; \arctan\left(\tfrac{\beta}{k}\tan(\beta a)\right) - ka = \frac{\pi}{2} - \tau_0\, k + \mathcal{O}(k^3) \tag{D.24a}$$

$$\delta_1 \;=\; \arctan\left(\tfrac{k}{\beta}\tan(\beta a)\right) - ka = -\tau_1\, k + \mathcal{O}(k^3) \tag{D.24b}$$

Here the series expansion for small values of k has been given additionally: Obviously the phases show a linear dependence for small wave numbers. The coefficients of the linear terms are given by: $\tau_0 = a + \hbar/\big(\sqrt{2mV_0}\,\tan(a\sqrt{2mV_0}/\hbar)\big)$; $\tau_1 = a - \hbar\,\tan(a\sqrt{2mV_0}/\hbar)/\sqrt{2mV_0}$.

D.2.2 Boundary conditions

As an example the boundary condition "incoming waves from the left *and* from the right" will be applied; according to (D.7) this can be expressed as $\binom{A}{B} = \binom{1}{1}$, which leads to $\binom{C_0}{C_1} = \frac{1}{\sqrt{2}}\binom{2}{0}$ as partial-wave coefficients, where (D.13) has been used.
Consequently, the asymptotic form of the wave function is the even function

$$\psi_{\mathrm{rl}}(x) = \phi_0(x) \overset{(D.5)}{=} 2e^{i\delta_0}\cos(k|x| + \delta_0) \tag{D.25}$$

It should be explicitly emphasized that (D.25) is the *general* form of the *asymptotic* wave function for the given boundary condition independent of V being of square-well type; the latter enters solely by the specific expression for the phase shift (D.24a).

Bibliography

[1] S. N. Bose: Plancks Gesetz und Lichtquantenhypothese, *Z. Phys.* **26**, *178-181 (1924)*

[2] A. Einstein: Quantentheorie des einatomigen idealen Gases: Zweite Abhandlung, *Sitzungsber. Preuss. Akad. Wiss. (Kl. Phys./Chem.)* **1925**, *3-14 (1925)*

[3] M. H. Anderson, J. R. Ensher, M. R. Matthews, C. E. Wieman, E. A. Cornell: Observation of Bose-Einstein Condensation in a Dilute Atomic Vapor, *Science* **269**, *198-201 (1995)*

[4] C. C. Bradley, C. A. Sackett, J. J. Tollett, R. G. Hulet: Evidence of Bose-Einstein Condensation in an Atomic Gas with attractive Interactions, *Phys. Rev. Lett.* **75**, *1687-1690 (1995)*

[5] K. B. Davis, M.-O. Mewes, M. R. Andrews, N. J. van Druten, D. S. Durfee, D. M. Kurn, W. Ketterle: Bose-Einstein Condensation in a Gas of Sodium Atoms, *Phys. Rev. Lett.* **75**, *3969-3973 (1995)*

[6] W. Nolting: Statistische Physik, *Vieweg, 3. Auflage 1998*

[7] K. Huang: Statistical Mechanics, *John Wiley & Sons Inc., New York, 2nd ed. 1987*

[8] Y. Castin: Bose-Einstein condensates in atomic gases: simple theoretical results, *cond-mat/0105058 (2001)*

[9] F. Dalfovo, S. Giorgini, L. P. Pitaevskii, S. Stringari: Theory of Bose-Einstein condensation in trapped gases, *Rev. Mod. Phys.* **71**, *463-512 (1999)*

[10] W. Ketterle, D. S. Durfee, D. M. Stamper-Kurn: Making, probing and understanding Bose-Einstein condensates, *cond-mat/9904034 (1999)*

[11] H. Haken: Quantenfeldtheorie des Festkörpers, *B. G. Teubner Stuttgart, 2. Auflage 1983*
(engl. version:) Quantum field theory of solids : an introduction, *North-Holland Amsterdam, 2nd ed. 1983*

[12] M. Edwards, R. J. Dodd, C. W. Clark, K. Burnett: Zero-Temperature, Mean-Field Theory of Atomic Bose-Einstein Condensates, *J. Res. Natl. Inst. Stand. Technol.* **101**, *553-565 (1996)*

[13] H. B. Thacker, David Wilkinson: Inverse scattering transform as an operator method in quantum field theory, *Phys. Rev. D* **19**, *3660-3665 (1979)*

[14] W. Nolting: Elektrodynamik, *Vieweg, 5. Auflage 2000*

[15] G. P. Agrawal: Nonlinear Fiber Optics, *Academic Press, 2nd ed. 1995*

[16] F. X. Kärtner: Optische Solitonen – Grundlagen und Anwendungen, *Physik in unserer Zeit* **26(4)**, *152-161 (1995)*

[17] Fedor Mitschke, Michael Böhm: Solitonen in Glasfasern, *Phys. Blätt.* **56(2)**, *25-30 (2000)*

[18] V. E. Zakharov, A. B. Shabat: Exact theory of two-dimensional self-focusing and one-dimensional self-modulation of waves in nonlinear media, *Sov. Phys. JETP* **34(1)**, *62-69 (1972)*
(mistake in eq. (6) ib; the correct version is eq. (3.9) in this thesis)

[19] L. D. Landau, E. M. Lifschitz: Lehrbuch der theoretischen Physik, Band III: Quantenmechanik, *Akademie-Verlag Berlin, 4. Auflage 1971 (german edition)*

[20] F. Schwabl: Quantenmechanik, *Springer, 5. Auflage 1998*

[21] N. J. Zabusky, M. D. Kruskal: Interactions of "solitons" in a collisionless plasma and the recurrence of initial states, *Phys. Rev. Lett.* **15**, *240-243 (1965)*

[22] A. M. Weiner: Dark optical solitons, in: *Optical solitons – theory and experiment, ed. by J. R. Taylor; Cambridge University Press 1992*

[23] K. M. Hilligsøe: Bright Atomic Solitons in Bose-Einstein Condensates, *Master Thesis, University of Aarhus/Universität Konstanz (2001); available under: http://hubble.physik.uni-konstanz.de/~kmh*

[24] C. M. Bender, S. A. Orszag: Advanced mathematical methods for scientists and engineers — Asymptotic methods and perturbation theory, *Springer, 1st ed. 1999*

[25] C. Matijn de Sterke, J. E. Sipe: Envelope-function approach for the electrodynamics of nonlinear periodic structures, *Phys. Rev. A* **38**, *5149-5165 (1988)*

[26] V. V. Konotop, M. Salerno: Modulational instability in cigar shaped Bose-Einstein condensates in optical lattices, *cond-mat/0106228*

[27] M. B. Dahan, E. Peik, J. Reichel, Y. Castin, C. Salomon: Bloch Oscillations of Atoms in an Optical Potential, *Phys. Rev. Lett.* **76**, *4508-4511 (1996)*

[28] E. Peik, M. B. Dahan, I. Bouchoule, Y. Castin, C. Salomon: Bloch Oscillations of atoms, adiabatic rapid passage, and monokinetic atomic beams, *Phys. Rev. A* **55**, *2989-3001 (1996)*

[29] B. Brezger, M. K. Oberthaler, A. Sizmann, B. Eiermann, J. Mlynek: An experimental scheme for bright atomic gap solitons, *unpublished, priv. comm.*

[30] S. Burger, K. Bongs, S. Dettmer, W. Ertmer, K. Sengstock: Dark solitons in Bose-Einstein Condensates, *Phys. Rev. Lett.* **83**, *5198-5201 (1999)*

[31] J. Denschlag et al.: Generating Solitons by Phase Engineering of a Bose-Einstein Condensate, *Science* **287**, *97-101 (2000)*

[32] Y. Lai, H. A. Haus: Quantum theory of solitons in optical fibers. I. Time-dependent Hartree approximation, *Phys. Rev. A* **40**, *844-853 (1989)*

[33] Y. Lai, H. A. Haus: Quantum theory of solitons in optical fibers. II. Exact solution, *Phys. Rev. A* **40**, *854-866 (1989)*

[34] T. Fliessbach: Quantenmechanik - Lehrbuch zur Theoretischen Physik III, *Spektrum Akademischer Verlag, 2. Auflage 1995*

[35] M. R. Andrews, C. G. Townsend, H.-J. Miesner, D. S. Durfee, D. M. Kurn, W. Ketterle: Observation of Interference Between Two Bose Condensates, *Science* **275**, *637-641 (1997)*

[36] I. Bloch, T. W. Hänsch, T. Esslinger: Measurement of the spatial coherence of a trapped Bose gas at the phase transition, *Nature* **403**, *166-170 (2000)*

[37] R. Loudon: The Quantum Theory of Light, *Clarendon Press Oxford, 2nd ed. 1983*

[38] M. Naraschewski, R. J. Glauber: Spatial coherence and density correlations of trapped Bose gases, *Phys. Rev. A* **59**, *4595-4607 (1999)*

[39] *Computeralgebra Software:* Mathematica, Ver. 4.1; *Wolfram Research, Inc., Champaign 2000*

[40] S. Wolfram: The Mathematica Book, *Wolfram Media, Champaign, 4th ed. 1999*

[41] Mathematica-/Maple-Kurs – Skript (computeralgebra compact course; concept/author: Matthias Söhn), *available under: http://hubble.physik.uni-konstanz.de/msoehn/mamakurs/public_html*

[42] C. S. Gardner, J. M. Greene, M. D. Kruskal, R. M. Miura: Method for solving the Korteweg-De-Vries equation, *Phys. Rev. Lett.* **19**, *1095-1097 (1967)*

[43] P. G. Drazin: Solitons, *Cambridge University Press, 1983*

[44] P. D. Lax: Integrals of nonlinear equations of evolution and solitary waves, *Comm. Pure Appl. Math.* **21**, *467-490 (1968)*

[45] J. H. Eberly: Quantum Scattering Theory in One Dimension, *Am J. Phys.* **33**, *771-773 (1965)*
Mind some errors in this paper:
• eq. (10), third line; correct is: $\cdots = \sum_{l=0,1} \frac{1}{2}\epsilon_{\_}^{l}(-\underline{i})^{l} \ldots$
• p. 773, middle of left column; correct is: $\psi_{\text{int}} = \sum_{l=0,1} \epsilon^{l} B_l \cos(\beta r \underline{+ l\pi/2})$.
• Also mind the rectification [47] of this paper.

[46] Y. Nogami, C. K. Ross: Scattering from a nonsymmetric potential in one dimension as a coupled-channel problem, *Am J. Phys.* **64**, *923-928 (1996)*

[47] J. Formánek: On phase shift analysis of one-dimensional scattering, *Am J. Phys.* **44**, *778-779 (1976)*

Epilog

... Was er sah, war sinnverwirrend. In einer krausen, kindlich dick aufgetragenen Schrift [...] bedeckte ein phantastischer Hokuspokus, ein Hexensabbat verschränkter Runen die Seiten. Griechische Schriftzeichen waren mit lateinischen und mit Ziffern in verschiedener Höhe verkoppelt, mit Kreuzen und Strichen durchsetzt, ober- und unterhalb waagerechter Linien bruchartig aufgereiht, durch andere Linien zeltartig überdacht, durch Doppelstrichelchen gleichgewertet, durch runde Klammern zusammengefaßt, durch eckige Klammern zu großen Formelmassen vereinigt. Einzelne Buchstaben, wie Schildwachen vorgeschoben, waren rechts oberhalb der umklammerten Gruppen ausgesetzt. Kabbalistische Male, vollständig unverständlich dem Laiensinn, umfaßten mit ihren Armen Buchstaben und Zahlen, während Zahlenbrüche ihnen voranstanden und Zahlen und Buchstaben ihnen zu Häupten und Füßen schwebten. Sonderbare Silben, Abkürzungen geheimnisvoller Worte waren überall eingestreut, und zwischen den nekromantischen Kolonnen standen geschriebene Sätze und Bemerkungen in alltäglicher Sprache, deren Sinn gleichwohl so hoch über allen menschlichen Dingen war, daß man sie lesen konnte, ohne mehr davon zu verstehen als von einem Zaubergemurmel.

Th. Mann; aus dem Roman *Königliche Hoheit*